HHS Public Access

Author manuscript

Adv Mater. Author manuscript; available in PMC 2023 March 01.

Published in final edited form as:

Adv Mater. 2022 March ; 34(10): e2106787. doi:10.1002/adma.202106787.

Recent Progress in Materials Chemistry to Advance Flexible Bioelectronics in Medicine

Gaurav Balakrishnan, **Jiwoo Song**, **Chenchen Mou**, **Christopher J. Bettinger**

Carnegie Mellon University, 5000 Forbes Avenue, 15213, USA

Abstract

Designing bioelectronic devices that seamlessly integrate with the human body is a technological pursuit of great importance. Bioelectronic medical devices that reliably and chronically interface with the body can advance neuroscience, health monitoring, diagnostics, and therapeutics. Recent major efforts focus on investigating strategies to fabricate flexible, stretchable, and soft electronic devices, and advances in materials chemistry have emerged as fundamental to the creation of the next generation of bioelectronics. In this review, we summarize contemporary advances and forthcoming technical challenges related to three principal components of bioelectronic devices: (i) substrates and structural materials, (ii) barrier and encapsulation materials, and (iii) conductive materials. Through notable illustrations from the literature, integration and device fabrication strategies and associated challenges for each material class are highlighted.

Graphical Abstract

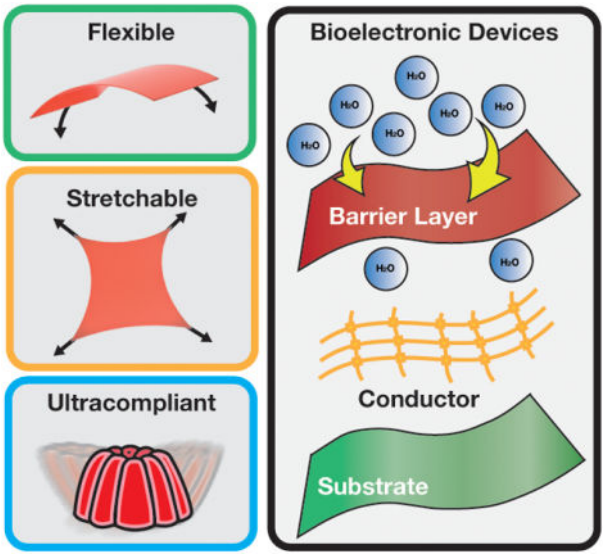

Flexible, stretchable and soft electronics interfaced with the human body hold immense potential to unlock a variety of diagnostic, therapeutic, and health monitoring applications. Materials chemistry plays a crucial role in determining the interaction and integration of these

cbetting@andrew.cmu.edu .

devices with biological systems. Recent progress in materials chemistry-enabled bioelectronics is presented and challenges, opportunities, and future research directions are highlighted.

Keywords

flexible bioelectronics; materials chemistry; bioresorbable; soft electronics; encapsulation; extensible conductors

1. Introduction

Reliable interfacing of flexible, stretchable, and soft electronics with the human body could advance a wide range of medical technologies such as chronic brain-computer interfaces,[1–6] implantable electrophysiological sensors,[7–10] active drug delivery systems,[11–16] wearable health monitoring devices,[17–24] and electrical stimulatory therapeutic devices.[25–33] Electronic devices with flexible and compliant form factors permit conformal integration with tissues in the human body, which are often soft, curvilinear, and dynamic.[34–36] While the prospects for biomedical applications are promising, transforming flexible electronics from laboratory curiosities into robust and reliable medical devices creates new challenges in fabrication and deployment. Advances in materials chemistry and polymer science contribute to the design of flexible electronic devices for biomedical applications.[37–40] Decades of research in flexible bioelectronics have standardized materials and processing techniques that serve as cornerstone technologies within the bioelectronics scientific community. This has included advances in the processing and integration of traditional electronics materials,[41–46] the design of novel biocompatible polymer substrates,[47–52] and investigating intrinsically flexible and stretchable organic electronics.[53–58] Furthermore, novel materials and new fabrication techniques enable new form factors and increase the parameter space for both mechanical and electrical properties, and structural adaptability. Here we discuss how materials chemistry can accelerate progress in bioelectronics in three specific areas: (1) substrate and structural materials, (2) packaging and barrier layers, and (3) flexible and stretchable conductors. We will examine contemporary instances of materials development, process design, and implementations of flexible bioelectronics systems, with an emphasis on implantable devices, through a lens of materials chemistry. Furthermore, we will present emerging challenges, bottlenecks, and opportunities for innovation in the field.

1.1. Defining Key Terms in Flexible Electronics

Terms such as flexibility, stretchability, mechanical compliance, softness, and extensibility are often used interchangeably. However, precisely defining this beforehand will clarify the forthcoming technical discussion. As such, this article will assign bioelectronic devices as flexible, stretchable, or ultracompliant roughly based on the intrinsic mechanical properties of the structural materials. These classifications, albeit artificial, facilitate discussions on the role of materials chemistry in flexible bioelectronic devices.

Mechanical flexibility and compliance are interchangeably defined as the inverse of stiffness, a parameter that refers to the ability of a body to resist deflection or deformation

and can be expressed as the ratio of applied force to the deformation.[74,75] While a material can be subject to varying modes of deformation, flexibility specifically refers to the ability of a material to undergo bending.[76] In the context of bioelectronics, the minimum bending radius and bending stiffness can be valuable measures of flexibility that provides direct insight into the ability of a film to conform to topographically complex curvilinear targets. The minimum bending radius of a film $r_{b,min}$ is dependent on the elastic modulus of the material and the thickness of the film, given by:[75,77]

$$r_{b,\,min} = \frac{Eh}{2\sigma_y}. \quad (1)$$

The bending stiffness of a film is:

$$D = \frac{Eh^3}{12\left(1-\nu^2\right)} \quad (2)$$

where E is the Young's modulus of the material, h is film thickness, σ_y is yield strength, and ν is the Poisson's ratio. "Flexible bioelectronics" will refer to inextensible devices with an effective elastic modulus typically between 0.1–100 GPa and bending stiffness on the order of 10^{-9}–10^{-15} N m^2.[78] With the broad range of possible bending stiffnesses, this class of devices are useful in a variety of applications such as intracortical probes, conformal neural probes, retinal implants, cochlear implants, etc.[79–81]

The term "stretchability" is somewhat vaguer in the context of bioelectronics, sometimes referring to the ability for a system to accommodate strain without failure in the elastic regime and other times expanding the requirement to include plastic regime.[82–84] Concluding an effort to define stretchability in the context of electronics, Lipomi states "stretchable electronics comprise materials and devices that accommodate strain, or do not accommodate strain, depending on your perspective, by a variety of mechanisms: elastic deformation, plastic deformation, strain-evolved formation of buckles, and even formation of cracks".[85] In this article, we will define "stretchable electronics" as devices that are able to withstand a non-zero strain that is useful to its intended application prior to device and/or material failure. They are typically extensible devices whose effective elastic moduli lie between 0.1–100 MPa. Extensibility of materials is similarly understood as the extent to which a material can be stretched before failure and can be quantified by the percent elongation at failure. Stretchable devices can be deployed in mechanically dynamic applications such as cardiac sensors, wearable devices, and peripheral nervous interfaces.[86–90]

Lastly, softness broadly refers to the property of low mechanical modulus materials to deform under small, applied stresses. Unlike flexibility, softness extends beyond elastic deformation by bending, encompassing low modulus polymeric materials, such as viscoelastic hydrogels and supramolecular networks with mesoscale organization. In this article, devices based on such materials will be discussed under the title of "ultracompliant bioelectronics". Furthermore, "ultracompliant electronics" comprise devices with elastic

moduli between 0.1–100 kPa. Ultracompliant devices are most useful in forming seamless interfaces with soft tissues such as the brain.[91–94]

1.2. Guidelines for Designing Implantable Flexible Bioelectronics

Implantable flexible bioelectronic devices present unique additional design constraints compared to wearable devices. Implantable flexible bioelectronic devices will ideally be composed of non-toxic biocompatible materials to promote integration of the device with the biological environment.[34,95,96] Biocompatibility is used as an all-encompassing term to describe materials that do not induce severe foreign body and inflammatory responses, and are able to function in their intended application without causing harm to local tissue or overall human health.[97,98] Strategies commonly employed to improve biocompatibility of implantable devices involve the following: (i) using non-toxic, biologically derived, or biomimetic materials, (ii) engineering the surface chemistry and topography to camouflage the device, improve biointegration, and minimize the consequences of bio-fouling; (iii) target localized release of drugs or other bioactive compounds to manage the inflammatory response.[99–106]

In addition to managing *in vivo* responses to implanted devices, it is also imperative to understand the mechanical environment of the biological environment at site of tissue integration. As illustrated in Figure 1, various organs exhibit different mechanical environments, such as elastic modulus, extensibility, dynamic versus static loading condition, etc. A holistic picture of these conditions should greatly influence the materials selection and device design of the bioelectronics. For instance, a long-term device meant to conformally contact heart tissue must be a fatigue resistant, stretchable device that can withstand several thousand cycles of loading per operational day.[107–110] A conformal neural interface, on the other hand, can be made of ultrathin flexible materials that don't need to be stretchable or fatigue resistant.[111–113]

A final consideration that requires additional thought and planning in all implantable bioelectronics applications is designing for processability and practicality. While there might be several attractive materials for use in bioelectronics for their interesting mechanical or functional properties, they must be amenable to integration with microelectronics processing techniques or propose the development of novel device integration methods. Furthermore, practical challenges such as interfacing devices with input and output data and power transmission cables must be considered from an early stage in the design process.[114–116]

2. Substrates and Structural Materials for Flexible Bioelectronics

Substrates are structural elements that provide mechanical integration for device components, such as logic elements, electrodes, traces, and interconnects. Active devices and supporting components are often composed of micropatterned thin film architectures <1 μm in thickness, while substrate materials are of macroscopic dimensions and are often >100 μm in thickness.[54] Thus, the substrate often dictates the mechanics, form factor, and toxicity profile of the overall device.

In the following discussion on substrates, the materials will be classified into the four following categories, employing definitions presented in Section 1.1 and Figure 2: (i) flexible substrates, (ii) stretchable substrates, (iii) ultracompliant substrates, and (iv) structurally adaptive substrates. Figure 2 represents a non-exhaustive survey of a trend towards softer and more compliant substrates for bioelectronic devices. Using this chronological perspective, this section will utilize a bottom-up approach to summarizing trends in this domain. This sub-topic will review chemical composition, then macromolecular networks and polymer processing, and then finally microstructural aspects of materials that are commonly used as substrates and structural materials in bioelectronic devices.

2.1. Flexible Substrate Materials in Bioelectronics

This section focuses on thin films of high modulus inextensible polymers (1–10 GPa, <250 μm), such as Parylene C, polyesters, polyimides, and SU-8, and their use as substrates in bioelectronics. The commercial availability of such polymers and compatibility with microelectronics processing techniques has accelerated progress in flexible bioelectronics. With early bioelectronic implants typically comprising rigid bulk inorganic components and packaging, flexible substrates significantly improved mechanical matching across the biotic-abiotic interface.[131–134] These materials offer exceptional processability as they are amenable to thin film processing, patterning, molding, etching, and other diverse types of subtractive and additive fabrication techniques.[47,135–137] Here, we briefly highlight contemporary and historical examples of polymers as substrate materials in flexible bioelectronic devices.

2.1.1. Polyesters—Polyesters have found wide use as substrate materials in flexible bioelectronics, ranging from the crude early demonstrations of flexible multielectrode arrays for medical applications in the 1970s, to intricate devices with active on-board electronics for applications in conformal cardiac sensors.[109,117] As a widely used commercial and industrial polymer, the infrastructure surrounding polyester processing can be leveraged to engineer these materials as substrates for flexible bioelectronic devices.[28,159,160]

Polyethylene terephthalate (PET) and polyethylene naphthalate (PEN) are two aromatic thermoplastic polyesters commonly used as substrates in flexible bioelectronic devices.[109,160–162] PET and PEN both feature ester links between monomers with aromatic groups in the polymer backbone which confer chemical stability and produce stable semi-crystalline hydrophobic domains that resist biodegradation. One versus two aromatic rings in PET and PEN, respectively, has a direct impact on the glass transition temperature ($T_{g,\mathrm{PET}}$ = 75–85 °C; $T_{g,\mathrm{PEN}}$ = 114–125 °C), crystallinity, and therefore also the Young's modulus (E_{PET} = 2.95 GPa; E_{PEN} = 5.5 GPa).[163] As thermoplastics, PET and PEN are manufactured through a combination of molten extrusion and cold rolling to produce films of desired thicknesses.[164,165] As a result, it can be more challenging to integrate pre-rolled polyesters with microelectronics manufacturing methods compared to polymer substrates that can be deposited or spin coated. However, the thermal and chemical stability of polyesters have encouraged researchers to develop several approaches to implement PET and PEN as substrates for bioelectronics.

PET is a versatile thermoplastic that has been successfully in implemented in a variety of systems that utilize differing substrate thicknesses (1–50 μm) and processing methods. A 1974 study demonstrated the use of a relatively thick PET film (50 μm) in an early prototype of a multielectrode array for a flexible cochlear implant.[117] More recently, ultrathin PET substrates (1–3 μm) have also been successfully integrated for a range of wearable and in vivo applications. Lee et al. presented the fabrication of an ultraflexible multielectrode array on 1.5 μm PET substrates for *in vivo* cardiac monitoring in 10-week old rats.[109] Traces are deposited using thermal evaporation through a shadow mask and passivated with a Parylene-C insulation layer. In addition to engineering an extremely low bending radius (<10 μm) in their ultrathin PET film, the authors utilized a patterned adhesive polyvinyl acetate (PVA) hydrogel to improve electrode interfacial adhesion and create a highly conformal contact with the cardiac tissue. As a result, the ultrathin device with PVA coated electrodes showed stable signal amplitudes of 8 mV with a 0.1 mV noise level, in contrast to uncoated electrodes showing fluctuating signal amplitudes from 5–7 mV with a 1.5 mV noise level. Sung et al. designed a wireless implantable controlled release system on PET substrates for delivery of neurotherapeutics directly to the cerebral cortex (Figure 3, A-i,ii).[159] The device features SU-8 drug reservoirs with nominal volumes of 1.5 nL capped with Au membranes, Ti conductive traces to deliver 1.1 mA cm^{-2} DC current to electrochemically dissolve the Au, and an SU-8 passivation layers, all fabricated on a PET film 25 μm in thickness. (Figure 3, A-iii). PET substrates were specifically selected in this application as a result of its compatibility with UV adhesive-based bonding and to provide necessary flexibility and handling for deploying the device into the subdural space.

Similar to PET, PEN has also been widely used as a substrate for bioelectronics for its thermal and chemical stability, especially in cases that benefit from its higher Young's Modulus compared to PET. Someya et al. and Fuketa et al. integrated 100 μm and 1 μm thick PET films respectively with patterned metal thin film conductors and organic semi-conductors to fabricate wearable sensors.[127,161] These examples also illustrate the compatibility of PEN substrates with manufacturing techniques, such as laser cutting and micromachining for feature and form-factor definition.

PEN substrates have also been used for inkjet printing and 3D printing of functional inks containing nanomaterials such as gold, silver, and carbon nanoparticles.[160,166,167] Inkjet printing of gold nanoparticles described by Khan et al. was used to fabricate a flexible impedance sensing electrode array to detect pressure ulcers in rat models (Figure 3, B).[168] PEN served as a reliable substrate that could undergo 1000 twist cycles without damage to the device.

2.1.2. Polyimides—Polyimides are commercially available polymers that have been used extensively as substrates in flexible bioelectronics due to the combination of chemical stability and compatibility with many existing microfabrication processes.[169,170] By definition, polyimides contain imide ($-R_1CO-NR_2-COR_3-$) groups in the polymer backbone. Delocalized electrons in the imide group help to confer thermal and chemical resistance as a result of stable delocalized electronic configuration.[169,171] Polyimides are commodity materials used in adhesives, electronic device insulation and packaging, and flexible printed circuit boards.[172] Polyimides can be prepared using aliphatic or aromatic

monomers (Figure 4). Polyimides with aromatic groups such as poly(*4,4'*-oxydiphenylene pyromellitimide) (PMDAODA PI) or Kapton and biphenyltetracarboxylic dianhydridde/ para-phenylenediamine (BPDA-PPD) or U-Varnish are of particular interest as substrate materials in bioelectronics.[173] Although most polymers used in bioelectronics are aromatic or semi-aromatic as a result of superior thermal and chemical resistance, aliphatic polyimides are becoming materials of interest for optoelectronics applications due to their higher optical transparency (~90%) compared to commercial polyimides such as Kapton (~70%).[174,175]

In addition to its chemical and thermal resistance, polyimide is biocompatible, strongly bonds photoresists to facilitate photolithography, and is compatible with etching techniques.[170,176] Furthermore, polyimides are thermosets that can be produced as liquid polymer precursors that can be solution processed at room temperature (drop casted, spin coated, and molded) and baked to produce irreversibly cured polymer films.[177–179] As a result, polyimides have been used as substrates in early instantiations of cochlear implants, an early example of implantable bioelectronic devices.[180] In this study, microfabrication processes were optimized and standardized for polyimide substrates, including spin-coating on Si handling wafers, photopatterning, and the use of tantalum adhesion layers for metallization.

More contemporary examples exploit polyimides for their compatibility with nanofabrication methods to design complex implantable devices in cardiac and neural sensing applications.[181–183] Silicon nanomembrane transistors were integrated with a 288-electrode array for on-board amplification and multiplexing on flexible polyimide substrates to measure cardiac electrophysiology.[182] Multilayer architectures use two thin (~1.5 μm) spin-coated PI 2545 (HD Microsystems, NJ, USA) intermediary insulation layers and a Kapton (DuPont, DE, USA) polyimide substrate 12.5 μm in thickness bonded the to the device using a plasma activated silicone adhesive. When interfaced with a porcine heart, the device can map the cardiac wavefront with 800 μm resolution and signal-to-noise ratios (SNR) of ~34 dB. As one of the first instances of Si-based devices in implantable systems, this project highlights the potential of leveraging silicon-based microfabrication technology for robust yet flexible bioelectronic devices. Recently, a similar fabrication scheme was used to design a capacitively-coupled 396-node cardiac sensor and a 1008-node electrocorticography (ECoG) sensor that allowed for a completely encapsulated device without any exposed electronic components for long-term electrophysiology monitoring and high resolution (~400 μm) mapping (SNR ~42 dB) (Figure 4, A).[184,185]

Polyimides are amenable to micropatterning which can be used to create porous ordered mesh networks as substrates, improving the conformability of bioelectronic devices.[112,186,187] This is possible through a variety of techniques, such as dry etching using reactive ions, conventional photopatterning, and laser cutting. Seminal work in this field was reported by Kim et al. where photolithographic techniques were employed to pattern and metallize 2 μm thick Kapton PI films, followed by dry etching of PI to pattern the substrate into a mesh (Figure 4, B).[112] Dissolvable silk films were used as a temporary stiffener to deploy the devices in *in vivo* applications. A hemispherical mechanical model to estimate minimum adhesion energy per unit area showed that the polyimide mesh required a 10× lower adhesion energy compared to a film of the same thickness (γ_{sheet} = 29 mJ/m^2, γ_{mesh}

= 2.4 mJ/m^2, thickness = 2.5 μm). An *in vivo* demonstration of the structures on a feline visual cortex showed that the mesh-based devices had the highest mean signal amplitude and the lowest error ($V_{RMS,mesh}$ = 5.7±3), suggesting that compliant electrodes are in closer contact with neural tissue compared to the unpatterned sheet devices ($V_{RMS,sheet\ 76\mu m}$ = 5.2±3.9, $V_{RMS,sheet\ 2.5\mu m}$ = 5.2±3.9).

2.1.3. Liquid Crystal Polymers—Liquid crystalline polymers (LCP) are highly crystalline polymer networks whose use as substrates in flexible bioelectronics evolved from their use as packaging materials in microelectronic devices. LCP are unique thermoplastics composed of low molecular weight aromatic subunits called mesogens that can self-assemble and align into liquid crystals upon heating or dissolution.[188–190] Crystalline domains confer chemical and thermal stability (T_{deg} ~380°C), comparatively large elastic moduli for polymers (E~10 GPa), and low water absorptivity (moisture absorption <0.04wt%).[119,142] These properties, in addition to research suggesting that commonly used commercial LCP films are biocompatible for *in vivo* applications, have made them compelling for use in bioelectronics.[191–193]

LCP have been used as substrates for various devices including neural interfaces and retinal prosthetics.[194] Lee et al. used LCP as a substrate for peripheral neural interfaces to record from the sciatic nerve of murine subjects (Figure 2, A3). Multi-electrode arrays are fabricated on LCP by depositing Ti/Au metal stacks using sputtering and then patterning using wet etching.[195] Conformal retinal prosthetics have also been prepared using electronics integrated with LCP-based substrates.[119,196] Rabbits implanted with surrogate devices showed no adverse effects after 2.5 years post-implantation.[193] Lastly, LCP substrates can be integrated with ultrathin Si-based radio frequency integrated circuits to enable more sophisticated functions including *in vivo* wireless communication.[192]

Aligned and crystalline networks in LCP produce some challenges for use in flexible bioelectronics. First, aligned polymer chains generate robust, yet highly anisotropic mechanical properties. For example, the anisotropy ratio of tensile strength and elastic modulus of commercial 1-mm thick Vectra A950 films are $\frac{UTS_{\parallel}}{UTS_{\perp}} = 3.6$ and $\frac{E_{\parallel}}{E_{\perp}} = 3.6$ respectively.[197,198] However, using modified film extrusion processes, biaxial LCP films that have polymer chains orientation equally distributed in two perpendicular directions (−45° and +45°) exhibit isotropic mechanical properties.[199] The high melting point of LCPs coupled with the low viscosity of LCP melts limit their processing into films to extrusion-based methods (Velctra A-950: T_m =280°C, melt viscosity η = <100 Pa s).[142,200] As a result, most reports that use LCPs as substrates in bioelectronic devices use commercially available films with thicknesses greater than 25 μm. This lower limit of thickness bounds the flexibility of LCP-based devices and prevents their use from applications requiring high conformability. Dry etching and laser based-thinning can reduce the thickness of LCP substrates for applications where thicknesses <25 μm are required.[143,201]

2.1.4. Epoxies—Epoxies are widely used as photoresists in microelectronics fabrication but have also gained traction as a substrate material in flexible electronics.[202–205]

Commercially available SU-8 photoresist contains a UV-activated photoacid generator that protonates epoxide groups on multifunctional oligomers and yields highly cross-linked networks.[145] The resulting polymer is mechanically robust and thermally stable with a Young's Modulus up to $E \sim 5$ GPa and shows no detectable structural degradation at temperatures up to 380°C.[206] In photolithography, the non-crosslinked polymer can easily be dissolved with an SU-8 developer like 1-methoxy-2-propanol acetate. SU-8 films of a broad range of thicknesses (0.2–300 μm) can be fabricated by spin coating precursors with varying viscosities.[207,208] In addition to the favorable processing capabilities and mechanical properties, demonstrations of the biocompatibility of SU-8 implants have made it a compelling material for bioelectronics.[209–211]

Flexible bioelectronic devices fabricated on bulk SU-8 substrates have been extensively investigated for diverse applications, including peripheral and cortical nerve interfaces. Photopatterned SU-8 with thin-film gold electrodes was used to fabricate grooved microprobes aimed at channeling the regrowth of sciatic nerves in a rat model.[204] This structure measured nervous impulses for 51 weeks *in vivo* with a signal-to-noise ratio (SNR) >2 and no indication of adverse inflammatory reactions. SU-8-based cortical probes exploit the robust in-plane mechanical properties combined with out-of-plane flexural compliance to accommodate insertion forces without buckling.[212] Altuna et al. presented a multimodal device capable of microfluidic drug delivery into the brain in addition to measuring neural responses (Figure 5, A-i,ii,iii).[203] Devices deployed *in vivo* can detect local field potentials and single cell activity in conjunction with localized delivery of precise drug volumes within the brain of murine subjects (Figure 5, A-iv).

Photo-definable features of SU-8 lend itself to the manufacturing of substrates with complex features. Ultra-thin SU-8 films (300–400 nm) can be photo-patterned to create porous substrates with over 90% free space (Figure 5, B-i).[213] These structural elements with bending stiffnesses as low as 0.104 nN-m (compared to 3000 nN-m for standard 25 μm polyimide thin films) can be compressed and delivered through a needle with a diameter as low as 100 μm (Figure 5, B-ii).[214] Porous SU-8 substrates support the integration of passive sensors for measuring local field potentials and mapping single neurons in the cortex of mice with limited detectable chronic immune response for 12 months.[128,214,215] Mesh-based multielectrode arrays record stable signals with low background noise and RMS amplitudes of $V_{RMS} = 300$ μV and stable recordings from spikes for >6 months. "Syringe-injectable electronics" use several features of SU-8 substrates, including precise film thicknesses, facile patterning, and heterogeneous integration with thin film electronics. The ability to deploy such devices through a syringe offers a minimally invasive implantation technique through a stereotaxic injection. When combined with extreme miniaturization, patterned mesh SU-8 substrates can enable exciting new concepts in electrophysiological recording.

One of the major challenges in implementing SU-8 as substrates in flexible electronics is poor adhesion with metallic interconnects when deposited using conventional deposition methods. This challenge can be overcome through the use of adhesive layers and different deposition methods like ion implantation.[202] While there are several challenges and limitations in using SU-8, it stands uniquely among other substrate materials as a high-

aspect ratio photoresist that is capable of precise direct photopatterning. Additionally, the demonstration of SU-8 mesh electronics makes the interesting proposition of using patterned substrates to create viscoelastic flexible bioelectronic devices that can be implanted using minimally invasive approaches.

2.1.5. Parylene C—A material developed broadly for packaging applications such as microelectronics insulation, implant coatings, and food encapsulants, Parylene C possesses several properties that make it attractive for bioelectronics.[216–223] Parylene C is a chlorinated member of a larger family of poly(*p*-xylylene) polymers that are typically synthesized using chemical vapor deposition (CVD).[216] Parylene synthesis schemes produce vapors by subliming solid dipara-xylylene precursors at ~150 °C.[224] At ~700 °C and 0.1 torr, dimers pyrolyze into the vapor-phase monomer para-xylylene. When this gas encounters a substrate, it forms a semi-crystalline conformal transparent layer of poly(*p*-xylylene). Highly crystallinity and dense packing in Parylene C produce Young's moduli in the range of $E_{\text{Para-C}}$ = 1–3 GPa for both thin and bulk films alike. Parylene C films have been used as substrates for flexible electronics with thicknesses ranging from several nm to 100 μm.[148] The extensibility of Parylene C is typically limited to ε_{yield} = ~4% with $\varepsilon_{failure}$ = ~25–200% at σ_{yield} = 60–80 MPa.[149,225] Parylene C is attractive for use in bioelectronics because it features robust mechanical properties, facile processing and integration with photolithography and etching, and has an established record of low toxicity.[226,227]

Parylene C can be fabricated by micromachining and thermoforming to create both 2D and 3D structural elements for bioelectronics.[228–232] Highlighted in Figure 2, A2, Parylene was used in one of the earliest demonstrations of flexible neural probes with 3D form factors by Suzuki et al. in 2003 through micromachining.[118] This study processed Parylene using dry etching and sacrificial layers to release Parylene structures and create structural pillars used as probes for multi-channel recording from the brain. More recently, a dry-etching technique was utilized to pattern kirigami designs into Parylene substrates that allowed over 800% strain (Figure 6, A).[233] 10-channel platinum multielctrode arrays on kirigami patterned Parylene C can record electrocardiograms of a beating mouse heart with a stable signal amplitude of V_{RMS}~4 mV. Thermoforming has been extensively used to anneal and fix Parylene based devices into form factors for specific applications including sheaths and tubes for neural interfaces and curved surfaces for retinal implants.[234–237] Hara et al. built on previous literature on sheath designs of cortical probes to demonstrate device viability in chronic applications.[238] A signal-to-noise ratio >5.5 was observed that increases over a 22-week post-implantation period as the device integrated with surrounding neurites.

Beyond conventional inorganic thin-film flexible devices, Parylene C can serve as a substrate for organic bioelectronics.[227,239–243] An organic electrochemical transistor array of doped poly(3,4-ethylenedioxythiophene) polystyrene sulfonate (PEDOT:PSS) was fabricated on Parylene C substrates using photolithographic patterning methods and used to measure cortical activity *in vivo* from human epileptic patients (Figure 6, B).[220] Additionally, with a growing interest in bio-optoelectronics, Parylene C became an obvious choice as a substrate for optical devices given its transparent optical properties in addition to robust mechanical and dielectric properties (Figure 6, C).[244–247] In 2020, Kim et al. exploited recent advances in organic semiconductors to fabricate a Parylene C-based

flexible array of organic light-emitting diodes with an *in vivo* demonstration of optogenetic stimulation of the sciatic nerve in mouse models.[248]

A major challenge of fabricating inorganic thin-film electronics on Parylene C involves its thermal instability during deposition and patterning processing as a result of its thermoplastic nature and low oxidative degradation temperatures (T_{deg} ~125°C).[222,249] This can result in the formation of bubbles, cracks, and damage during the manufacturing process. However, if needed, high temperature stable varieties of Parylene such as Parylene HT can be explored as substrates.[235]

2.2. Stretchable Substrate Materials in Flexible Bioelectronics

Elastomers have gained traction as structural materials for medical devices owing to their mechanical flexibility (E < 10 MPa), extensibility(ε_{yield} > 10%, typically well over 100%), and facile processability.[54,250,251] As designing stable biological interfaces with low mechanical impedance mismatch has become important, the role of elastomers has become prominent because of the intrinsic stretchability of several biological tissues.

However, the use of elastomers for implantable bioelectronics as a stretchable substrate is relatively recent due to technical challenges when integrating rigid electronic components with compliant substrates. The last two decades have seen a tremendous rise in the utilization of stretchable substrates to enable a wide range of biological applications such as dynamic bioelectronic cardiac patches, conformal wearable devices, and soft central and peripheral nervous interfaces.[35,252–254] The recent success of stretchable bioelectronics suggests that integrating elastomers with high performance electronic components will continue to grow as commercialization becomes imminent.[34,255,256]

2.2.1. Silicone-based Elastomers—Silicones are named after their inorganic silicon-oxygen backbone, with organic functional groups attached to each Si. Polydimethylsiloxane (PDMS), the most common variety of silicone in bioelectronics, has two methyl groups that are bonded to each Si atom in the polymer backbone (Figure 7). Silicones such as PDMS exhibit thermal stability, chemical resistance in physiological solutions, and dielectric properties (Resistivity ρ_{PDMS} = 4×10^3 Ω-m, dielectric constant ε_{PDMS}=2.3–2.8, degradation temperature T_{deg}=400–650°C), which are attributed to electron delocalization along the backbone and Si-O bond energies of 452 kJ mol^{-1} compared to 348 kJ mol^{-1} in C-C bonds.[257–260] PDMS resists enzymatic biodegradation pathways due to its partial inorganic character.[261] As a result, dozens of medical devices that use silicones have been approved by the FDA including shunts, catheters, contact lenses, soft tissue implants, and stimulation leads.[262,263]

Commercial PMDS silicones (e.g., Sylgard, Ecoflex, and Silbione) are widely used as structural materials in stretchable bioelectronic devices.[264–266] Silicone can be processed into 2D and 3D deterministic architectures and combined with inorganic thin films to confer stretchability to flexible bioelectronic devices.[121,267–270] Minev et al. micropatterned PDMS substrates for use as synthetic electronic dura mater capable of simultaneous electrical measurements and microfluidic drug delivery in neural interfaces for up to 6 weeks.[123] These devices were fabricated using soft lithography for patterning drug

microchannels, plasma-activated covalent bonding for assembly, and thermal evaporation and stencil printing for patterning conductors.

The versatility of silicones was further demonstrated by Afanasenkau et al. in their demonstration of a multi-material 3D printing approach utilized to simultaneously print silicone elastomers and Pt conductive inks that form conductive composites *in situ* (Figure 7, A).[271] At a physiologically estimated maximum operational strain of 20%, the printed devices showed a 10-fold increase in impedance at 20 kΩ compared to the unstrained composite, still being conductive enough to retain device functionality. Through this technique, several neuromuscular interfaces with unique form factors were reported with applications including spinal cord stimulation and recording, sciatic nerve recording, and electromyogram recording.

Materials chemistry has played an important role in designing modified silicone-based materials to overcome limitations of commercial PDMS. Commercial silicones suffer from poor adhesiveness that impacts devices both during processing and deployment.[272] Jeong et al. designed and synthesized soft, stretchable, and adhesive PDMS by adding small volumes (20–40 μL in 10 g of PDMS) of ethoxylated polyethyleneimine (PEIE) with PDMS precursors prior to curing (Figure 7, B). PEIE additives induce heterogeneity and increase sol content, thereby reducing the modulus to $E_{\text{PDMS+PEIE}}$ = 24 kPa from E_{PDMS} = 1 MPa and increasing the force of interfacial adhesion forces to $F_{ad,\text{PDMS+PEIE}}$ = 1.2 N compared to $F_{ad,\text{PDMS}}$ < 0.1 N (Sylgard 184).[273] Compared to PDMS, PEIE-modified silicones increase mechanical compliance and adhesion which can improve integration with ultrafine tissue targets and reduce subsequent fibrous capsule formation *in vivo*.[102] Silicones can also be modified with photoactive groups to achieve photocrosslinkable analogues. Choi et al. reported a new class of photocrosslinkable silicones that use urethanes with pendant methacrylate groups as photoactive groups.[274] Photocrosslinkable silicones were originally designed as materials for high resolution nanometer scale patterning and soft lithographic molding. However, photocrosslinkable silicones could also be used as structural materials with micron-scale features for stretchable bioelectronics.

Devices interfaced with regenerating or growing tissue can experience small stresses and rates of strain (~1 mm/day) over long periods of time as the tissue expands. Conventional silicone elastomers are too stiff to operate in this context.[275] However, this can be addressed through engineering an increased viscoelastic response in PDMS elastomers. This was accomplished by designing a chemically modified PDMS with isophorone bisurea (IU) and *4,4′*-methylenebis(phenyl urea) (MPU) and blending PDMS-IU with PDMS-$IU_{0.6}$-$MPU_{0.4}$.[276–278] By balancing the dynamic bonding of IU and hydrogen bonding of MPU, the PDMS blend is capable of a Young's modulus of 0.4 MPa at a strain rate of 50% s^{-1}. This material was integrated with a plasticized PEDOT:PSS conductor for stable chronic neuromodulation and nerve growth monitoring tested on the sciatic nerve of fast growing rats over a period of 4 weeks (140% increase in nerve diameter) (Figure 7, C).

2.2.2. Block Copolymer-based Elastomers—Block copolymer (BCP)-based elastomers are polymer networks with physical crosslinks that have been used in medical devices, such as catheters, drug delivery systems, and materials for regenerative medicine.

[279–284] Polystyrene-based ABA triblock polymers are a prominent example of this molecular architecture, in which polystyrene A blocks flank a central B block with variable composition.[285] Typically, the middle block chain is composed of an aliphatic monomer, resulting in two rigid hydrophobic polystyrene blocks linked by a flexible polymer chain. However, any reasonable combination of A and B blocks that are immiscible with one another can serve as ABA triblocks. Populations of ABA triblocks self-assemble into rigid domains of A blocks that serve as physical crosslinks with flexible interstitial phases that are rich in B blocks.[286,287] BCP-based elastomers possess tunable mechanical and viscoelastic properties that can be optimized by varying the volume fraction and lengths of the A and B blocks. This controls the morphology and volume fraction of the rigid microdomain blocks, ϕ_m, of the physically crosslinked species, A.[285,288] The higher volume fraction of the rigid microdomains understandably produces elastomers with higher elastic moduli.[289] For instance, ABA triblocks composed of polystyrene (A) and polybutadiene (B) can be modulated to form both viscous polymer lubricants and robust physically crosslinked elastomeric polymer networks by varying ϕ_m.[255–257] Polymer networks with physical crosslinking expands the range of processability to include casting, extrusion, electrospinning, and molding.[284,290–293] The combination of processability and unique mechanical properties makes them useful as substrates in bioelectronics.

In Figure 2 B2, we see an early use of BCP-based elastomers, specifically poly(styrene-*b*-butadiene-*b*-styrene) (SBS), as a substrate for a highly stretchable transistors for wearable tactile sensing applications.[122] The authors employ electrospinning to cast a film of the SBS elastomer, and all device elements, including the Au nanosheet conductor, PH3T polymeric semiconductor, and PEG-based ionic dielectric, were integrated using a stamp transfer printing technique.[122] This work demonstrates a robust integration technique for fabricating devices on BCs. Molina-Lopez et al. demonstrated the versatility of processing BCP-based elastomers by fabricating a multilayer inkjet-printed synaptic transistor arrays on a styrene-ethylene-butylene-styrene (SEBS) substrate for use as low voltage (~1 V) wearable devices.[294] The ionic nature of these transistors closely mimic the synaptic behavior of neurons, making them exciting devices for neural interfaces and neuromorphic processing. BCP networks with physical crosslinks exhibit significant hysteresis compared to elastomers with chemical crosslinks.[284] This can be an undesired characteristic for stretchable electronic systems that experience dynamic loading conditions. Proposed solutions for this issue involve chemically crosslinking the BCP to create more rigid anchors in the polymer network.[295,296]

2.3. Ultracompliant Substrate Materials in Flexible Bioelectronics

Matching the modulus of the substrate at the tissue-device interface is a dominant principle when designing devices for seamless integration with excitable tissue.[297,298] In many instances, the mechanics and chemistry of electronically excitable soft tissues are dominated by the extracellular matrix.[299–303] Therefore, integrating active electronic components to materials that mimic this native environment could ostensibly offer advantages. Specifically, integrating sensors, traces, and other active components on ultracompliant substrates, such as hydrogels, is an important step in this evolution.[59] Hydrogels have been used extensively as coatings for rigid silicon-based neural implants and 1D recording wires to modulate the

chemistry at the tissue-device interface, but to date have seldom been used as structural materials.[304–310] Hydrogels are challenging to process into mechanically robust electronic devices since they are fundamentally incompatible with many microfabrication strategies that require vacuum, elevated temperature, or exotic organic solvents.[311–313] New concepts in materials processing strategies and heterogeneous integration catalyzed recent advances in hydrogel-based bioelectronics.[314–320]

With the development of intrinsically conductive polymers capable of electropolymerization, such as PEDOT, *in situ* polymerization of conductive traces within hydrogel substrates has been explored. Sekine et al. electropolymerized PEDOT on a microfabricated Pt pattern within a newly crosslinked agarose network (Figure 8, A-i).[321] Repeated electrochemical actuation using the same set-up is employed to peel off the hydrogel easily. This simple technique is generalizable to any crosslinkable hydrogel (Figure 8, A-ii). Ido et al. improve the conductivity of PEDOT electrodes in hydrogel-based networks by pre-polymerizing PEDOT on Pt traces in acetonitrile, a solvent system that is optimized for electropolymerization as opposed to hydrogel processing.[322] This can be followed by casting the hydrogel and PEDOT solution and following the same procedure laid out previously. These procedures have been used to fabricate advanced electronic tissue engineering platforms and wearable sensors.[323]

Another important development that enabled the fabrication of such hydrogel-based devices was an aqueous phase transfer printing process developed by Wu et al.[324] They demonstrated a versatile technique to transfer print microfabricated metal traces from wafers with water-soluble sacrificial layers to aqueous pre-swollen hydrogels. This is done by photopatterning the metal traces on a polyacrylic acid (PAA) sacrificial layer. Hydrogel precursors are then cast and cured on the substrate before releasing the sacrificial layer.

This method was adapted by Huang et al. to fabricate a multielectrode array on polyethylene glycol-dopamine (PEG-Dopa) hydrogels for a peripheral nerve interface (Figure 8, B).[126] As a widely used hydrogel system for a variety of biomedical applications, PEG-based hydrogels are a natural choice for use in bioelectronics.[325–328] The catechol motifs found in dopamine improve interfacial adhesion with Parylene C insulating layers, thus facilitating transfer printing.[329,330] Multi-electrode arrays fabricated using this technique were used as peripheral nerve interfaces to record from the dorsal root ganglia in feline models.

2.3.1. Tough Hydrogels—Most hydrogel networks have polymer fractions of $\phi_2 <$ 0.1 and therefore exhibit small elastic moduli because of the volumetric dilution of crosslinks. The molecular topology endows networks with mechanical compliance at the expense of toughness with tensile toughness on the order of 10 J m^{-2} compared to 10,000 J m^{-2} for typical silicone-based elastomers.[157,331] The typical brittle properties of hydrogels limit extensibility and therefore bound the potential use as structural materials for flexible bioelectronic devices. However, the toughness of hydrogels can be increased by incorporating interpenetrating double networks. For example, polyacrylamide (PAAM) and alginate double network hydrogels exhibit maximum strains of ε_{max} >2000% and fracture energies of ~9000 J m^{-2} (Figure 9, i–iii).[157] This toughness is a result of the combination of a covalently crosslinked network polyacrylamide providing stability by remaining intact

on deformation and the mobile ionically crosslinked alginate that reversibly unzips on deformation.

Lin et al. demonstrated the use of the PAAM-Alginate double network (DN) hydrogel-based hybrid electronic and diffusive drug delivery devices demonstrated as a proof-of-concept for wound healing applications (Figure 9, iv).[158] The conductive traces are preformed titanium wire that is bent into serpentine structures to enable stretchability. Additionally, they demonstrate a rigid-island based strategy to bond conventional electronic components to the hydrogel substrate where the electronic components are encapsulated by PDMS and bonded to the hydrogel with a silanized glass slide as an intermediary structure. This method is a promising steppingstone in designing hydrogel-based stretchable electronics. Beyond Ti wires, conductive elements could include transfer printed metal films, electrodeposited conducting polymers, or other structures, such as 3D printed colloidal metals.

Other approaches to develop tough hydrogels have involved innovation in supramolecular polymer networks, nano-clay hydrogel composites, and other combinations of interpenetrating networks.[332–335] While these strategies have resulted in materials with promising properties for application in bioelectronics, there has yet to be broad adoption of tough hydrogels as structural materials in flexible bioelectronic devices, with a few notable exceptions.[29,336,337]

2.4. Structurally Adaptive Substrates for Bioelectronics

2.4.1. Biodegradable Polymers—Flexible bioelectronic devices fabricated on transient substrates have several compelling advantages as medical implants. In principle, transient devices can be implanted and resorbed within the body without the need for secondary extraction surgeries as in the case for non-degradable systems. To date, transient electronics have been integrated with naturally derived materials such as silk fibrion, cellulose, gelatin, and collagen, and synthetic polymers such as poly(lactic-co-glycolic acid (PLGA), polyurethanes, and poly(*1,8*-octanediol-*co*-citrate) (POC).[130,338–342] These polymers possess a range of varying mechanical properties and degradation characteristics engineered for unique applications. A common trait of all biodegradable polymers in implantable electronics is that their degradation by-products must be non-toxic to prevent an inflammatory response.[343–347]

Biologically Derived Biodegradable Polymers: Silk fibroin is a high molecular weight protein isolated from the cocoon of the *Bombyx mori* that is solution processable into various form factors and exhibits tunable mechanical properties, degradation characteristics, and crystallinity thus making it an attractive choice as a structural material for transient bioelectronics.[348–356] The crystallinity and β-sheet content can be tuned by processing treatments and post-processing conditions, such as treatment with methanol.[357–360] Crystalline methanol treated films deposited using a layer-by-layer technique are brittle with a mechanical modulus of 6–8 GPa, ultimate tensile strength of 100 MPa, and exhibit slower degradation kinetics compared to their amorphous silk fibroin counterparts.[361–363] The high tensile strength of silk films allows for them to serve as ultrathin substrates in flexible bioelectronic devices that are intended to conform to curvilinear tissues.[364,365] On the other

hand, an acetone solvent induced sol-gel transition can be used to fabricate transparent silk fibroin hydrogels with compressive moduli ranging from 0.4 to 11.5 kPa.[366] Lastly, silk has served as a particularly unique material in soft electronics as it has been demonstrated that cross-linking in silk can be controlled by electron-beam radiation.[367,368] This has allowed silk to be directly exploited as a lithographic resist that can be processed using only water.[367]

Biologically derived structural polymers such as gelatin and collagen can processed into films and used as substrates in bioelectronics.[369–373] Through the use of additives such as glycerol, citric acid, and glucose, Baumgartner et al. process tough gelatin biogels that can accommodate strains of up to ε_{max} = 300%. Conductive zinc traces were defined through laser patterning to fabricate a wearable sensor capable of monitoring a number of different parameters such as temperature, humidity, and strain.[130] Mammalian collagen-based glutaraldehyde cross-linked hydrogels have also been used as substrates.[374] The extent of crosslinking is controlled to demonstrate tunable degradation properties, and a transfer printing method is optimized to fabricate multilayer device stacks on collagen-based substrates.

Synthetic Biodegradable Polymers: Aliphatic polyesters such as polylactic acid (PLA) and poly (lactic-co-glycolic acid) (PLGA) were among the first synthetic polymers investigated as biodegradable substrates for potential applications in bioelectronics. From extensive characterization in drug delivery applications, modulation of degradation profiles of PLA and PLGA is well understood and has been extended to biodegradable electronics applications.[341,375,376] PLA substrates have been used to fabricate bioresorbable stents with integrated bioelectronic sensing of temperature and arterial blood flow.[377] Transfer printing methods have been developed to fabricate complex Si-based semi-conductor devices on PLGA substrates.[378] Transient silicon nanomembrane devices have been used for high resolution spatial mapping of cortical activity, monitoring intercranial pressure in rats, and wireless bioresorbable cardiac pacemakers.[379–381]

Biodegradable elastomers have also garnered interest as substrate materials for bioresorbable electronics. Poly(1,8-octanediol-*co*-citrate) (POC) is one such biodegradable elastomer initially developed for tissue engineering applications that has been explored as a substrate for bioelectronics.[382–385] Silicon nanomembranes linked into functional devices can be transferred to POC for use in stretchable pH sensors and wearable electrophysiological sensors.[386] More recently, Choi et al. developed a bioresorbable dynamic covalent polyurethane (b-DCPU) elastomer for use as a substrate in an electronic stimulation device for neuromuscular regeneration (Figure 10).[340] Thermally activated dynamic bonding of the polymer network enables robust self-adhesion (~500 J m^{-2}), and with inorganic device components, such as Si, Mo, SiO_2, and Mg (>850 J m^{-2}), facilitates facile processing of stable devices. Additionally, with a controllable elastic modulus between 0.5–3.8 MPa and yield and failure strains of 25% and 170% respectively, b-DCPU devices are able to withstand the dynamic environment around the sciatic nerve in mice. The device reliably stimulates and records *in vivo* for ~30 days, with complete bioresorption within 6 weeks.

2.4.2. Mechanically Adaptive Polymers—Stiffness tuning or softening polymers are a compelling choice as substrates in applications requiring the insertion of bioelectronics into soft tissue, as in the case of cortical probes. As described previously, soft neural probes with comparable mechanical properties to cortical tissue show lower inflammatory response and glial scarring compared to stiffer implants.[387–393] However, soft cortical probes must be able to withstand the insertion forces without buckling. Considering the insertion of a cortical neural interface where forces up to ~12–40 mN are needed to penetrate the dura mater of the brain, a material capable of undergoing a stiff-soft-transition offers unique advantages with a rigid regime during insertion and soft regime during operation within the brain.[394–398] This problem has been tackled using several approaches, including hydration-induced softening, rapidly dissolving stiffeners, shape memory polymer transitions, and stiff nanofiber and hydrogel composites.[399–405]

A seminal breakthrough towards designing materials capable of significant change in mechanical modulus was reported by Capadona et al.[406] Bioinspired nanocomposites of stiff cellulose nanofibers (1.43 GPa) in a soft poly(vinyl acetate) (PVAc) matrix undergo a chemically regulated transition from 4200 MPa to 1.6 MPa upon hydration. Specifically, sulfate groups are introduced onto cellulose nanofiber surface in order to mediate their interaction through competitive hydrogen-bonding with solvent molecules. This material has been investigated for use as substrates for neural probes, showing that the softening material shows significantly lower neuroinflammatory response and improved proximity of neural cells in chronic use post-implantation in comparison to stiff materials.[394,407] While this material has shown great promise as an adaptable substrate for neural probes, it presents challenges in integration with microfabrication strategies as it is incompatible with typical wet chemicals and temperatures exceeding 100 °C. However, Hess-Dunning et al. presented a microfabrication strategy involving utilizing a conformal Parylene C protective coating prior to proceeding with standard microfabrication methods.[408] Multielectrode arrays fabricated using this procedure were implanted in the primary motor cortex of rats and showed stable recording capability of neural responses (mean SNR ~4) over a period of 16 weeks.

An alternate approach towards designing mechanically adaptable polymers has been through softening shape memory polymer (SMP) networks on the exposure to elevated body temperatures. The highly selective thiol-ene chemistry has been utilized to design shape memory polymers capable of such mechanical transitions.[409,410] A similar thiol-ene/acrylate polymer system was engineered by Ware et al. in 2012 for use as a biocompatible softening substrate for responsive neural interfaces.[411–415] This thiol-ene/acrylate polymeric system is composed of tricyclodecanedimethanol diacrylate and 1,3,5-triallyl-1,3,5-triazine-2,4,6(1H,3H,5H)-trione monomers that are polymerized under UV light in the presence of a photoinitiator, 2,2-dimethoxy-2-phenylacetophenone. As a result of challenges in using conventional electronics processing techniques with this SMP as a substrate, a transfer-by-polymerization method was used to transfer metallic traces from a glass-Parylene C substrate by exploiting the weak adhesion of Parylene C on glass, followed by laser micromachining to define the form factor. Ware et al. illustrated a reduction in elastic modulus from 1 GPa to 18 MPa upon heating to the physiological temperature of

37 °C. Through successful recording of brain activity for 4 weeks in mice, Ware et al. demonstrated a unique approach to solving the challenge of designing probes stiff enough to be inserted into soft tissue while remaining highly compliant post-implantation.[416]

2.4.3. Adaptive Liquid Crystal Elastomers—Liquid crystal elastomers (LCEs) are a unique class of LCP that possess a combination of stretchability and polymer chain self-organization that can be used more for shape-changing functional bioelectronics (Figure 2, D4). LCEs are crosslinked polymeric networks with mesogen groups as side chains that confer smectic arrangements.[417–421] Some LCEs possess the unique capability of pre-programmed field-responsive shape change based on the alignment of the polymer chains during the processing of the LCE film.[422–428] In addition to this active functionality, LCEs still possess the high thermal and chemical resistance and mechanical robustness of conventional LCP.[429] Kim et al. showed the first instance of stimulus-responsive 3D electronics systems that are based on LCE substrates by demonstrating a morphing helical antenna.[129] To achieve this, the LCE precursors were photopolymerized after aligning azobenzene-dye molecules to program the shape change. The 3D transformation of the structure occurs through an order-disorder transition at temperatures below the cross-linking temperature. Similar processing methods were used to fabricate helical LCE-based multichannel cables integrated with a 16-channel nerve cuff electrode array for peripheral nerve interfaces and deployable cortical probes.[430]

As a material with rapidly growing interest for applications not just in bioelectronics but also soft robotics, there is significant progress being made towards processing and patterning methods of LCEs. While early applications of LCEs utilized techniques such as mechanical loading or magnetic fields to align the polymer chains within the LCE network, Ware et al. demonstrate a unique materials chemistry that enables highly sensitive photoalignment of defined volumes within the LCE polymer network.[431] Since this work, voxelated LCEs have been utilized for the 3D printing of structures capable of programmable shape change.[432,433] Additionally, a similar platform has also been used to engineer LCE films with localized domains with varying stiffnesses.[434] There is significant opportunity in utilizing the progress in processing LCEs to designing unique functional and adaptive bioelectronics.[435]

3. Packaging and Barrier Layers for Flexible Bioelectronics

3.1. Overview of Technical Challenges

Implantable electronic devices require appropriate insulation from the external environment to maintain reliable function. Liquid water, dissolved oxygen, ions, water vapor, and other small molecules can diffuse through barrier layers or defects in barrier layers, accumulate near sensitive electronic components, and ultimately contribute to device failure. Oftentimes, it is the performance of the barrier and packaging layers that determines the functional lifetime of implantable electronic devices.[78,436,437] Packaging strategies and materials for barrier layers for implantable electronics can be informed from innovations in more mature industries such as consumer electronics.[438,439] However, flexible electronics intended for use in biomedical applications afford significant additional challenges. Implanted

devices may be continuously exposed to mechanically dynamic environments, elevated temperatures, and aqueous solutions with high concentrations of highly mobile and potentially debilitating ions such as sodium.[440–442] Furthermore, chronically implanted devices are subject to enzymatic reactions and other biological milieu that can contribute to additional failure modes.[443] Additionally, barrier layers of implantable electronics must encapsulate the entire device. From a materials chemistry perspective, the ideal barrier layer is composed of a material(s) that is (i) insulating, (ii) impermeable to moisture and ions through highly conformal and low defect density films with negligible diffusivities, (iii) stable in the presence of proteins and other biomolecules, (iii) highly mechanically compliant, interact (or not) with the surroundings in the desired manner, and lastly, (iv) able to maintain these properties over the functional lifetime of the device.

There have been a variety of materials and combinations thereof that have been investigated as barrier layers for flexible and stretchable bioelectronics. Materials that have been tested include metallic thin films like Al and Ti, ceramic oxides and nitrides like SiO_2, Al_2O_3, HfO_2, Si_3N_4, and TiN, and organic polymers like Parylene C, polyimide, and a variety of dielectric elastomers.[182,217,444–451] These materials have been used both on their own and in composites in attempts to protect electronic devices from contaminants found in the physiological environment. The rigid materials (inorganic oxides, nitrides, and metals) achieve a desired flexural modulus through the use of ultrathin layers that enable flexibility but not stretchability. On the other hand, the mechanical properties of the organic barrier layers are determined by the intrinsic properties of the polymer, allowing for both flexibility and stretchability. Rapid soak tests to evaluate water and ion penetration have shown that ultrathin ceramic layers perform significantly better than commonly used polymeric barrier layers. In the next few sections, the advantages and drawbacks of each of these materials will be presented, in an effort to highlight the importance for careful materials selection based on the application of the bioelectronic system and the immense scope for innovation in flexible and stretchable barrier layers.[452,453]

3.2. Techniques to Measure Barrier Layer Performance

Several standardized methods have been established to evaluate the performance of barrier layers (Figure 11). For flexible barrier layers in bioelectronics, a common method for the evaluation of barrier function involves soak tests in a solution of phosphate-buffered saline (PBS), to mimic typical ionic concentrations of biofluids. Often, these tests are performed in an accelerated format at higher temperatures to extrapolate the characteristics of the barrier layers at long timescales. The Arrhenius relationship can be leveraged to estimate true operational time to failure from the accelerated soak tests by calculating the acceleration factor.[469–471]

$$AF = Q_{10}^{\frac{T_{accelerated} - T_{target}}{10}}, \tag{3}$$

where Q_{10}, $T_{accelerated}$, and T_{target} refer to the quantity by which the reaction rate increases for a 10°C increase in temperature, the accelerated temperature at which the test is conducted, and the target operational temperature of the device.

Another common qualitative approach researchers have used involves depositing the barrier layer over arrays of metals that are known to have high reactivity with water, such as Mg or Ca.[450,472] The arrays are then subject to aqueous conditions and monitored optically over time. This method, while qualitative, provides a simple visual way to characterize barrier performance.

The method described above can be modified to provide quantitative information on the Water Vapor Transmission Rate (WVTR), one the most common metrics measured in g m^{-2} day^{-1} used to evaluate barrier layers.[473] Commonly referred to as the 'Ca Test', the electrical conductivity or optical transmittance can be measured to precisely measure very small rates of water vapor permeation.[474] A more common method for measuring WVTR requires specialized instrumentation (Ametek MOCON, Minnesota, USA) that uses precise moisture sensors to measure the permeation of water vapor through barrier layers. Although these devices are widely used in the electronics packaging community, they are limited by their minimum measurable WVTR of ~10^{-3} g m^{-2} day^{-1}.[475] Apart from the Ca test, multiple research groups have created their own experimental set-ups to measure ultra-low WVTR (lower than 10^{-6} g m^{-2} day^{-1}) values by employing tritiated water that can be mapped using a scintillation counter.[476,477] While WVTR values are an important metric to evaluate biofluid barrier, in practice, the same material can show a wide range of WVTRs because the fabrication method and defect densities will greatly determine fluid permeation.

The temporal evolution of insulating properties of barrier layers can be evaluated during soak tests by measuring the electrical properties of test structures.[455,478,479] Electrochemical Impedance Spectroscopy (EIS) is valuable tool to evaluate multiple aspects of barrier layer function because of its sensitivity to changes in dielectric properties. By modeling the system as a combination of resistors and capacitors, the EIS spectrum can provide information on barrier function and the degree of delamination between the substrate and barrier layer.[480] The percentage of water uptake can be described through the following relationship:

$$\phi = k \quad \frac{\log(C_t/C_0)}{\log \epsilon_W}, \tag{4}$$

where C_t, C_0, ϵ_W, and k refer to capacitance at time t, capacitance of the dry film, dielectric constant of water, and swelling constant of the film respectively.

3.3. Polymeric Barrier Layers

High-performance polymeric barrier layers for use in flexible bioelectronics is a region of active investigation. Polymers typically have a significantly lower flexural rigidity than inorganics and can be designed with intrinsic stretchability, making them a promising candidate for barrier layers. High-modulus inextensible plastics such as polyimide, Parylene C, SU-8, and LCPs demonstrate superior barrier function compared to low-modulus amorphous elastomeric polymers such as PDMS, styrene-ethylene-butylene-styrene (SEBS), and polyisobutylene (PIB). However, several of these materials continue to find successful use in applications that play to the material strengths. A wide variety of organics have been used and tested as barrier layers including several of the polymers discussed under

the section entitled *Substrates and Structural Materials*. However, even the gold standards of polymeric barrier layers (i.e. LCP and Parylene C) fall short in barrier function in comparison to many inorganic materials including oxides and nitrides (e.g. SiO_2, Al_2O_3, and SiN_3).[78,436,437] In this section, we present a discussion on the different types of polymeric barrier layers, their advantages and shortcomings, and most importantly, opportunities for designing the next generation of this important class of materials.

3.3.1. Flexible Polymers as Barrier Layers—Inextensible high-modulus polymers derive their barrier functionality from the packing density of the polymer chains within a film, with a greater density corresponding to lower diffusivity of moisture and ions across the barrier.[482–486] Notably, the high mechanical modulus and inextensible nature of polymers can also be attributed to the polymer chain packing within a polymer network. The packing of polymer chains is predominantly controlled by two parameters: crystallinity and crosslinking density.[487–489] Among the common inextensible polymeric barriers that will be discussed in this article, Parylene C, polyimides, and LCPs are crystalline in nature, and SU-8 is amorphous but highly crosslinked.[490,491] The crystallinity in polyimides, Parylene C, and LCPs arises from the ordering of long linear polymer chains, with rigid aromatic components contributing to increased alignment and crystallinity.

Poly(*4,4*-oxydiphenylene-pyromellitimide) (PMDA-ODA; Kapton, Dupont Wilmington DE, USA) is a polyimide used as a structural material for flexible electronics, but less often as a barrier layer due to its susceptibility to hydrolytic degradation.[492,493] In contrast to Kapton polyimides, biphenyltetracarboxylic bianhydride/para-phenylenediamine (BPDA-PPD; PI2611, U-Varnish-S) is a polyimide that is more commonly used as a barrier layer. PI2611 (HD Microsystems, NJ, USA) films (9 μm in thickness) have WVTR of 6 g m^{-2} day^{-1}.[456] Devices encapsulated in BPDA-PPD can operate for up to 12 months *in vivo* and >20 months *in vitro*.[493–495]

Parylene C films show a greater degree of crystallinity than Kapton or PI2611 with a WVTR as low as 0.08 g m^{-2} day^{-1}.[496] This increased crystallinity is attributed to alignment of chlorinated *para*-xylylene monomers. Approximately 70–90% of neural implants encapsulated in Parylene C barrier layers retain function after 29 weeks in an *in vitro* soak test as measured by EIS (10% decrease in relative impedance).[455] Additionally, accelerated testing of Parylene C suggests that devices can maintain function for >1 year in physiological buffers at 37°C. With a lower WVTR than PI, Parylene C encapsulated devices promise more stable device for long-term use. Other accelerated lifetime tests have also shown that a 10 μm thick Parylene C encapsulated devices have retained function for 117 days at 75 °C, indicating around a 4.5-year lifetime at physiological temperatures.[454] However, the major roadblock in implementing Parylene C-based encapsulation is its poor adhesion with several substrates and metals commonly used in bioelectronics.[249,497] Techniques such as silanization, O_2 plasma treatment, mechanical interlocking, and annealing improve adhesion and reduce risk of delamination between layers.[149,498–500]

LCP are a promising candidate for encapsulation materials because the high degree of crystallinity results confers excellent barrier properties. In an effort to compare barrier function of LCP to PI and Parylene C, Lee et al. performed an accelerated lifetime test in

a physiological buffer solution at 75 °C where the PI and Parylene C devices fail in 66 and 117 days respectively while the LCP devices are functional for >300 days.[454] LCP are most commonly purchased as pre-formed films and can be bonded with like films using thermal-press bonding.[143,501,502] This ability makes LCP attractive for applications where it serves as both substrate and barrier as a monolithic encapsulation.

3.3.2. Dielectric Elastomers as Barrier Layers—Dielectric elastomers are a viable barrier layer owing to the combination of dielectric properties and extensibility. Silicone-based rubbers like PDMS and Silbione, SEBS, and PIB have all be used as extensible barrier layers.[449] However, the molecular structure that is a necessary meso-scale component of extensibility in elastomers is a liability with respect to barrier properties. More specifically, the characteristically high free volume of elastomers, which confers elastomeric properties also provides a larger mean free path for diffusion and will make the material susceptible to high moisture and ionic permeation rates.[503–505] This is primarily because elastomeric polymeric networks are amorphous and low density as a result of low crosslinking densities. A comprehensive study presented by Floch et al. employed electrochemical impedance measurements to evaluate the fundamental limits of dielectric elastomers (PDMS, PIB, and SEBS).[449] After soaking the test structure in PBS for one week, the impedance of the elastomers falls by 10^2–10^6, suggesting water and ion penetration into the polymer network. Additionally, the dielectric elastomer required a minimum thickness of 40 μm to maintain electric function for 1 year of implantation, reducing the benefits of using elastomers by increasing the flexural rigidity of the material.

While these results indicate that elastomers are not an ideal material for biofluid barriers, it is valuable to recognize the scope for innovation in materials chemistry to develop elastomeric materials with improved barrier properties. Additionally, there is an important role that elastomeric composite multilayer barriers can play that is highlighted in Section 3.5.

3.4. Ceramic Barrier Layers

Inorganic materials are the dominant barrier and packaging materials for conventional rigid electronics. While macro-scale and some micro-scale electronics have used metallic barriers like Ti, ceramic oxides and nitrides like SiO_2, Si_3N_4, Al_2O_3, HfO_2, and TiN have become the most commonly used barriers in microelectronics.[506–509] In addition to being good insulators, the high packing density of these ceramics enable extremely small water and ion permeation rates.[510–512] As the interest in mechanically compliant electronics has increased, researchers have found innovative ways to use similar materials and fabrication methods to create flexible barrier layers. Taking advantage of the cubic relation between thickness of a material and its flexural rigidity, numerous studies have created flexible barrier layers by depositing thin layers of these ceramics. However, the square relationship between time and length scales for diffusion becomes an important design consideration. While thin inorganic barriers with a low flexural rigidity improve the mechanical compliance of the system, they suffer a higher fluid and ion permeation as a result of the lower diffusion length. It is important to note here that thin inorganic materials, while flexible, are not intrinsically extensible. Additionally, the ceramics used

as biofluid barriers typically degrade through hydrolysis and extremely thin layers run the risk of significantly losing their barrier function over their lifetime.[513–515] However, they are compelling options owing to their ease of fabrication and integration with conventional fabrication. Advances in chemistry and fabrication methods have the potential to leverage the benefits of high-performance inorganic barrier layers with the desired mechanical compliance provided by polymers.

Ceramic thin films, most commonly oxides and nitrides, have been investigated extensively as barrier layers for flexible electronics, with the promise of superior barrier function compared to organic materials. These thin films can be fabricated using a variety of synthesis schemes, such as chemical vapor deposition (CVD), atomic layer depostion (ALD), and thermal evaporation. An important process parameter to note is the deposition temperatures for each of these processes. Plasma-enhanced CVD (PECVD) and ALD are often the most widely used synthesis techniques used in flexible barrier layers because of their low processing temperatures (150–400 °C).[461,516,517] This can often be crucial, depending on the process design, for bioelectronics commonly use polymeric materials that are unstable at high temperatures. With a more controlled process and highly conformal film production, ALD films have shown a significantly lower WVTR than CVD films.[481] However, both CVD and ALD face the challenge of having a non-trivial defect density that significantly lowers the barrier function as a result of impurities, and chemical effects during the deposition. While thermally grown oxides show a significantly lower defect density, it can be challenging to transfer these films and integrate them with bioelectronics.

3.4.1. Silicon-based Barrier Layers—Si-based oxides and nitrides have been widely explored for their high degree of integration with traditional electronics fabrication strategies. SiO_2 and SiN_x barrier layers can be synthesized through all the processes mentioned earlier. PECVD SiO_2 is typically synthesized with a Silane or Disilane (SiH_4, Si_2H_6) precursor in the presence of nitrous oxide (N_2O) and nitrogen gas (N_2) at approximately 350 °C at low pressures (0.2–1 torr).[481] Optimized barrier layers yields WVTR as low as 0.1 g m^{-2} day^{-1}.[458,481] However, these films are affected by the significant defect densities produced by the PECVD process. Thermally grown SiO_2 has a significantly smaller defect density compared to oxides prepared from deposition techniques thus achieving superior barrier function compared to films prepared using deposition techniques, with an ultra-low WVTR of 2×10^{-8} g m^{-2} day^{-1} (100 nm film).[457,459] Furthermore, recent studies have overcome the processing and integration challenges of thermally grown SiO_2 by developing a physical transfer method.[457] This method involves the thermal oxidation of Si at ~1100 °C on device-grade Si wafers followed by etching techniques and mechanical grinding of the wafer from the bottom to expose SiO_2 films for device encapsulation. Accelerated lifetime tests show that devices integrated with t-SiO_2 barriers dissolve at a rate of ~15 nm/year, indicating a multi-decade functional implanted lifetime.[437,457] Figure 12 shows a t-SiO_2 film integrated with a Si nanomembrane transistor array and polyimide substrate to form capacitively coupled interfaces with cardiac tissue and record electrocardiograms. Although t-SiO_2 has been used only as a barrier on one side of this device, t-SiO_2 can also be used for completely encapsulating thin-film electronic devices.[185]

SiN_x thin films are most commonly used as a capping secondary layer on a SiO_2 layer to improve the barrier function and reduce the water and ion permeability. SiN_x can be synthesized using CVD and ALD techniques and are often done in plasma-enhanced conditions to lower the process temperatures. The CVD process to synthesize SiN_x uses a Silane precursor (SiH_4) in the presence of Ammonia (NH_3) and Nitrogen gas (N_2) at low pressures (~1 torr) with an operating temperature of approximately 350 °C.[518,519] As a result of a higher density than SiO_2, PECVD SiN_x has shown WVTR as low as 0.01 g m^{-2} day^{-1}.[520] A 200 nm thick LPCVD SiN_x used as an encapsulation layer for NMOS transistors maintained stable electrical performance for just under 2 days at 96°C.[447] These LPCVD SiN_x films were found to dissolve at a rate of 0.3 nm day^{-1} at 37°C, explaining the inferior barrier performance compared to SiO_2. There is also interest in used plasma enhanced ALD techniques to deposit SiN_x layers with a lower defect density which have intrinsic WVTR properties as low as 10^{-6} g m^{-2} $day^{-1}$for a 10 nm layer.[461]

Other approaches to utilizing Si-based materials as barrier layers involve silicon carbide (SiC) and metal silicides such as titanium silicide ($TiSi_2$).[448,521,522] Diaz-Botia et al. presented a unique SiC-based neural interface with amorphous SiC as the barrier material and locally doped SiC as the conductive electrodes.[522] An accelerated aging study performed at 96°C showed that an amorphous SiC film of 360 nm thickness had leakage currents lower than 70 nA cm^{-2} after 60 hours of aging. The excellent barrier properties were further supplemented by extremely slow dissolution rates compared to SiO_2 and SiN_x.[523,524] Li et al. demonstrate another approach to stable barriers with low dissolution rates through interfacing a TiS_2 layer on active p-doped Si devices.[521] This was achieved by depositing titanium on the Si followed by thermal annealing. Accelerated lifetime analyses performed at 96°C showed that a Si/TiS_2 (140 nm/50 nm) provided stable encapsulation for a period of 21 days.

3.4.2. Al_2O_3 Barrier Layers—ALD Al_2O_3 is among the most prevalent materials under investigation for flexible barrier layers, as a result of its high packing density, low pinhole and defect densities, and its chemical inertness.[525–527] In the ALD process, Al_2O_3 is typically fabricated using a sequential self-limiting reaction in a chamber with alternating flows of trimethylaluminum $(CH_3)_3Al$ followed by H_2O or O_3.[528,529] This process can be undertaken at much lower temperatures than CVD synthesis methods (80–200 °C). The controlled reaction results in a much lower defect density, resulting in superior barrier properties.[530] Al_2O_3 barriers synthesized by ALD methods have shown WVTR values in the range of 10^{-3} to 10^{-6} g m^{-2} day^{-1} (t = 25–100 nm).[462,531]

3.5. Multilayer Barrier Layers

Multilayer barriers have a significantly better barrier function than single layers by relieving the detrimental effects of critical defects, such as pinholes and grain boundaries. This can be intuitively understood as an increase in complexity of the path a water molecule or ion needs to take to penetrate the barrier. Additionally, the multilayer barrier can be designed with materials with different strengths, achieving a more universal barrier. Researchers have pursued a variety of composite strategies, from ceramic nanolaminates, to inorganic-organic multilayers, to organic multilayers.

Ceramic nanolaminates have shown among the highest performance in terms of barrier function in flexible electronics. For instance, alternating 2 nm layers of Al_2O_3 and ZrO_2 synthesized using ALD with a total height of 30 nm have shown strong barrier function with a WVTR of lower than 2×10^{-4} g m^{-2} day^{-1}.[465] Additionally, Al_2O_3/SiO_2 multilayers deposited by ALD with an 86 nm height have WVTRs as low as 5×10^{-5} g m^{-2} day^{-1}.[476] While many of these studies have been performed in the context of optoelectronics and OLEDs, there are a few instances of ceramic bilayers in flexible bioelectronics. Song et al. reported a flexible biofluid barrier comprised of a thermally grown SiO_2 layer capped with a layer of HfO_2 deposited using ALD that extends device lifetimes by >10x compared to single layer of thermally grown SiO_2 by slowing the dissolution rate of the SiO_2 layer, the primary failure mode of thermal SiO_2 barriers.[463]

Conventional approaches to organic-inorganic multilayer barriers have typically involved enhancing the moisture barrier functions of Parylene C by supplementing it with a ceramic thin film. The barrier functionality of Parylene C has been shown to improve multiple-fold with the addition of SiN_x, Al_2O_3, SiO_2, and TiO_2.[467,479] However, there is also the potential for engineering composite multilayers to possess unique functionality that is difficult to achieve with a single material type. Song et al. demonstrate the value of such composite structures through *in vitro* accelerated lifetime tests with trilayer assemblies of t-SiO_2, HfO_2, and Parylene C with thicknesses of 50, 50, and 100 nm respectively.[450] Devices encapsulated with this barrier assembly fail after 13 days at 95°C in pH 7.4 PBS solution, indicating a multi-decade stability of over 50 years under physiological conditions.

As described previously, the lack of extensibility is a major shortcoming of the inorganic barrier layers that otherwise seem to have superior function. Floch et al. presented a compelling attempt to engineer extensibility in typically rigid materials like SiO_2 by depositing it on a pre-stretched elastomeric substrate.[532] This is a technique commonly employed in generating stretchable interconnects from conventionally rigid materials but has not been thoroughly investigated for the purpose of barrier layers.[533–535] In this work, the authors demonstrate that a wrinkled SiO_2 layer remains intact after 10000 cycles of strain at 100%. This is a promising strategy for stretchable ceramics that have potential use as a barrier layer in flexible implantable medical devices.

3.6. Novel Bioinspired Barrier Layers

Barrier layers comprise the vast majority of the surface area of an implantable device. As such, the surface chemistry of barrier layers dictates the abiotic-biotic interface and govern the downstream response to implantable devices. As a result, there is an emerging interest in engineering encapsulation materials that confer biocompatibility, dictate cellular responses, and control bioresorption *in vivo*. Here, we outline a few key advances in such designer biocompatible barrier materials.

In transient bioelectronic implants, there is a need for robust and controllable encapsulation materials to be developed. While hydrolytically degradable inorganic ceramic barriers are promising for transient devices, they are stiff, brittle, and challenging to integrate with soft electronics. In contrast, common degradable polymers are hydrophilic and swell in water, making them poor insulation materials. Choi et al. reported a class of UV-curable

biodegradable hydrophobic polyanhydrides with tunable mechanical (E = 5–25 MPa, ε_{max} = ~30%) and degradation (0.05–1.15 mg/day) characteristics (Figure 13, A).[536] Through controlling the thickness of the polyanhydride film, functional device lifetime was modulated between 13 and 95 hours in PBS at 37 °C.

To improve biocompatibility and cellular adhesion in implantable devices, Ju et al. proposed a bioactive photo-cross-linkable silk fibroin (PSF) capable of being patterned using conventional photolithographic techniques (Figure 13, B).[537] By grafting methacrylate groups onto pendant hydroxyl species on the silk fibroin, a crosslinked silk films can be produced with enhanced crystallinity compared to unmodified silk fibroin films. The resultant PSF films (E=15.6±1.1 GPa) insulate thin-film metal electrodes for 21 days with a less than 20% decrease in impedance. Additionally, *in vitro* cell culture studies on PSF indicated significantly improved cellular adhesion compared to glass and SU-8 substrates.

For non-transient bioelectronic applications, a similar effort to improve interfacial adhesion and biocompatibility was described through an aramid nanofiber and epoxy composite.[538] Device soak tests using interdigitating electrodes structures sandwiched between the nanocomposite films indicated an order of magnitude higher impedance compared to Parylene C encapsulated structures after 45 days. *In vitro* cell culture studies indicate a significantly improved cell adhesion on the nanocomposite substrate compared to Parylene C.

3.7. Future Outlook on Barrier Layers

Although barrier layers are an area of active investigation with significant progress being made in the recent years, barrier layers remain a bottleneck in the realization of chronic implantable bioelectronics. With new barrier layers and processing technologies continuing to emerge, there is considerable friction in their implementation by the broader bioelectronics community. Existing barriers like Parylene C, polyimide, and dielectric elastomers are often suitable for demonstrating novel device concepts in academic settings due to their satisfactory performance, ease of processing, and versatility. However, therapeutic bioelectronic devices for use in humans will almost certainly need breakthroughs in the chemistry and processing of barrier layers. While recent progress in integrating thin film ceramic barrier layers and multilayer structures is highly promising, heterogenous integration, film adhesion, and delamination remain as critical bottlenecks.[539,540] With the need to account for the intrinsic trade-off between stretchability and barrier properties, the robust and repeatable integration of high-performance inorganic barrier layers and composite multilayer structures with mechanically compliant electronics will emerge as a particular area for improvement. Materials chemists will continue to play critical roles in developing the next generation of barrier layers that will promote implantable bioelectronic devices from laboratory curiosities into powerful therapeutic tools.

4. Flexible Electronic, Ionic, and Hybrid Conductors

As with the other components of a soft bioelectronics device, the ideal conductive layer will also be mechanically compliant and biocompatible. Conductive materials used in traditional electronics tend to be rigid and may degrade in biological conditions. Biologically inert

conductive materials (e.g. Au, Pt, Mo), while rigid in bulk, may be structured in various nanoscale and microscale configurations capable of extending to strains necessary for *in vivo* applications (e.g. 30% for cardiac applications) without breaking ohmic contact.[20] We present the most promising biocompatible conductive materials by highlighting recent exemplary *in vivo* applications with demonstrated robustness and potential for clinical translation.

4.1. Nanowires and 1D Materials

Nanowires have gained considerable interest in recent years for stretchable applications, owing to its high stretchability, high conductance, low percolation threshold, and potential for biocompatibility.[39,544,545] Carbon nanotubes (CNTs),[546] silver nanowires (AgNW),[547] and gold-coated titanium dioxide nanowires (Au-TiO_2 NW)[548] have been the most commonly applied materials for biomedical applications. However, concerns of toxicity from CNTs have limited its biomedical applications to epidermal sensors, while early reports of cytotoxicity from AgNW have prompted some researchers to study other materials.[107,547,549] Still, AgNW may be the most prominent material for in vivo applications of nanowires in recent years, and representative recent reports of AgNW and Au-TiO_2 NW are presented.

Silver nanowires have recently been used in an epicardial bioelectronic patch by Sim et al. (Figure 14, A).[542] A stretchable AgNW/PDMS composite was used as the conductive traces, while novel rubbery transistors made of AuNP-coated AgNW/PDMS electrodes were used in a 5×5 active matrix for spatiotemporal mapping. The transistors showed no degradation over a few weeks in biofluid while encapsulated in PDMS. All components in the device had Young's moduli in the range of 0.1–10 MPa, improving upon prior epicardial devices that utilized rigid materials and approaching those of the heart. [20,110,550,551][20] The authors noted that their rubbery transistor could be stretched to a maximum of 30% strain, but slight changes to the field-effect mobility, threshold voltage, and on/off ratio were observed which partially recovered upon releasing back to 0% strain.

AgNW have recently been explored as a transparent and flexible conductor for optical biointerfacing by Chen et al. (Figure 14, B).[542] as an alternative to previously reported brittle indium tin oxide (ITO)[552] and potentially cytotoxic carbon nanotubes (CNT).[552,553] As a proof-of-concept, AgNW microelectrodes embedded in PDMS were used to measure a blue light excitable opsin, channelrhodopsin-2, which is commonly measured to evaluate atrioventricular block in mice.[554,555] Measurements from the AgNW microelectrodes closely aligned with those from the commercial reference (9.7 ± 0.5 and 9.8 ± 0.4 ms respectively) while demonstrating high optical transparency (>90.0% transmittance at 550 nm), low impedance (3.4–15 Ω cm^{-2} at f=1 kHz), and low sheet resistance (4.1–25 Ω cm^{-2}).[553] Chen et al. further demonstrated the possibility of using AgNW for optical mapping of a common fluorescent dye (i.e. di-4-ANEPPS) in a rat heart to obtain high transmittance values (81.4% and 82.4% at 530 and 705 nm respectively). The devices were found to cause mild inflammation four weeks after implantation, and further investigation is necessary for chronic applications.

Concerns over the toxicity of silver in implanted devices have led researchers to explore alternative structures.[107,549] Gold-coated titanium dioxide nanowires (Au-TiO_2 NW) embedded in PDMS were used in a porcine study for continuous heart volume monitoring via strain measurements by Dual et al. (Figure 14, C).[543] The heart volume and stroke volume measurements from the implantable strain sensor showed moderate to high correlation (R^2 = 0.44 to 0.79) with values from the clinical standard (i.e. ultrasound) and demonstrated a lower error versus the clinical standard (7.1 mL and 14.0 mL respectively) when compared to impedance measurements. The robustness of the sensor was demonstrated by showing little resistance change after autoclaving and immersing in Ringer solution for seven days. Continuous monitoring of the resistance during cycling at 30% strain over 72 h ex vivo (compared to the 48 h typically needed for heart monitoring post-surgery) showed a modest increase in resistance, which is expected to confound heart volume measurements. The authors attributed this to the reorientation and disconnection of the Au-TiO_2 NW over time, which are shorter than modern AgNW (~10 μm vs >20 μm), and argue that preconditioning the strain sensor before implantation would allow the resistance changes to reach a plateau.

4.2. Nanoparticles and Low-Dimensional Colloids

Conductive paths of nanoparticles are capable of reorganizing to a greater degree than other materials, leading to a strain dependent percolation threshold and allowing the material to be incorporated in other networks, such as those of crosslinked polymers.[39,559] Ag nanoparticles (AgNP) continue to be the most widely used nanoparticle conductor for in vivo applications, perhaps owing to its established use in the health industry as antibacterial agents, cosmetics, and food storage,[560] while other materials (e.g. Au nanoparticles) have seen limited use as stretchable conductors but are favored for other applications (e.g. analytical chemistry).[561,562]

By using Ag flakes instead of nanowires, conductivity can be incorporated into a wider range of polymers, allowing for more diverse applications. Song et al. recently incorporated Ag flakes into a self-healing polymer composite ((PDMS)-4,4’-methylenebis(phenyl urea) $(MPU)_{0.4}$-isophorone bisurea units $(IU)_{0.6}$)) to interface with a sciatic rat nerve (Figure 15, A).[556] The Ag flake composite self-bonded to the encapsulating layers (which were also composed of self-healing polymers) without requiring additional adhesive layers due to the homogenous interface. The reduced mechanical mismatch allowed for a robust chronic implantation, retaining a signal-to-noise ratio of 1.76 after 6 weeks. The authors further demonstrated reduced leakage of Ag ions from the implant by including an Au nanomembrane, although some leakage was observed after a long time (17.03 ppm after 32 weeks).

Ag ions can be incorporated into commercial polyurethane (PU) fibers to create robust, sensitive, and biocompatible capacitive strain sensors, as reported by Lee et al. using a simple fabrication process (Figure 15, B).[557,563] The commercial PU-based spandex fibers are cleaned then immersed in a 40 wt% $AgCF_3COO$/ethanol solution for 30 mins to incorporate the ions, then reduced in a 1:1 hydrazine hydrate/ethanol solution for 5 mins to convert the ions into nanoparticles. Bundling the filaments together allowed for a resistive

strain sensor (gauge factor ~35 for strains up to 100%) that can measure bladder filling and voiding in ex vivo porcine subjects. Lee et al. further demonstrated the material in a passive wireless resistor-inductor-capacitor (RLC) strain sensor by configuring two filaments into a double helix. Each filament was individually coated in Ecoflex and the dielectric core was kept hollow, allowing for a sensitivity of 12 (defined as $\delta(\Delta C/C_0)/\delta\varepsilon$, which exceeded those of prior capacitive strain sensors.[564,565] Porcine leg strains were measured wirelessly in vivo using this passive circuit, and maintained its efficacy over 3 weeks. While the device did not impede the growth of cardiac microvascular endothelial cells over 3 weeks in vitro, the authors reported that future works may replace the Ag nanoparticles with Au to improve biocompatibility.

To address hysteresis commonly found in sensors based on viscoelastic materials, sensors based on poroelastic networks have potential applications for rapid long-term cycling, such as epicardial recording. Kim et al. incorporated poroelasticity into a 3D-printed PDMS/SiO_2-PS silica mix via steaming (Figure 15, C).[558] The rapid evaporation/absorption of water molecules turned the ink into a sponge-like foam with pore diameters ranging from 5 to 50 μm. The pore diameters were well-suited for the incorporation of Ag flakes, which was simply added via immersion in a hexane-Ag flake solution, then plated with Cu and Au. The resulting device had a maximum strain greater than 100%, bending stiffness of 8.0×10^7 GPa μm^4, an elastic modulus of 29 kPa, an impedance of 1.0 kΩ at $f = 1$ kHz, and a reduced hysteresis of 4.3 ± 0.5 kJ m^{-4} compared to that of the unsteamed control (23.6 ± 8.7 kJ m^{-4}). The mesh layout of the poroelastic material combined with the low bending stiffness allowed the device to adhere to the epicardium tissue via capillary adhesion and conformal contact, allowing for a robust measurement of electrocardiogram (ECG) signals on murine and porcine hearts without slipping. While no cytotoxicity was seen over 24 h, significant inflammation was observed after 14 days, and long-term continuous recording (>24 h) was not obtained, indicating more work is needed for chronic implantation.

4.3. Thin Film Metals

The possibility of incorporating established nanofabrication methods from the silicon industry into stretchable materials may be the most compelling reason for the study of stretchable thin film metals as a scalable technology. In addition, thin film metals can utilize a wide range of inert materials (e.g. Au, Pt), leave a minimal footprint for bioresorbable applications, and provide the uniformity necessary for sensing applications. While not intrinsically stretchable, developments in structural designs of thin films have allowed for strains typically in the range of 30–50%, and up to 100%, enabling its use in a wide variety of recent in vivo applications.[569–571]

The thin film method is ideal in highly sensitive electrochemical sensing applications, where good uniformity in thickness and an ultrathin (30–300 nm) nanomembrane layer are typically desired.[572,573] For example, nitric oxide (NO) is an important biomarker linked to neurotransmission, immune responses, and cardiovascular systems, among others.[574,575] However, its detection requires either indirect methods (e.g. by measurement of nitrite ion NO_2^-) or real time measurements due to its short half-life, low concentration (nM to μM), and chemical interference.[576] A highly sensitive (3.97 nmol detection limit) NO sensor

was developed by Li et al. by implementing ultrathin (32 nm) Au nanomembranes with a poly(eugenol) coating in a bioresorbable polymer (Figure 16, A).[566] The sensor was implanted in a rabbit and detected NO over a wide range (0.01–100 μM) while maintaining selectivity for NO due to its poly(eugenol) coating. In addition, the sensor could withstand strains of 50% with minimal resistance changes after 1000 cycles and fully dissolved in PBS after 15 weeks.

A common and facile approach for imparting extensibility onto thin metal films is to use well-established photolithography approaches to form serpentine paths of metal, typically encapsulated in polyimide, which can deflect out of plane and extend up to 300% strain.[577] This idea has been extended into various three dimensional geometries, and their extensibility mechanism has been characterized in terms of compressive buckling.[267] Han, Chen, Aras et al. have recently used this thin film approach to create an extensible sensor array on a balloon catheter (Figure 16, C).[568] Pressure, temperature, and strain sensors were incorporated into an 8×8 array with 3D serpentine gold interconnects capable of withstanding strains up to 30%. By using thin (300 nm) and uniform gold films, the design was shown to be scalable and reproducible with high linearity ($R^2 > 0.996$), uniform sensitivity (mean 8.2×10^{-5} kPa^{-1}, s.d. 7.8×10^{-6} kPa^{-1}), and low hysteresis (difference in $\Delta R/R < 0.014\%$). Han, Chen, Aras et al. further demonstrated the *ex vivo* robustness of the sensor in both rabbits and humans. While the balloon catheter approach may preclude the possibility of chronic implantation, the authors propose this stretchable sensor design as a proof-of-concept for diagnostic measurements during short-term and minimally invasive procedures.

Stretchable thin film conductors can be easily integrated with rigid components using established techniques in microfabrication, allowing for small and sophisticated devices. For example, Ausra et al. have recently developed a wireless and battery-free optogenetic stimulator with the LED probe attached via a serpentine copper trace (17.5 μm thick) (Figure 16, B).[567] The device consists of commercial components, including a microcontroller, capacitor, inductive coil, and an antenna, powered wireless by magnetic resonant coupling. The fully implantable device had a maximum dimension of 13.50 mm and was implanted onto a murine skull without penetrating the blood-brain barrier. The stretchable copper trace exhibited a maximum strain of 100% and linked the LED probe and the rigid components. The flexibility offered by the stretchable conductor allowed for a facile and precise application to the skull, while its compatibility with the conductive material of the rigid components simplified the fabrication process. While the study lacks the possibility of chronic implantation due to the use of toxic materials, the proof-of-concept demonstrated that the use of well-established components and fabrication methods can lead to robust wireless devices for in vivo applications.

4.4. Other Conductors

Conductive polymers continue to be an active research topic for biomaterials and have demonstrated record tensile strains (>100%), low moduli (kPa-MPa), and conductivity (10^1–10^4 S m^{-1}),[578–582] among other tunable characteristics such as anisotropy,[583] adhesiveness,[156,584–586] and biodegradability.[587] A wide range of polymers are being

explored as stretchable semiconductors, optimizing for charge carrier mobility,[587–589] device density,[590] ionic transport,[591] and neuromorphic computing.[592] Typically, carrier mobilities of 10^{-1}–10^{0} cm^2 V^{-1} s^{-1} are reported, with minimal variation under applied strains of >100%. Conductive polymers limit the overall impedance of devices due to their mixed conductor characteristic allowing them to be modeled as a capacitor and resistor in parallel, and have been used as device coatings.[309,593–596] While the potential for unique properties abound, significant barriers for clinical translation exist, including lack of regulatory approval for new materials, minimal toxicity and stability research, and limited compatibility with established microfabrication techniques. However, a few notable conductive polymers have been demonstrated in recent *in vivo* applications - e.g. PEDOT:PSS for electrophysiological recording, [276,594,597–599] polypyrrole (PPy) as an anisotropic cardiac patch,[583] and poly[3-hexylthiophene] (P3HT) nanoparticles for neuronal photostimulation[600] - and are the nearest candidates for clinical translation.

Metallic glasses have gained interest as a next generation fiber material owing to their high conductivity, elasticity, fracture toughness, hardness, and corrosion resistance.[601–605] However, their complex formation mechanisms have been difficult to characterize and sensitive to experimental details.[606] In recent years, Yan et al. have developed a thermal drawing method, similar to the manufacturing process of optical fibers, that is capable of generating metallic glass fibers with extreme aspect ratios (i.e. 40 nm to 20 μm in thickness, >28 m in length).[607–609] By choosing a polymer and metallic glass with similar crystallization kinetics (i.e. polyetherimide and $Pt_{57.5}Cu_{14.7}Ni_{5.3}P_{22.5}$), the co-drawn material can be scalably redrawn at 260°C in multiple steps to reduce the thickness from 20 μm to 40 nm while generating lengths up to 28 m. The authors state that the method could potentially be used to generate kilometer-scale fibers. Yan et al. implemented the metallic glass fibers in a murine neural implant, which successfully recorded neural activity for up to six weeks, after which the signal-to-noise ratio became inhibitive. This initial proof-of-concept allows for new potential applications in flexible electronics that require high density and aspect ratio fibers, such as in optoelectronics, wearables, and neuroscience.

5. Conclusion

This article emphasized how advancements in materials chemistry contributed to furthering the goal of integrating soft electronics with the human body. The materials most frequently explored by soft electronics researchers in recent years were presented categorically by the three major components of any bioelectronics system: substrates, barrier layers, and conductors. While many notable and scientifically interesting examples exist, we highlighted recent major works that demonstrated robustness via thorough *in vivo* investigations.

In these discussions, we described specific challenges that must be addressed as we look towards the future of flexible bioelectronics. Broadly, there are several bottlenecks and opportunity gaps for the widespread adoption of flexible bioelectronics in medicine. First, there is a need for the development of versatile materials for encapsulating not just flexible inextensible devices but also stretchable and ultracompliant devices for long-term use in the human body. With inorganic materials showing the most superior barrier function but the poorest mechanical biocompatibility and polymers displaying the exact opposite,

there is an opportunity to develop robust composites or novel materials that can sustain dynamic biomechanical loading conditions for a multi-decade device lifetime. Second, there is a need for a thorough follow-up to successful bioelectronic device implementations with an emphasis on repeatable and scaled manufacturing methods. While demonstrations of implanted soft devices abound, robust chronic implantation has yet to be thoroughly demonstrated. With increased interest in designing custom functional materials for specific applications, materials chemistry will be crucial to designing scalable manufacturing methods.

Acknowledgements

The authors acknowledge funding from the following sources: National Institutes of Health Grants R21EB026073 and R21EB028418.

Biographies

Gaurav Balakrishnan received his B.S. degree in Materials Science and Engineering (MSE) with an additional major in Biomedical Engineering from Carnegie Mellon University in 2019. He is currently a Ph.D. candidate in MSE, working under the supervision Prof. Christopher J. Bettinger. His research interests include the design and fabrication of flexible and stretchable bioelectronics for implantable and ingestible applications.

Jiwoo Song received his B.S.E. degree in mechanical engineering, materials science, and chemistry from Duke University in 2020. He is currently pursuing a Ph.D. degree in materials science and engineering at Carnegie Mellon University, under the supervision of Prof. Christopher J. Bettinger. His research interests include translational medical devices and stretchable electronics.

Chenchen Mou received her B.S. degree in Biomedical Engineering (BME) from Sichuan University in 2011. She received her M.S. degree in Biomedical Engineering in 2016 and Ph.D. degree in Biomedical Engineering in 2021, both at Carnegie Mellon University, working under the supervision Prof. Christopher J. Bettinger. Her research interests include the design and fabrication of flexible and stretchable bioelectronics.

Christopher J. Bettinger is a Professor Materials Science & Engineering and Biomedical Engineering at Carnegie Mellon University. His group studies fundamental and applied aspects of polymer and materials chemistry for flexible bioelectronic devices.

References

[1]. Kipke DR, Shain W, Buzsáki G, Fetz E, Henderson JM, Hetke JF, Schalk G, J. Neurosci 2008, 28, 11830. [PubMed: 19005048]

[2]. Fetz EE, in Prog. Brain Res (Eds.: Dancause N, Nadeau S, Rossignol S), Elsevier, 2015, pp. 241–252.

[3]. Jackson A, Zimmermann JB, Nat. Rev. Neurol 2012, 8, 690. [PubMed: 23147846]

[4]. Zhang M, Tang Z, Liu X, Van der Spiegel J, Nat. Electron 2020, 3, 191.

[5]. Zhang A, Zhao Y, You SS, Lieber CM, Nano Today 2020, 31, 100821.

[6]. Nicolelis MAL, Nat. Rev. Neurosci 2003, 4, 417. [PubMed: 12728268]

[7]. Wei W, Song Y, Wang L, Zhang S, Luo J, Xu S, Cai X, Microsyst. Nanoeng 2015, 1, 1.

[8]. Hong YJ, Jeong H, Cho KW, Lu N, Kim D-H, Adv. Funct. Mater 2019, 29, 1808247.

[9]. Sunwoo SH, Lee JS, Bae S, Shin YJ, Kim CS, Joo SY, Choi HS, Suh M, Kim SW, Choi YJ, Kim T, Proc. Natl. Acad. Sci 2019, 116, 1146. [PubMed: 30617062]

[10]. Feiner R, Engel L, Fleischer S, Malki M, Gal I, Shapira A, Shacham-Diamand Y, Dvir T, Nat. Mater 2016, 15, 679. [PubMed: 26974408]

[11]. Vadlapatla R, Wong EY, Gayakwad SG, J. Drug Deliv. Sci. Technol 2017, 41, 359.

[12]. Khan AN, Ermakov A, Sukhorukov G, Hao Y, Appl. Phys. Rev 2019, 6, 041301.

[13]. Sjöström TA, Berggren M, Gabrielsson EO, Janson P, Poxson DJ, Seitanidou M, Simon DT, Adv. Mater. Technol 2018, 3, 1700360.

[14]. Yadav KS, Kapse-Mistry S, Peters GJ, Mayur YC, Drug Discov. Today 2019, 24, 1023. [PubMed: 30794860]

[15]. Pons-Faudoa FP, Ballerini A, Sakamoto J, Grattoni A, Biomed. Microdevices 2019, 21, 47. [PubMed: 31104136]

[16]. Lee J, Cho HR, Cha GD, Seo H, Lee S, Park C-K, Kim JW, Qiao S, Wang L, Kang D, Kang T, Ichikawa T, Kim J, Lee H, Lee W, Kim S, Lee S-T, Lu N, Hyeon T, Choi SH, Kim D-H, Nat. Commun 2019, 10, 5205. [PubMed: 31729383]

[17]. Izmailova ES, Wagner JA, Perakslis ED, Clin. Pharmacol. Ther 2018, 104, 42. [PubMed: 29205294]

[18]. Wang C, Li X, Hu H, Zhang L, Huang Z, Lin M, Zhang Z, Yin Z, Huang B, Gong H, Bhaskaran S, Gu Y, Makihata M, Guo Y, Lei Y, Chen Y, Wang C, Li Y, Zhang T, Chen Z, Pisano AP, Zhang L, Zhou Q, Xu S, Nat. Biomed. Eng 2018, 2, 687. [PubMed: 30906648]

[19]. Sempionatto JR, Lin M, Yin L, De la paz E, Pei K, Sonsa-ard T, de Loyola Silva AN, Khorshed AA, Zhang F, Tostado N, Xu S, Wang J, Nat. Biomed. Eng 2021, 5, 737. [PubMed: 33589782]

[20]. Kim D-H, Lu N, Ma R, Kim Y-S, Kim R-H, Wang S, Wu J, Won SM, Tao H, Islam A, Yu KJ, Kim T, Chowdhury R, Ying M, Xu L, Li M, Chung H-J, Keum H, McCormick M, Liu P, Zhang Y-W, Omenetto FG, Huang Y, Coleman T, Rogers JA, Science 2011, 333, 838. [PubMed: 21836009]

[21]. Jeong J-W, Yeo W-H, Akhtar A, Norton JJS, Kwack Y-J, Li S, Jung S-Y, Su Y, Lee W, Xia J, Cheng H, Huang Y, Choi W-S, Bretl T, Rogers JA, Adv. Mater 2013, 25, 6839. [PubMed: 24327417]

[22]. Jeong J-W, Kim MK, Cheng H, Yeo W-H, Huang X, Liu Y, Zhang Y, Huang Y, Rogers JA, Adv. Healthc. Mater 2014, 3, 642. [PubMed: 24132942]

[23]. Lv J, Yin L, Chen X, Jeerapan I, Silva CA, Li Y, Le M, Lin Z, Wang L, Trifonov A, Xu S, Cosnier S, Wang J, Adv. Funct. Mater 2021, 31, 2102915.

[24]. Bartlett MD, Markvicka EJ, Majidi C, Adv. Funct. Mater 2016, 26, 8496.

[25]. Jung YH, Kim JU, Lee JS, Shin JH, Jung W, Ok J, Kim T, Adv. Mater 2020, 32, 1907478.

[26]. Cingolani E, Goldhaber JI, Marbán E, Nat. Rev. Cardiol 2018, 15, 139. [PubMed: 29143810]

[27]. Cho Y, Park J, Lee C, Lee S, Bioelectron. Med 2020, 6, 23. [PubMed: 33292861]
[28]. Jonsson A, Song Z, Nilsson D, Meyerson BA, Simon DT, Linderoth B, Berggren M, Sci. Adv 2015, 1, e1500039. [PubMed: 26601181]
[29]. Han L, Lu X, Wang M, Gan D, Deng W, Wang K, Fang L, Liu K, Chan CW, Tang Y, Weng L-T, Yuan H, Small 2017, 13, 1601916.
[30]. Payne SC, Furness JB, Stebbing MJ, Nat. Rev. Gastroenterol. Hepatol 2019, 16, 89. [PubMed: 30390018]
[31]. Ward MP, Gupta A, Wo JM, Rajwa B, Furness JB, Powley TL, Nowak TV, J. Neurosci. Methods 2020, 336, 108631. [PubMed: 32087238]
[32]. Hokanson JA, Langdale CL, Sridhar A, Milliken P, Grill WM, Sci. Rep 2021, 11, 314. [PubMed: 33431964]
[33]. Koopman FA, Schuurman PR, Vervoordeldonk MJ, Tak PP, Best Pract. Res. Clin. Rheumatol 2014, 28, 625. [PubMed: 25481554]
[34]. Schiavone G, Fallegger F, Kang X, Barra B, Vachicouras N, Roussinova E, Furfaro I, Jiguet S, Seáñez I, Borgognon S, Rowald A, Li Q, Qin C, Bézard E, Bloch J, Courtine G, Capogrosso M, Lacour SP, Adv. Mater 2020, 32, 1906512.
[35]. Fallegger F, Schiavone G, Lacour SP, Adv. Mater 2020, 32, 1903904.
[36]. Lacour SP, Courtine G, Guck J, Nat. Rev. Mater 2016, 1, 1.
[37]. Chen X, Rogers JA, Lacour SP, Hu W, Kim D-H, Chem. Soc. Rev 2019, 48, 1431. [PubMed: 30849169]
[38]. Fang Y, Meng L, Prominski A, Schaumann EN, Seebald M, Tian B, Chem. Soc. Rev 2020, 49, 7978. [PubMed: 32672777]
[39]. Wang C, Wang C, Huang Z, Xu S, Adv. Mater 2018, 30, 1801368.
[40]. Zhao X, Chen X, Yuk H, Lin S, Liu X, Parada G, Chem. Rev 2021, 121, 4309. [PubMed: 33844906]
[41]. Chen Y, Zhang Y, Liang Z, Cao Y, Han Z, Feng X, Npj Flex. Electron 2020, 4, 1.
[42]. Liu Y, Wang H, Zhao W, Zhang M, Qin H, Xie Y, Sensors 2018, 18, 645.
[43]. Lacour SP, Wagner S, Huang Z, Suo Z, Appl. Phys. Lett 2003, 82, 2404.
[44]. Xu M, Obodo D, Yadavalli VK, Biosens. Bioelectron 2019, 124–125, 96.
[45]. Sunwoo S-H, Ha K-H, Lee S, Lu N, Kim D-H, Annu. Rev. Chem. Biomol. Eng 2021, 12, 359. [PubMed: 34097846]
[46]. Pham T-A, Nguyen T-K, Vadivelu RK, Dinh T, Qamar A, Yadav S, Yamauchi Y, Rogers JA, Nguyen N-T, Phan H-P, Adv. Funct. Mater 2020, 30, 2004655.
[47]. Simon D, Ware T, Marcotte R, Lund BR, Smith DW, Di Prima M, Rennaker RL, Voit W, Biomed. Microdevices 2013, 15, 925. [PubMed: 23852172]
[48]. Reeder J, Kaltenbrunner M, Ware T, Arreaga-Salas D, Avendano-Bolivar A, Yokota T, Inoue Y, Sekino M, Voit W, Sekitani T, Someya T, Adv. Mater 2014, 26, 4967. [PubMed: 24733490]
[49]. Adly N, Weidlich S, Seyock S, Brings F, Yakushenko A, Offenhäusser A, Wolfrum B, Npj Flex. Electron 2018, 2, 15.
[50]. Chiong JA, Tran H, Lin Y, Zheng Y, Bao Z, Adv. Sci 2021, 8, 2101233.
[51]. Shim HJ, Sunwoo S-H, Kim Y, Koo JH, Kim D-H, Adv. Healthc. Mater 2021, 10, 2002105.
[52]. Irimia-Vladu M, Chem. Soc. Rev 2013, 43, 588.
[53]. Wang C, Yokota T, Someya T, Chem. Rev 2021, 121, 2109. [PubMed: 33460327]
[54]. Wu X, Peng H, Sci. Bull 2019, 64, 634.
[55]. Someya T, Bao Z, Malliaras GG, Nature 2016, 540, 379. [PubMed: 27974769]
[56]. Baek P, Voorhaar L, Barker D, Travas-Sejdic J, Acc. Chem. Res 2018, 51, 1581. [PubMed: 29897228]
[57]. Rivnay J, Owens RM, Malliaras GG, Chem. Mater 2014, 26, 679.
[58]. Rivnay J, Inal S, Salleo A, Owens RM, Berggren M, Malliaras GG, Nat. Rev. Mater 2018, 3, 1.
[59]. Yuk H, Lu B, Zhao X, Chem. Soc. Rev 2019, 48, 1642. [PubMed: 30474663]

[60]. Griffin MF, Leung BC, Premakumar Y, Szarko M, Butler PE, J. Otolaryngol. - Head Neck Surg 2017, 46, 33. [PubMed: 28420435]

[61]. Borschel GH, Kia KF, Kuzon WM, Dennis RG, J. Surg. Res 2003, 114, 133. [PubMed: 14559438]

[62]. Millesi H, Zöch G, Reihsner R, Clin. Orthop 1995, 76.

[63]. Badea S, Wu W, in Nanoeng. Biomater. Regen. Med (Eds.: Mozafari M, Rajadas J, Kaplan) D, Elsevier, 2019, pp. 187–214.

[64]. Ma Z, Hu S, Tan JS, Myer C, Njus NM, Xia Z, J. Biomed. Mater. Res. A 2013, 101A, 2718.

[65]. Sherif R, Hani N, Narinder P, in Front. Bioeng. Biotechnol, 2016.

[66]. McKee CT, Last JA, Russell P, Murphy CJ, Tissue Eng. Part B Rev 2011, 17, 155. [PubMed: 21303220]

[67]. Amzulescu MS, De Craene M, Langet H, Pasquet A, Vancraeynest D, Pouleur AC, Vanoverschelde JL, Gerber BL, Eur. Heart J. - Cardiovasc. Imaging 2019, 20, 605. [PubMed: 30903139]

[68]. Qu Y, He Y, Zhang Y, Ma T, Zhu J, Miao Y, Dai C, Humayun M, Zhou Q, Chen Z, Biomed. Opt. Express 2018, 9, 4054. [PubMed: 30615733]

[69]. Bekerman I, Gottlieb P, Vaiman M, J. Ophthalmol 2014, 2014, 503645. [PubMed: 25431659]

[70]. Fallenstein GT, Hulce VD, Melvin JW, J. Biomech 1969, 2, 217. [PubMed: 16335085]

[71]. Leipzig ND, Shoichet MS, Biomaterials 2009, 30, 6867. [PubMed: 19775749]

[72]. Taylor Z, Miller K, J. Biomech 2004, 37, 1263. [PubMed: 15212932]

[73]. Chang James, Neligan Peter, Plastic Surgery, Elsevier, London, 2018.

[74]. Young WC, Budynas RG, Sadegh AM, Roark's Formulas for Stress and Strain, Eighth Edition, McGraw-Hill Education, 2012.

[75]. Steif P, Mechanics of Materials, Pearson, 2012.

[76]. Harris KD, Elias AL, Chung H-J, J. Mater. Sci 2016, 51, 2771.

[77]. Peng J, Snyder GJ, Science 2019, 366, 690. [PubMed: 31699925]

[78]. Song E, Li J, Won SM, Bai W, Rogers JA, Nat. Mater 2020, 19, 590. [PubMed: 32461684]

[79]. Rivnay J, Wang H, Fenno L, Deisseroth K, Malliaras GG, Sci. Adv 2017, 3, e1601649. [PubMed: 28630894]

[80]. Weiland JD, Liu W, Humayun MS, Annu. Rev. Biomed. Eng 2005, 7, 361. [PubMed: 16004575]

[81]. Zeng F-G, Rebscher S, Harrison W, Sun X, Feng H, IEEE Rev. Biomed. Eng 2008, 1, 115. [PubMed: 19946565]

[82]. Savagatrup S, Printz AD, O'Connor TF, Zaretski AV, Lipomi DJ, Chem. Mater 2014, 26, 3028.

[83]. Ocheje MU, Charron BP, Nyayachavadi A, Rondeau-Gagné S, Flex. Print. Electron 2017, 2, 043002.

[84]. Wang NG-J, Gasperini A, Bao Z, Adv. Electron. Mater 2018, 4, 1700429.

[85]. Lipomi DJ, Adv. Mater 2016, 28, 4180. [PubMed: 26601914]

[86]. Rogers JA, Ghaffari R, Kim D-H, Eds., Stretchable Bioelectronics for Medical Devices and Systems, Springer International Publishing, 2016.

[87]. Choi S, Lee H, Ghaffari R, Hyeon T, Kim D-H, Adv. Mater 2016, 28, 4203. [PubMed: 26779680]

[88]. Kim H, Kim Y-S, Mahmood M, Kwon S, Zavanelli N, Kim HS, Rim YS, Epps F, Yeo W-H, Adv. Sci 2020, 7, 2000810.

[89]. Bettinger CJ, Bioelectron. Med 2018, 4, 6. [PubMed: 32232082]

[90]. Wu P, Xiao A, Zhao Y, Chen F, Ke M, Zhang Q, Zhang J, Shi X, He X, Chen Y, Nanoscale 2019, 11, 21103. [PubMed: 31524919]

[91]. Szostak KM, Grand L, Constandinou TG, Front. Neurosci 2017, 11, 665. [PubMed: 29270103]

[92]. Nam J, Lim H-K, Kim NH, Park JK, Kang ES, Kim Y-T, Heo C, Lee O-S, Kim S-G, Yun WS, Suh M, Kim YH, ACS Nano 2020, 14, 664. [PubMed: 31895542]

[93]. Li S, Cong Y, Fu J, J. Mater. Chem. B 2021, 9, 4423. [PubMed: 33908586]

[94]. Xu J, Xu J, Moon H, Sintim HO, Lee H, ACS Appl. Polym. Mater 2020, 2, 528. [PubMed: 32490375]

[95]. Sheikh Z, Brooks PJ, Barzilay O, Fine N, Glogauer M, Materials 2015, 8, 5671. [PubMed: 28793529]

[96]. Bhunia S, Majerus S, Sawan M, Implantable Biomedical Microsystems: Design Principles and Applications, Elsevier, 2015.

[97]. Ratner BD, J Cardiovasc. Transl. Res 2011, 4, 523. [PubMed: 21710333]

[98]. Black J, Biological Performance of Materials: Fundamentals of Biocompatibility, CRC Taylor & Francis, Boca Raton, 2006.

[99]. Williams DF, Biomaterials 2008, 29, 2941. [PubMed: 18440630]

[100]. Taraballi F, Sushnitha M, Tsao C, Bauza G, Liverani C, Shi A, Tasciotti E, Adv. Healthc. Mater 2018, 7, 1800490.

[101]. Doloff JC, Veiseh O, de Mezerville R, Sforza M, Perry TA, Haupt J, Jamiel M, Chambers C, Nash A, Aghlara-Fotovat S, Stelzel JL, Bauer SJ, Neshat SY, Hancock J, Romero NA, Hidalgo YE, Leiva IM, Munhoz AM, Bayat A, Kinney BM, Hodges HC, Miranda RN, Clemens MW, Langer R, Nat. Biomed. Eng 2021, 1. [PubMed: 33483712]

[102]. Noskovicova N, Schuster R, van Putten S, Ezzo M, Koehler A, Boo S, Coelho NM, Griggs D, Ruminski P, McCulloch CA, Hinz B, Nat. Biomed. Eng 2021, 1. [PubMed: 33483712]

[103]. Welch NG, Winkler DA, Thissen H, Adv. Drug Deliv. Rev 2020, 167, 109. [PubMed: 32553685]

[104]. Biran R, Pond D, Adv. Drug Deliv. Rev 2017, 112, 12. [PubMed: 28042080]

[105]. Helmus MN, Gibbons DF, Cebon D, Toxicol. Pathol 2008, 36, 70. [PubMed: 18337223]

[106]. Goding JA, Gilmour AD, Aregueta-Robles UA, Hasan EA, Green RA, Adv. Funct. Mater 2018, 28, 1702969.

[107]. Park J, Choi S, Janardhan AH, Lee S-Y, Raut S, Soares J, Shin K, Yang S, Lee C, Kang K-W, Cho HR, Kim SJ, Seo P, Hyun W, Jung S, Lee H-J, Lee N, Choi SH, Sacks M, Lu N, Josephson ME, Hyeon T, Kim D-H, Hwang HJ, Sci. Transl. Med 2016, 8, 344ra86.

[108]. Choi S, Han SI, Jung D, Hwang HJ, Lim C, Bae S, Park OK, Tschabrunn CM, Lee M, Bae SY, Yu JW, Ryu JH, Lee S-W, Park K, Kang PM, Lee WB, Nezafat R, Hyeon T, Kim D-H, Nat. Nanotechnol 2018, 13, 1048. [PubMed: 30104619]

[109]. Lee S, Inoue Y, Kim D, Reuveny A, Kuribara K, Yokota T, Reeder J, Sekino M, Sekitani T, Abe Y, Someya T, Nat. Commun 2014, 5, 5898. [PubMed: 25523614]

[110]. Xu L, Gutbrod SR, Ma Y, Petrossians A, Liu Y, Webb RC, Fan JA, Yang Z, Xu R, Whalen JJ, Weiland JD, Huang Y, Efimov IR, Rogers JA, Adv. Mater 2015, 27, 1731. [PubMed: 25641076]

[111]. Xiao T, Zhou Z, Zheng F, Zhou Y, Xu F, Zhang S, Shi Z, Mao Y, Tao TH, in 2020 IEEE 33rd Int. Conf. Micro Electro Mech. Syst. MEMS, IEEE, Vancouver, BC, Canada, 2020, pp. 419–420.

[112]. Kim D-H, Viventi J, Amsden JJ, Xiao J, Vigeland L, Kim Y-S, Blanco JA, Panilaitis B, Frechette ES, Contreras D, Kaplan DL, Omenetto FG, Huang Y, Hwang K-C, Zakin MR, Litt B, Rogers JA, Nat. Mater 2010, 9, 511. [PubMed: 20400953]

[113]. Thukral A, Ershad F, Enan N, Rao Z, Yu C, IEEE Nanotechnol. Mag 2018, 12, 21.

[114]. Li H, Liu H, Sun M, Huang Y, Xu L, Adv. Mater 2021, 33, 2004425.

[115]. Liu Y, Urso A, Martins da Ponte R, Costa T, Valente V, Giagka V, Serdijn WA, Constandinou TG, Denison T, IEEE Solid-State Circuits Mag 2020, 12, 30.

[116]. Chen X, Villa NS, Zhuang Y, Chen L, Wang T, Li Z, Kong T, Adv. Energy Mater 2020, 10, 1902769.

[117]. Sonn M, Feist WM, Med. Biol. Eng 1974, 12, 778. [PubMed: 4282864]

[118]. Suzuki T, Mabuchi K, Takeuchi S, in First Int. IEEE EMBS Conf. Neural Eng. 2003 Conf. Proc, IEEE, Capri Island, Italy, 2003, pp. 154–156.

[119]. Lee SW, Seo J-M, Ha S, Kim ET, Chung H, Kim SJ, Invest. Opthalmol. Vis. Sci 2009, 50, 5859.

[120]. Tijero M, Gabriel G, Caro J, Altuna A, Hernández R, Villa R, Berganzo J, Blanco FJ, Salido R, Fernández LJ, Biosens. Bioelectron 2009, 24, 2410. [PubMed: 19167206]

[121]. Khang D-Y, Jiang H, Huang Y, Rogers JA, Science 2006, 311, 208. [PubMed: 16357225]

[122]. Shin M, Song JH, Lim G-H, Lim B, Park J-J, Jeong U, Adv. Mater 2014, 26, 3706. [PubMed: 24664816]

[123]. Minev IR, Musienko P, Hirsch A, Barraud Q, Wenger N, Moraud EM, Gandar J, Capogrosso M, Milekovic T, Asboth L, Torres RF, Vachicouras N, Liu Q, Pavlova N, Duis S, Larmagnac A, Voros J, Micera S, Suo Z, Courtine G, Lacour SP, Science 2015, 347, 159. [PubMed: 25574019]

[124]. Ahn Y, Lee H, Lee D, Lee Y, ACS Appl. Mater. Interfaces 2014, 6, 18401. [PubMed: 25347028]

[125]. Agarwala S, Lee JM, Ng WL, Layani M, Yeong WY, Magdassi S, Biosens. Bioelectron 2018, 102, 365. [PubMed: 29172145]

[126]. Huang W-C, Ong XC, Kwon IS, Gopinath C, Fisher LE, Wu H, Fedder GK, Gaunt RA, Bettinger CJ, Adv. Funct. Mater 2018, 28, 1801059.

[127]. Fuketa H, Yoshioka K, Shinozuka Y, Ishida K, Yokota T, Matsuhisa N, Inoue Y, Sekino M, Sekitani T, Takamiya M, Someya T, Sakurai T, IEEE Trans. Biomed. Circuits Syst 2014, 8, 824. [PubMed: 24951707]

[128]. Liu J, Fu T-M, Cheng Z, Hong G, Zhou T, Jin L, Duvvuri M, Jiang Z, Kruskal P, Xie C, Suo Z, Fang Y, Lieber CM, Nat. Nanotechnol 2015, 10, 629. [PubMed: 26053995]

[129]. Kim H, Gibson J, Maeng J, Saed MO, Pimentel K, Rihani RT, Pancrazio JJ, Georgakopoulos SV, Ware TH, ACS Appl. Mater. Interfaces 2019, 11, 19506. [PubMed: 31070344]

[130]. Baumgartner M, Hartmann F, Drack M, Preninger D, Wirthl D, Gerstmayr R, Lehner L, Mao G, Pruckner R, Demchyshyn S, Reiter L, Strobel M, Stockinger T, Schiller D, Kimeswenger S, Greibich F, Buchberger G, Bradt E, Hild S, Bauer S, Kaltenbrunner M, Nat. Mater 2020, 19, 1102. [PubMed: 32541932]

[131]. Lee HC, Ejserholm F, Gaire J, Currlin S, Schouenborg J, Wallman L, Bengtsson M, Park K, Otto KJ, J. Neural Eng 2017, 14, 036026. [PubMed: 28470152]

[132]. Jeon M, Cho J, Kim YK, Jung D, Yoon E-S, Shin S, Cho I-J, J. Micromech. Microeng 2014, 24, 025010.

[133]. Du ZJ, Kolarcik CL, Kozai TDY, Luebben SD, Sapp SA, Zheng XS, Nabity JA, Cui XT, Acta Biomater 2017, 53, 46. [PubMed: 28185910]

[134]. Woeppel K, Yang Q, Cui XT, Curr. Opin. Biomed. Eng 2017, 4, 21. [PubMed: 29423457]

[135]. Yang C, Zhang H, Liu Y, Yu Z, Wei X, Hu Y, Adv. Sci 2018, 5, 1801070.

[136]. Majumdar JD, Manna I, Int. Mater. Rev 2011, 56, 341.

[137]. Pyo SH, Lee MY, Jeon JJ, Lee JH, Yi MH, Kim JS, Adv. Funct. Mater 2005, 15, 619.

[138]. Bhushan B, Ma T, Higashioji T, J. Appl. Polym. Sci 2002, 83, 2225.

[139]. MacDonald WA, Looney MK, MacKerron D, Eveson R, Adam R, Hashimoto K, Rakos K, J. Soc. Inf. Disp 2007, 15, 1075.

[140]. DuPont, Kapton® HN General-Purpose Polyimide Film, 2018.

[141]. HD MicroSystems, Product Selection Guide, 2013.

[142]. Celanese Corporation, Design Guide for Velctra LCP, 2013.

[143]. Wang X, Engel J, Liu C, J. Micromech. Microeng 2003, 13, 628.

[144]. Celanese Corporation, VECTRA® A950 Datasheet, 2020.

[145]. Lorenz H, Despont M, Fahrni N, LaBianca N, Renaud P, Vettiger P, J. Micromech. Microeng 1997, 7, 121.

[146]. LaBianca N, Gelorme J, Lee K, Cooper E, O'Sullivan E, Shaw J, High Aspect Ratio Optical Resist Chemistry for MEMs Applications, 1995.

[147]. Chung S, Park S, J. Mech. Sci. Technol 2013, 27, 2701.

[148]. Jackson N, Stam F, O'Brien J, Kailas L, Mathewson A, O'Murchu C, Thin Solid Films 2016, 603, 371.

[149]. von Metzen RP, Stieglitz T, Biomed. Microdevices 2013, 15, 727. [PubMed: 23494595]

[150]. Kim BJ, Meng E, Polym. Adv. Technol 2016, 27, 564.

[151]. Para-coat Technologies, Parylene Guide, 2021.

[152]. Volkov A, in Encycl. Membr (Eds.: Drioli E, Giorno L), Springer, Berlin, Heidelberg, 2015, pp. 1–2.

[153]. Gao D, Parida K, Lee PS, Adv. Funct. Mater 2020, 30, 1907184.

[154]. "Ecoflex™ Series, Super-Soft, Addition Cure Silicone Rubbers," can be found under https://www.smooth-on.com/product-line/ecoflex/, 2021.

[155]. Huang W-C, Ali F, Zhao J, Rhee K, Mou C, Bettinger CJ, Biomacromolecules 2017, 18, 1162. [PubMed: 28245355]

[156]. Mou C, Ali F, Malaviya A, Bettinger CJ, J. Mater. Chem. B 2019, 7, 1690. [PubMed: 31372223]

[157]. Sun J-Y, Zhao X, Illeperuma WRK, Chaudhuri O, Oh KH, Mooney DJ, Vlassak JJ, Suo Z, Nature 2012, 489, 133. [PubMed: 22955625]

[158]. Lin S, Yuk H, Zhang T, Parada GA, Koo H, Yu C, Zhao X, Adv. Mater 2016, 28, 4497. [PubMed: 26639322]

[159]. Sung SH, Kim YS, Joe DJ, Mun BH, You BK, Keum DH, Hahn SK, Berggren M, Kim D, Lee KJ, Nano Energy 2018, 51, 102.

[160]. Khan Y, Pavinatto FJ, Lin MC, Liao A, Swisher SL, Mann K, Subramanian V, Maharbiz MM, Arias AC, Adv. Funct. Mater 2016, 26, 1004.

[161]. Someya T, Sekitani T, Iba S, Kato Y, Kawaguchi H, Sakurai T, Proc. Natl. Acad. Sci 2004, 101, 9966. [PubMed: 15226508]

[162]. Someya T, Kato Y, Sekitani T, Proc. Natl. Acad. Sci. U. S. A 2005, 102, 12321. [PubMed: 16107541]

[163]. Tonelli AE, Polymer 2002, 43, 637.

[164]. Vlachopoulos J, Strutt D, Mater. Sci. Technol 2003, 19, 1161.

[165]. Riley A, in Packag. Technol (Eds.: Emblem A, Emblem H), Woodhead Publishing, 2012, pp. 310–360.

[166]. de Oliveira RF, Casalini S, Cramer T, Leonardi F, Ferreira M, Vinciguerra V, Casuscelli V, Alves N, Murgia M, Occhipinti L, Biscarini F, Flex. Print. Electron 2016, 1, 025005.

[167]. Schnitker J, Adly N, Seyock S, Bachmann B, Yakushenko A, Wolfrum B, Offenhäusser A, Adv. Biosyst 2018, 2, 1700136.

[168]. Swisher SL, Lin MC, Liao A, Leeflang EJ, Khan Y, Pavinatto FJ, Mann K, Naujokas A, Young D, Roy S, Harrison MR, Arias AC, Subramanian V, Maharbiz MM, Nat. Commun 2015, 6, 6575. [PubMed: 25779688]

[169]. Lu Q-H, Zheng F, in Adv. Polyim. Mater, Elsevier, 2018, pp. 195–255.

[170]. Constantin CP, Aflori M, Damian RF, Rusu RD, Materials 2019, 12, 3166.

[171]. Ghosh M, Polyimides: Fundamentals and Applications, 2018.

[172]. Wilson D, Stenzenberger HD, Hergenrother PM, Polyimides, Springer Netherlands, 1990.

[173]. Ji D, Li T, Hu W, Fuchs H, Adv. Mater 2019, 31, 1806070.

[174]. Mathews AS, Kim I, Ha C-S, Macromol. Res 2007, 15, 114.

[175]. Pakhuruddin MZ, Ibrahim K, Aziz AA, Optoelectron. Adv. Mater. - Rapid Commun 2013, 7, 377.

[176]. Seo J-M, Kim SJ, Chung H, Kim ET, Yu HG, Yu YS, Mater. Sci. Eng. C 2004, 24, 185.

[177]. Kuliasha CA, Judy JW, Adv. Mater. Technol 2021, 6, 2100149. [PubMed: 34632047]

[178]. Stenzenberger H, Br. Polym. J 1988, 20, 383.

[179]. Abbott A, Gibson T, Tandon GP, Hu L, Avakian R, Baur J, Koerner H, Addit. Manuf 2021, 37, 101636.

[180]. Dunson DL, Synthesis and Characterization of Thermosetting Polyimide Oligomers for Microelectronics Packaging, Ph.D, Virginia Polytechnic Institute and State University, 2000.

[181]. Shamma-Donoghue SA, May GA, Cotter NE, White RL, Simmons FB, IEEE Trans. Electron Devices 1982, 29, 136.

[182]. Fang H, Yu KJ, Gloschat C, Yang Z, Song E, Chiang C-H, Zhao J, Won SM, Xu S, Trumpis M, Zhong Y, Han SW, Xue Y, Xu D, Choi SW, Cauwenberghs G, Kay M, Huang Y, Viventi J, Efimov IR, Rogers JA, Nat. Biomed. Eng 2017, 1, 0038. [PubMed: 28804678]

[183]. Viventi J, Kim D-H, Moss JD, Kim Y-S, Blanco JA, Annetta N, Hicks A, Xiao J, Huang Y, Callans DJ, Rogers JA, Litt B, Sci. Transl. Med 2010, 2, 24ra22.

[184]. Viventi J, Kim D-H, Vigeland L, Frechette ES, Blanco JA, Kim Y-S, Avrin AE, Tiruvadi VR, Hwang S-W, Vanleer AC, Wulsin DF, Davis K, Gelber CE, Palmer L, Van der Spiegel J, Wu

J, Xiao J, Huang Y, Contreras D, Rogers JA, Litt B, Nat. Neurosci 2011, 14, 1599. [PubMed: 22081157]

[185]. Chiang C-H, Won SM, Orsborn AL, Yu KJ, Trumpis M, Bent B, Wang C, Xue Y, Min S, Woods V, Yu C, Kim BH, Kim SB, Huq R, Li J, Seo KJ, Vitale F, Richardson A, Fang H, Huang Y, Shepard K, Pesaran B, Rogers JA, Viventi J, Sci. Transl. Med 2020, 12, eaay4682. [PubMed: 32269166]

[186]. Xiang Z, Liu J, Lee C, Microsyst. Nanoeng 2016, 2, 1.

[187]. Vomero M, Porto Cruz MF, Zucchini E, Ciarpella F, Delfino E, Carli S, Boehler C, Asplund M, Ricci D, Fadiga L, Stieglitz T, Biomaterials 2020, 255, 120178. [PubMed: 32569863]

[188]. Collyer AA, Liquid Crystal Polymers: From Structures to Applications, Springer Netherlands, Dordrecht, 1993.

[189]. Noël C, Navard P, Prog. Polym. Sci 1991, 16, 55.

[190]. Fink JK, in High Perform. Polym. Second Ed (Ed.: Fink JK), William Andrew Publishing, 2014, pp. 381–400.

[191]. Bae SH, Che J-H, Seo J-M, Jeong J, Kim ET, Lee SW, Koo K, Suaning GJ, Lovell NH, “Dan” Cho D-I, Kim SJ, Chung H, Invest. Ophthalmol. Vis. Sci 2012, 53, 2653. [PubMed: 22427592]

[192]. Hwang G-T, Im D, Lee SE, Lee J, Koo M, Park SY, Kim S, Yang K, Kim SJ, Lee K, Lee KJ, ACS Nano 2013, 7, 4545. [PubMed: 23617401]

[193]. Jeong J, Bae SH, Seo J-M, Chung H, Kim SJ, J. Neural Eng 2016, 13, 025004. [PubMed: 26905477]

[194]. Rihani R, Tasnim N, Javed M, Usoro JO, D’Souza TM, Ware TH, Pancrazio JJ, Neuromodulation Technol. Neural Interface 2021, ner.13364.

[195]. Lee CJ, Oh SJ, Song JK, Kim SJ, Mater. Sci. Eng. C 2004, 24, 265.

[196]. Jeong J, Shin S, Lee GJ, Gwon TM, Park JH, Kim SJ, in 2013 35th Annu. Int. Conf. IEEE Eng. Med. Biol. Soc. EMBC, 2013, pp. 5295–5298.

[197]. GmbH Ticona, Vectra, Liquid Crystal Polymer (LCP) Brochure, 2001.

[198]. Wang J, Labes MM, Macromolecules 1992, 25, 5790.

[199]. Harvey AC, Lusignea RW, Rubin LS, Liquid Crystal Polymer Film, 1994, US5288529A.

[200]. Zhang T, Johnson W, Farrell B, Lawrence MS, in SPIE Proc. Ser, 2002, pp. 1–9.

[201]. Jeong J, Min KS, Kim SJ, Microelectron. Eng 2019, 216, 111096.

[202]. Marelli M, Divitini G, Collini C, Ravagnan L, Corbelli G, Ghisleri C, Gianfelice A, Lenardi C, Milani P, Lorenzelli L, J. Micromech. Microeng 2011, 21, 045013.

[203]. Altuna A, Menendez de la Prida L, Bellistri E, Gabriel G, Guimerá A, Berganzo J, Villa R, Fernández LJ, Biosens. Bioelectron 2012, 37, 1. [PubMed: 22633740]

[204]. Cho S-H, Lu HM, Cauller L, Romero-Ortega MI, Lee J-B, Hughes GA, IEEE Sens. J 2008, 8, 1830.

[205]. Zhang J, Tan KL, Gong HQ, Polym. Test 2001, 20, 693.

[206]. del Campo A, Greiner C, J. Micromech. Microeng 2007, 17, R81.

[207]. Lorenz H, Despont M, Fahrni N, Brugger J, Vettiger P, Renaud P, Sens. Actuators Phys 1998, 64, 33.

[208]. Keller S, Blagoi G, Lillemose M, Haefliger D, Boisen A, J. Micromech. Microeng 2008, 18, 125020.

[209]. Márton G, Tóth EZ, Wittner L, Fiáth R, Pinke D, Orbán G, Meszéna D, Pál I, Győri EL, Bereczki Z, Kandrács Á, Hofer KT, Pongrácz A, Ulbert I, Tóth K, Mater. Sci. Eng. C 2020, 112, 110870.

[210]. Nemani KV, Moodie KL, Brennick JB, Su A, Gimi B, Mater. Sci. Eng. C 2013, 33, 4453.

[211]. Baëtens T, Begard S, Pallecchi E, Thomy V, Arscott S, Halliez S, Mater. Today Commun 2020, 24, 101073.

[212]. Huang S-H, Lin S-P, Chen J-JJ, Sens. Actuators Phys 2014, 216, 257.

[213]. Schuhmann TG, Zhou T, Hong G, Lee JM, Fu T-M, Park H-G, Lieber CM, J. Vis. Exp 2018, 58003.

[214]. Zhou T, Hong G, Fu T-M, Yang X, Schuhmann TG, Viveros RD, Lieber CM, Proc. Natl. Acad. Sci 2017, 114, 5894. [PubMed: 28533392]

[215]. Fu T-M, Hong G, Zhou T, Schuhmann TG, Viveros RD, Lieber CM, Nat. Methods 2016, 13, 875. [PubMed: 27571550]

[216]. Golda-Cepa M, Engvall K, Hakkarainen M, Kotarba A, Prog. Org. Coat 2020, 140, 105493.

[217]. Hsu J-M, Rieth L, Normann RA, Tathireddy P, Solzbacher F, IEEE Trans. Biomed. Eng 2009, 56, 23. [PubMed: 19224715]

[218]. Seymour JP, Elkasabi YM, Chen H-Y, Lahann J, Kipke DR, Biomaterials 2009, 30, 6158. [PubMed: 19703712]

[219]. Kale V, Riley T, IEEE Trans. Parts Hybrids Packag 1977, 13, 273.

[220]. Khodagholy D, Gelinas JN, Thesen T, Doyle W, Devinsky O, Malliaras GG, Buzsáki G, Nat. Neurosci 2015, 18, 310. [PubMed: 25531570]

[221]. Li W, Rodger DC, Meng E, Weiland JD, Humayun MS, Tai Y-C, J. Microelectromech. Syst 2010, 19, 735.

[222]. Ortigoza-Diaz J, Scholten K, Larson C, Cobo A, Hudson T, Yoo J, Baldwin A, Weltman Hirschberg A, Meng E, Micromachines 2018, 9, 422.

[223]. Wang X, Hirschberg AW, Xu H, Slingsby-Smith Z, Lecomte A, Scholten K, Song D, Meng E, J. Microelectromech. Syst 2020, 29, 499.

[224]. Fortin JB, Lu T-M, Chemical Vapor Deposition Polymerization: The Growth and Properties of Parylene Thin Films, Kluwer Academic Publishers, Boston, 2004.

[225]. Shih VC-Y, Harder TA, Tai Y-C, in Symp. Des. Test Integr. Packag. MEMSMOEMS 2003, 2003, pp. 394–398.

[226]. del Valle J, de la Oliva N, Müller M, Stieglitz T, Navarro X, in 2015 7th Int. IEEEEMBS Conf. Neural Eng. NER, 2015, pp. 442–445.

[227]. Mandelli JS, Koepp J, Hama A, Sanaur S, Rae GA, Rambo CR, Biomed. Microdevices 2021, 23, 2. [PubMed: 33386434]

[228]. Kim BJ, Chen B, Gupta M, Meng E, J. Micromech. Microeng 2014, 24, 065003.

[229]. Kim BJ, Chen B, Gupta M, Meng E, in 2013 IEEE 26th Int. Conf. Micro. Electro. Mech. Syst. MEMS, 2013, pp. 339–342.

[230]. Williams KR, Gupta K, Wasilik M, J. Microelectromech. Syst 2003, 12, 761.

[231]. Noh H-S, Huang Y, Hesketh PJ, Sens. Actuators B Chem 2004, 102, 78.

[232]. Wang X-Q, Lin Q, Tai Y-C, in Tech. Dig. IEEE Int. MEMS 99 Conf. Twelfth IEEE Int. Conf. Micro Electro Mech. Syst. Cat No99CH36291, 1999, pp. 177–182.

[233]. Morikawa Y, Yamagiwa S, Sawahata H, Numano R, Koida K, Ishida M, Kawano T, Adv. Healthc. Mater 2018, 7, 1701100.

[234]. Zhao Z, Kim E, Luo H, Zhang J, Xu Y, J. Micromech. Microeng 2017, 28, 015012.

[235]. Rodger D, Fong A, Li W, Ameri H, Ahuja A, Gutierrez C, Lavrov I, Zhong H, Menon P, Meng E, Sens. Actuators B Chem 2008, 132, 449.

[236]. Kim BJ, Kuo JTW, Hara SA, Lee CD, Yu L, Gutierrez CA, Hoang TQ, Pikov V, Meng E, J. Neural Eng 2013, 10, 045002. [PubMed: 23723130]

[237]. Kuo JTW, Kim BJ, Hara SA, Lee CD, Gutierrez CA, Hoang TQ, Meng E, Lab Chip 2013, 13, 554. [PubMed: 23160191]

[238]. Hara SA, Kim BJ, Kuo JTW, Lee CD, Meng E, Pikov V, J. Neural Eng 2016, 13, 066020. [PubMed: 27819256]

[239]. Berggren M, Richter-Dahlfors A, Adv. Mater 2007, 19, 3201.

[240]. Fang Y, Li X, Fang Y, J. Mater. Chem. C 2015, 3, 6424.

[241]. Marszalek T, Gazicki-Lipman M, Ulanski J, Beilstein J. Nanotechnol 2017, 8, 1532. [PubMed: 28884059]

[242]. Zhang S, Hubis E, Tomasello G, Soliveri G, Kumar P, Cicoira F, Chem. Mater 2017, 29, 3126.

[243]. Khodagholy D, Doublet T, Quilichini P, Gurfinkel M, Leleux P, Ghestem A, Ismailova E, Hervé T, Sanaur S, Bernard C, Malliaras GG, Nat. Commun 2013, 4, 1575. [PubMed: 23481383]

[244]. Chamanzar M, Denman DJ, Blanche TJ, Maharbiz MM, in 2015 28th IEEE Int. Conf. Micro Electro Mech. Syst. MEMS, 2015, pp. 682–685.

[245]. Yamagiwa S, Ishida M, Kawano T, Appl. Phys. Lett 2015, 107, 083502.

[246]. Reddy JW, Lassiter M, Chamanzar M, Microsyst. Nanoeng 2020, 6, 1. [PubMed: 34567616]

[247]. Machorro R, Regalado LE, Siqueiros JM, Appl. Opt 1991, 30, 2778. [PubMed: 20700274]

[248]. Kim D, Yokota T, Suzuki T, Lee S, Woo T, Yukita W, Koizumi M, Tachibana Y, Yawo H, Onodera H, Sekino M, Someya T, Proc. Natl. Acad. Sci 2020, 117, 21138. [PubMed: 32817422]

[249]. Ortigoza-Diaz J, Scholten K, Meng E, J. Microelectromech. Syst 2018, 27, 874.

[250]. Yu X, Mahajan BK, Shou W, Pan H, Micromachines 2017, 8, 7.

[251]. Joshipura ID, Finn M, Tan STM, Dickey MD, Lipomi DJ, MRS Bull 2017, 42, 960.

[252]. Koo JH, Song J-K, Kim D-H, Son D, ACS Mater. Lett 2021, 1528.

[253]. Kim J, Ghaffari R, Kim D-H, Nat. Biomed. Eng 2017, 1, 1.

[254]. Bolonduro OA, Duffy BM, Rao AA, Black LD, Timko BP, Nano Res 2020, 13, 1253.

[255]. Tan E, Jing Q, Smith M, Kar-Narayan S, Occhipinti L, MRS Adv 2017, 2, 1721.

[256]. Nyns ECA, Poelma RH, Volkers L, Plomp JJ, Bart CI, Kip AM, van Brakel TJ, Zeppenfeld K, Schalij MJ, Zhang GQ, de Vries AAF, Pijnappels DA, Sci. Transl. Med 2019, 11, eaau6447. [PubMed: 30814339]

[257]. Shit SC, Shah P, Natl. Acad. Sci. Lett 2013, 36, 355.

[258]. Brandrup J, Immergut EH, Grulke EA, Eds., Polymer Handbook, 4th Edition, Wiley, New York ; Chichester, 2004.

[259]. Kučera M, Láníková J, J. Polym. Sci 1961, 54, 375.

[260]. Camino G, Lomakin SM, Lazzari M, Polymer 2001, 42, 2395.

[261]. Rościszewski P, Łukasiak J, Dorosz A, Galiński J, Szponar M, Macromol. Symp 1998, 130, 337.

[262]. Ratner BD, Ed., Biomaterials Science: An Introduction to Materials in Medicine, Elsevier/ Academic Press, Amsterdam ; Boston, 2013.

[263]. Brindley GS, Polkey CE, Rushton DN, Cardozo L, J. Neurol. Neurosurg. Psychiatry 1986, 49, 1104. [PubMed: 3491180]

[264]. Rodeheaver N, Herbert R, Kim Y, Mahmood M, Kim H, Jeong J, Yeo W, Adv. Funct. Mater 2021, 2104070.

[265]. Qi D, Zhang K, Tian G, Jiang B, Huang Y, Adv. Mater 2021, 33, 2003155.

[266]. Jang T-M, Lee JH, Zhou H, Joo J, Lim BH, Cheng H, Kim SH, Kang I-S, Lee K-S, Park E, Hwang S-W, Sci. Adv 2020, 6, eabc9675. [PubMed: 33177091]

[267]. Xu S, Yan Z, Jang K-I, Huang W, Fu H, Kim J, Wei Z, Flavin M, McCracken J, Wang R, Badea A, Liu Y, Xiao D, Zhou G, Lee J, Chung HU, Cheng H, Ren W, Banks A, Li X, Paik U, Nuzzo RG, Huang Y, Zhang Y, Rogers JA, Science 2015, 347, 154. [PubMed: 25574018]

[268]. Kim D-H, Ahn J-H, Choi WM, Kim H-S, Kim T-H, Song J, Huang YY, Liu Z, Lu C, Rogers JA, Science 2008, 320, 507. [PubMed: 18369106]

[269]. Lacour SP, Chan D, Wagner S, Li T, Suo ZG, Appl. Phys. Lett 2006, 88, DOI 10.1063/1.2201874.

[270]. Fan JA, Yeo W-H, Su Y, Hattori Y, Lee W, Jung S-Y, Zhang Y, Liu Z, Cheng H, Falgout L, Bajema M, Coleman T, Gregoire D, Larsen RJ, Huang Y, Rogers JA, Nat. Commun 2014, 5, 3266. [PubMed: 24509865]

[271]. Afanasenkau D, Kalinina D, Lyakhovetskii V, Tondera C, Gorsky O, Moosavi S, Pavlova N, Merkulyeva N, Kalueff AV, Minev IR, Musienko P, Nat. Biomed. Eng 2020, 4, 1010. [PubMed: 32958898]

[272]. Tokachichu DR, Bhushan B, IEEE Trans. Nanotechnol 2006, 5, 228.

[273]. Jeong SH, Zhang S, Hjort K, Hilborn J, Wu Z, Adv. Mater 2016, 28, 5830. [PubMed: 27167137]

[274]. Choi KM, Rogers JA, J. Am. Chem. Soc 2003, 125, 4060. [PubMed: 12670222]

[275]. Fu SY, Gordon T, Mol. Neurobiol 1997, 14, 67. [PubMed: 9170101]

[276]. Liu Y, Li J, Song S, Kang J, Tsao Y, Chen S, Mottini V, McConnell K, Xu W, Zheng Y-Q, Tok JB-H, George PM, Bao Z, Nat. Biotechnol 2020, 38, 1031. [PubMed: 32313193]

[277]. Döhler D, Kang J, Cooper CB, Tok JB-H, Rupp H, Binder WH, Bao Z, ACS Appl. Polym. Mater 2020, 2, 4127.

[278]. Liu K, Jiang Y, Bao Z, Yan X, CCS Chem 2019, 1, 431.

[279]. Tang X, Wang B, Eristoff S, Zhang H, Bettinger CJ, Macromol. Rapid Commun 2020, 41, 1900551.

[280]. Tang X, Bettinger CJ, J. Mater. Chem. B 2018, 6, 545. [PubMed: 29657715]

[281]. Zhu C, Bettinger CJ, Macromolecules 2015, 48, 1563.

[282]. Otsuka H, Nagasaki Y, Kataoka K, Curr. Opin. Colloid Interface Sci 2001, 6, 3.

[283]. Kutikov AB, Song J, ACS Biomater. Sci. Eng 2015, 1, 463. [PubMed: 27175443]

[284]. You I, Kong M, Jeong U, Acc. Chem. Res 2019, 52, 63. [PubMed: 30586291]

[285]. Bates FS, Fredrickson GH, Phys. Today 1999, 52, 32.

[286]. The Physics of Block Copolymers, Oxford University Press, Oxford, New York, 1999.

[287]. Lazzari M, Liu G, Lecommandoux S, Eds., Block Copolymers in Nanoscience, Wiley-VCH ; John Wiley, Weinheim : Chichester, 2006.

[288]. Torres VM, LaNasa JA, Vogt BD, Hickey RJ, Soft Matter 2021, 17, 1505. [PubMed: 33355580]

[289]. Hamley IW, Ed., Developments in Block Copolymer Science and Technology, J Wiley Chichester, West Sussex ; Hoboken, NJ, 2004.

[290]. Alexandridis P, Spontak RJ, Curr. Opin. Colloid Interface Sci 1999, 4, 130.

[291]. Wang Y, Yokota T, Someya T, NPG Asia Mater 2021, 13, 1.

[292]. Fong H, Reneker DH, J. Polym. Sci. Part B Polym. Phys 1999, 37, 3488.

[293]. Chen L, Wang S, Yu Q, Topham PD, Chen C, Wang L, Soft Matter 2019, 15, 2490. [PubMed: 30860535]

[294]. Molina-Lopez F, Gao TZ, Kraft U, Zhu C, Öhlund T, Pfattner R, Feig VR, Kim Y, Wang S, Yun Y, Bao Z, Nat. Commun 2019, 10, 2676. [PubMed: 31213599]

[295]. Cho S, Song JH, Kong M, Shin S, Kim Y-T, Park G, Park C-G, Shin TJ, Myoung J, Jeong U, ACS Appl. Mater. Interfaces 2017, 9, 44096. [PubMed: 29181972]

[296]. Hayashi M, Matsushima S, Noro A, Matsushita Y, Macromolecules 2015, 48, 421.

[297]. Sridharan A, Rajan SD, Muthuswamy J, J. Neural Eng 2013, 10, 066001. [PubMed: 24099854]

[298]. Salatino JW, Ludwig KA, Kozai TDY, Purcell EK, Nat. Biomed. Eng 2017, 1, 862. [PubMed: 30505625]

[299]. Parker KK, Ingber DE, Philos. Trans. R. Soc. B Biol. Sci 2007, 362, 1267.

[300]. Urbanczyk M, Layland SL, Schenke-Layland K, Matrix Biol 2020, 85–86, 1.

[301]. Frantz C, Stewart KM, Weaver VM, J. Cell Sci 2010, 123, 4195. [PubMed: 21123617]

[302]. Fomovsky GM, Thomopoulos S, Holmes JW, J. Mol. Cell. Cardiol 2010, 48, 490. [PubMed: 19686759]

[303]. Nicolas J, Magli S, Rabbachin L, Sampaolesi S, Nicotra F, Russo L, Biomacromolecules 2020, 21, 1968. [PubMed: 32227919]

[304]. Spencer KC, Sy JC, Ramadi KB, Graybiel AM, Langer R, Cima MJ, Sci. Rep 2017, 7, 1952. [PubMed: 28512291]

[305]. Rao L, Zhou H, Li T, Li C, Duan YY, Acta Biomater 2012, 8, 2233. [PubMed: 22406507]

[306]. Winter JO, Cogan SF, Rizzo JF, J. Biomed. Mater. Res. B Appl. Biomater 2007, 81B, 551.

[307]. Liu J, Qu S, Suo Z, Yang W, Natl. Sci. Rev 2021, 8, nwaa254. [PubMed: 34691578]

[308]. Goding J, Vallejo-Giraldo C, Syed O, Green R, J. Mater. Chem. B 2019, 7, 1625. [PubMed: 32254905]

[309]. Golabchi A, Wu B, Cao B, Bettinger CJ, Cui XT, Biomaterials 2019, 225, 119519. [PubMed: 31600673]

[310]. Trel'ová D, Salgarella AR, Ricotti L, Giudetti G, Cutrone A, Šrámková P, Zahoranová A, Chorvát D, Haško D, Canale C, Micera S, Kronek J, Menciassi A, Lacík I, Langmuir 2019, 35, 1085. [PubMed: 29792034]

[311]. Lee Y, Song WJ, Sun J-Y, Mater. Today Phys 2020, 15, 100258.

[312]. Fan H, Gong JP, Macromolecules 2020, 53, 2769.

[313]. Liu X, Liu J, Lin S, Zhao X, Mater. Today 2020, 36, 102.

[314]. Lu B, Yuk H, Lin S, Jian N, Qu K, Xu J, Zhao X, Nat. Commun 2019, 10, 1043. [PubMed: 30837483]

[315]. Yuk H, Lu B, Lin S, Qu K, Xu J, Luo J, Zhao X, Nat. Commun 2020, 11, 1604. [PubMed: 32231216]

[316]. Sridhar V, Takahata K, Sens. Actuators Phys 2009, 155, 58.

[317]. Yin Chin S, Cheung Poh Y, Kohler A-C, Compton JT, Hsu LL, Lau KM, Kim S, Lee BW, Lee FY, Sia SK, Sci. Robot 2017, 2, eaah6451. [PubMed: 31289767]

[318]. Jo YJ, Kwon KY, Khan ZU, Crispin X, Kim T, ACS Appl. Mater. Interfaces 2018, 10, 39083. [PubMed: 30360103]

[319]. Qi J, Wang AC, Yang W, Zhang M, Hou C, Zhang Q, Li Y, Wang H, Nano Energy 2020, 67, 104206.

[320]. Yang C, Suo Z, Nat. Rev. Mater 2018, 3, 125.

[321]. Sekine S, Ido Y, Miyake T, Nagamine K, Nishizawa M, J. Am. Chem. Soc 2010, 132, 13174. [PubMed: 20825188]

[322]. Ido Y, Takahashi D, Sasaki M, Nagamine K, Miyake T, Jasinski P, Nishizawa M, ACS Macro Lett 2012, 1, 400.

[323]. Sasaki M, Karikkineth BC, Nagamine K, Kaji H, Torimitsu K, Nishizawa M, Adv. Healthc. Mater 2014, 3, 1919. [PubMed: 24912988]

[324]. Wu H, Sariola V, Zhu C, Zhao J, Sitti M, Bettinger CJ, Adv. Mater 2015, 27, 3398. [PubMed: 25903565]

[325]. D'souza AA, Shegokar R, Expert Opin. Drug Deliv 2016, 13, 1257. [PubMed: 27116988]

[326]. Veronese FM, Pasut G, Drug Discov. Today 2005, 10, 1451. [PubMed: 16243265]

[327]. Hutanu D, Mod. Chem. Appl 2014, 02, 1.

[328]. Zhu J, Biomaterials 2010, 31, 4639. [PubMed: 20303169]

[329]. North MA, Del Grosso CA, Wilker JJ, ACS Appl. Mater. Interfaces 2017, 9, 7866. [PubMed: 28177600]

[330]. Han L, Lu X, Liu K, Wang K, Fang L, Weng L-T, Zhang H, Tang Y, Ren F, Zhao C, Sun G, Liang R, Li Z, ACS Nano 2017, 11, 2561. [PubMed: 28245107]

[331]. Lake GJ, Rubber Chem. Technol 1995, 68, 435.

[332]. Gaharwar AK, Dammu SA, Canter JM, Wu C-J, Schmidt G, Biomacromolecules 2011, 12, 1641. [PubMed: 21413708]

[333]. Haraguchi K, Takehisa T, Adv. Mater 2002, 14, 1120.

[334]. Okumura Y, Ito K, Adv. Mater 2001, 13, 485.

[335]. Illeperuma WRK, Sun J-Y, Suo Z, Vlassak JJ, Extreme Mech. Lett 2014, 1, 90.

[336]. Liu Y, Yang T, Zhang Y, Qu G, Wei S, Liu Z, Kong T, Adv. Mater 2019, 31, 1902783.

[337]. Carvalho FM, Lopes P, Carneiro M, Serra A, Coelho J, de Almeida AT, Tavakoli M, ACS Appl. Electron. Mater 2020, 2, 3390.

[338]. Kim D-H, Kim Y-S, Amsden J, Panilaitis B, Kaplan DL, Omenetto FG, Zakin MR, Rogers JA, Appl. Phys. Lett 2009, 95, 133701. [PubMed: 20145699]

[339]. Hwang S-W, Tao H, Kim D-H, Cheng H, Song J-K, Rill E, Brenckle MA, Panilaitis B, Won SM, Kim Y-S, Song YM, Yu KJ, Ameen A, Li R, Su Y, Yang M, Kaplan DL, Zakin MR, Slepian MJ, Huang Y, Omenetto FG, Rogers JA, Science 2012, 337, 1640. [PubMed: 23019646]

[340]. Choi YS, Hsueh Y-Y, Koo J, Yang Q, Avila R, Hu B, Xie Z, Lee G, Ning Z, Liu C, Xu Y, Lee YJ, Zhao W, Fang J, Deng Y, Lee SM, Vázquez-Guardado A, Stepien I, Yan Y, Song JW, Haney C, Oh YS, Liu W, Yoon H-J, Banks A, MacEwan MR, Ameer GA, Ray WZ, Huang Y, Xie T, Franz CK, Li S, Rogers JA, Nat. Commun 2020, 11, 5990. [PubMed: 33239608]

[341]. Bettinger CJ, Bao Z, Adv. Mater 2010, 22, 651. [PubMed: 20217767]

[342]. Zhao D, Zhu Y, Cheng W, Chen W, Wu Y, Yu H, Adv. Mater 2021, 33, 2000619.

[343]. Uva A, Lin A, Babi J, Tran H, J. Chem. Technol. Biotechnol 2021, jctb.6790.

[344]. Singh R, Bathaei MJ, Istif E, Beker L, Adv. Healthc. Mater 2020, 9, 2000790.

[345]. Jin Tan M, Owh C, Lin Chee P, Ko Kyaw AK, Kai D, Jun Loh X, J. Mater. Chem. C 2016, 4, 5531.

[346]. Hosseini ES, Dervin S, Ganguly P, Dahiya R, ACS Appl. Bio Mater 2021, 4, 163.

[347]. Cha GD, Kang D, Lee J, Kim D-H, Adv. Healthc. Mater 2019, 8, 1801660.

[348]. Wang C, Xia K, Zhang Y, Kaplan DL, Acc. Chem. Res 2019, 52, 2916. [PubMed: 31536330]

[349]. Altman GH, Diaz F, Jakuba C, Calabro T, Horan RL, Chen J, Lu H, Richmond J, Kaplan DL, Biomaterials 2003, 24, 401. [PubMed: 12423595]

[350]. Yucel T, Lovett ML, Kaplan DL, J. Controlled Release 2014, 190, 381.

[351]. Wray LS, Hu X, Gallego J, Georgakoudi I, Omenetto FG, Schmidt D, Kaplan DL, J. Biomed. Mater. Res. B Appl. Biomater 2011, 99B, 89.

[352]. Janani G, Kumar M, Chouhan D, Moses JC, Gangrade A, Bhattacharjee S, Mandal BB, ACS Appl. Bio Mater 2019, 2, 5460.

[353]. Johari N, Moroni L, Samadikuchaksaraei A, Eur. Polym. J 2020, 134, 109842.

[354]. Patil AC, Xiong Z, Thakor NV, Small Methods 2020, 4, 2000274.

[355]. Thurber AE, Omenetto FG, Kaplan DL, Biomaterials 2015, 71, 145. [PubMed: 26322725]

[356]. Partlow BP, Hanna CW, Rnjak-Kovacina J, Moreau JE, Applegate MB, Burke KA, Marelli B, Mitropoulos AN, Omenetto FG, Kaplan DL, Adv. Funct. Mater 2014, 24, 4615. [PubMed: 25395921]

[357]. Barreiro DL, Yeo J, Tarakanova A, Martin-Martinez FJ, Buehler MJ, Macromol. Biosci 2019, 19, 1800253.

[358]. Cao Y, Wang B, Int. J. Mol. Sci 2009, 10, 1514. [PubMed: 19468322]

[359]. Hofmann S, Wong Po Foo CT, Rossetti F, Textor M, Vunjak-Novakovic G, Kaplan DL, Merkle HP, Meinel L, J. Controlled Release 2006, 111, 219.

[360]. Xie C, Li W, Liang Q, Yu S, Li L, Appl. Surf. Sci 2019, 492, 55.

[361]. Horan RL, Antle K, Collette AL, Wang Y, Huang J, Moreau JE, Volloch V, Kaplan DL, Altman GH, Biomaterials 2005, 26, 3385. [PubMed: 15621227]

[362]. Jiang C, Wang X, Gunawidjaja R, Lin Y-H, Gupta MK, Kaplan DL, Naik RR, Tsukruk VV, Adv. Funct. Mater 2007, 17, 2229.

[363]. Qi Y, Wang H, Wei K, Yang Y, Zheng R-Y, Kim I, Zhang K-Q, Int. J. Mol. Sci 2017, 18, 237.

[364]. Zhu B, Wang H, Leow WR, Cai Y, Loh XJ, Han M-Y, Chen X, Adv. Mater 2016, 28, 4250. [PubMed: 26684370]

[365]. Wen D-L, Sun D-H, Huang P, Huang W, Su M, Wang Y, Han M-D, Kim B, Brugger J, Zhang H-X, Zhang X-S, Microsyst. Nanoeng 2021, 7, 1. [PubMed: 34567721]

[366]. Mitropoulos AN, Marelli B, Ghezzi CE, Applegate MB, Partlow BP, Kaplan DL, Omenetto FG, ACS Biomater. Sci. Eng 2015, 1, 964. [PubMed: 33429527]

[367]. Kim S, Marelli B, Brenckle MA, Mitropoulos AN, Gil E-S, Tsioris K, Tao H, Kaplan DL, Omenetto FG, Nat. Nanotechnol 2014, 9, 306. [PubMed: 24658173]

[368]. Liu J, Shao J, Zheng J, J. Appl. Polym. Sci 2004, 91, 2028.

[369]. Chen M, Fu X, Chen Z, Liu J, Zhong W-H, Adv. Funct. Mater 2021, 31, 2006744.

[370]. Zheng M, Wang X, Yue O, Hou M, Zhang H, Beyer S, Blocki AM, Wang Q, Gong G, Liu X, Guo J, Biomaterials 2021, 276, 121026. [PubMed: 34298443]

[371]. Zhang S, Chen Y, Liu H, Wang Z, Ling H, Wang C, Ni J, Çelebi-Saltik B, Wang X, Meng X, Kim H, Baidya A, Ahadian S, Ashammakhi N, Dokmeci MR, Travas-Sejdic J, Khademhosseini A, Adv. Mater 2020, 32, 1904752.

[372]. Ding S, Jiang Z, Chen F, Fu L, Lv Y, Qian Y, Zhao S, ACS Appl. Mater. Interfaces 2020, 12, 27572. [PubMed: 32453541]

[373]. Ren K, Cheng Y, Huang C, Chen R, Wang Z, Wei J, J. Mater. Chem. B 2019, 7, 5704. [PubMed: 31482926]

[374]. Moreno S, Keshtkar J, Rodriguez-Davila RA, Bazaid A, Ibrahim H, Rodriguez BJ, Quevedo-Lopez MA, Minary-Jolandan M, Adv. Electron. Mater 2020, 6, 2000391.

[375]. Shasteen C, Choy YB, Biomed. Eng. Lett 2011, 1, 163.

[376]. Budhian A, Siegel SJ, Winey KI, Int. J. Pharm 2008, 346, 151. [PubMed: 17681683]

[377]. Son D, Lee J, Lee DJ, Ghaffari R, Yun S, Kim SJ, Lee JE, Cho HR, Yoon S, Yang S, Lee S, Qiao S, Ling D, Shin S, Song J-K, Kim J, Kim T, Lee H, Kim J, Soh M, Lee N, Hwang CS, Nam S, Lu N, Hyeon T, Choi SH, Kim D-H, ACS Nano 2015, 9, 5937. [PubMed: 25905457]

[378]. Hwang S-W, Song J-K, Huang X, Cheng H, Kang S-K, Kim BH, Kim J-H, Yu S, Huang Y, Rogers JA, Adv. Mater 2014, 26, 3905. [PubMed: 24692101]

[379]. Yu KJ, Kuzum D, Hwang S-W, Kim BH, Juul H, Kim NH, Won SM, Chiang K, Trumpis M, Richardson AG, Cheng H, Fang H, Thompson M, Bink H, Talos D, Seo KJ, Lee HN, Kang S-K, Kim J-H, Lee JY, Huang Y, Jensen FE, Dichter MA, Lucas TH, Viventi J, Litt B, Rogers JA, Nat. Mater 2016, 15, 782. [PubMed: 27088236]

[380]. Kang S-K, Murphy RKJ, Hwang S-W, Lee SM, Harburg DV, Krueger NA, Shin J, Gamble P, Cheng H, Yu S, Liu Z, McCall JG, Stephen M, Ying H, Kim J, Park G, Webb RC, Lee CH, Chung S, Wie DS, Gujar AD, Vemulapalli B, Kim AH, Lee K-M, Cheng J, Huang Y, Lee SH, Braun PV, Ray WZ, Rogers JA, Nature 2016, 530, 71. [PubMed: 26779949]

[381]. Choi YS, Yin RT, Pfenniger A, Koo J, Avila R, Benjamin Lee K, Chen SW, Lee G, Li G, Qiao Y, Murillo-Berlioz A, Kiss A, Han S, Lee SM, Li C, Xie Z, Chen Y-Y, Burrell A, Geist B, Jeong H, Kim J, Yoon H-J, Banks A, Kang S-K, Zhang ZJ, Haney CR, Sahakian AV, Johnson D, Efimova T, Huang Y, Trachiotis GD, Knight BP, Arora RK, Efimov IR, Rogers JA, Nat. Biotechnol 2021, 1. [PubMed: 33376248]

[382]. Yang J, Webb AR, Pickerill SJ, Hageman G, Ameer GA, Biomaterials 2006, 27, 1889. [PubMed: 16290904]

[383]. Yang J, Webb AR, Ameer GA, Adv. Mater 2004, 16, 511.

[384]. Kang Y, Yang J, Khan S, Anissian L, Ameer GA, J. Biomed. Mater. Res. A 2006, 77A, 331.

[385]. Serrano MC, Carbajal L, Ameer GA, Adv. Mater 2011, 23, 2211. [PubMed: 21557337]

[386]. Hwang S-W, Lee CH, Cheng H, Jeong J-W, Kang S-K, Kim J-H, Shin J, Yang J, Liu Z, Ameer GA, Huang Y, Rogers JA, Nano Lett 2015, 15, 2801. [PubMed: 25706246]

[387]. Lecomte A, Descamps E, Bergaud C, J. Neural Eng 2018, 15, 031001. [PubMed: 28885187]

[388]. Lo M, Wang S, Singh S, Damodaran VB, Ahmed I, Coffey K, Barker D, Saste K, Kals K, Kaplan HM, Kohn J, Shreiber DI, Zahn JD, J. Neural Eng 2018, 15, 036002. [PubMed: 29485103]

[389]. Lecomte A, Castagnola V, Descamps E, Dahan L, Blatché MC, Dinis TM, Leclerc E, Egles C, Bergaud C, J. Micromech. Microeng 2015, 25, 125003.

[390]. Tien LW, Wu F, Tang-Schomer MD, Yoon E, Omenetto FG, Kaplan DL, Adv. Funct. Mater 2013, 23, 3185.

[391]. Biran R, Martin DC, Tresco PA, Exp. Neurol 2005, 195, 115. [PubMed: 16045910]

[392]. Jorfi M, Skousen JL, Weder C, Capadona JR, J. Neural Eng 2014, 12, 011001. [PubMed: 25460808]

[393]. Jeong J-W, Shin G, Park SI, Yu KJ, Xu L, Rogers JA, Neuron 2015, 86, 175. [PubMed: 25856493]

[394]. Harris JP, Hess AE, Rowan SJ, Weder C, Zorman CA, Tyler DJ, Capadona JR, J. Neural Eng 2011, 8, 046010. [PubMed: 21654037]

[395]. Haj Hosseini N, Hoffmann R, Kisban S, Stieglitz T, Paul O, Ruther P, in 2007 29th Annu. Int. Conf. IEEE Eng. Med. Biol. Soc, IEEE, Lyon, 2007, pp. 4711–4714.

[396]. Singh S, Lo M-C, Damodaran VB, Kaplan HM, Kohn J, Zahn JD, Shreiber DI, Sensors 2016, 16, 330.

[397]. Smith Z, Mechanical Characterization of Compliant Neural Probes, Their Insertion Regimes and a Rule of Thumb Design, 2019.

[398]. Shoffstall AJ, Srinivasan S, Willis M, Stiller AM, Ecker M, Voit WE, Pancrazio JJ, Capadona JR, Sci. Rep 2018, 8, 122. [PubMed: 29317748]

[399]. He F, Lycke R, Ganji M, Xie C, Luan L, iScience 2020, 23, 101387. [PubMed: 32745989]

[400]. Hosseini SM, Rihani R, Batchelor B, Stiller AM, Pancrazio JJ, Voit WE, Ecker M, Front. Mater 2018, 5, 66.

[401]. Zátonyi A, Orbán G, Modi R, Márton G, Meszéna D, Ulbert I, Pongrácz A, Ecker M, Voit WE, Joshi-Imre A, Fekete Z, Sci. Rep 2019, 9, 2321. [PubMed: 30787389]

[402]. Agorelius J, Tsanakalis F, Friberg A, Thorbergsson PT, Pettersson LME, Schouenborg J, Front. Neurosci 2015, 9, DOI 10.3389/fnins.2015.00331.

[403]. Shen W, Karumbaiah L, Liu X, Saxena T, Chen S, Patkar R, Bellamkonda RV, Allen MG, Microsyst. Nanoeng 2015, 1, 1.

[404]. Lind G, Linsmeier CE, Thelin J, Schouenborg J, J. Neural Eng 2010, 7, 046005. [PubMed: 20551508]

[405]. Lo M, Wang S, Singh S, Damodaran VB, Kaplan HM, Kohn J, Shreiber DI, Zahn JD, Biomed. Microdevices 2015, 17, 34. [PubMed: 25681971]

[406]. Capadona JR, Shanmuganathan K, Tyler DJ, Rowan SJ, Weder C, Science 2008, 319, 1370. [PubMed: 18323449]

[407]. Nguyen JK, Park DJ, Skousen JL, Hess-Dunning AE, Tyler DJ, Rowan SJ, Weder C, Capadona JR, J. Neural Eng 2014, 11, 056014. [PubMed: 25125443]

[408]. Hess-Dunning A, Tyler DJ, Micromachines 2018, 9, 583.

[409]. Hoyle CE, Bowman CN, Angew. Chem. Int. Ed 2010, 49, 1540.

[410]. Nair DP, Cramer NB, Scott TF, Bowman CN, Shandas R, Polymer 2010, 51, 4383. [PubMed: 21072253]

[411]. Ware T, Simon D, Arreaga-Salas DE, Reeder J, Rennaker R, Keefer EW, Voit W, Adv. Funct. Mater 2012, 22, 3470.

[412]. Ware T, Simon D, Hearon K, Liu C, Shah S, Reeder J, Khodaparast N, Kilgard MP, Maitland DJ, Rennaker RL, Voit WE, Macromol. Mater. Eng 2012, 297, 1193. [PubMed: 25530708]

[413]. Ware T, Simon D, Hearon K, Kang TH, Maitland DJ, Voit W, Macromol. Biosci 2013, 13, 1640. [PubMed: 24115484]

[414]. Do D-H, Ecker M, Voit WE, ACS Omega 2017, 2, 4604. [PubMed: 30023725]

[415]. Shoffstall AJ, Ecker M, Danda V, Joshi-Imre A, Stiller A, Yu M, Paiz JE, Mancuso E, Bedell HW, Voit WE, Pancrazio JJ, Capadona JR, Micromachines 2018, 9, 486.

[416]. Ware T, Simon D, Liu C, Musa T, Vasudevan S, Sloan A, Keefer EW, Rennaker RL, Voit W, J. Biomed. Mater. Res. B Appl. Biomater 2014, 102, 1. [PubMed: 23666562]

[417]. White TJ, Broer DJ, Nat. Mater 2015, 14, 1087. [PubMed: 26490216]

[418]. Nguyen T-S, Selinger JV, Eur. Phys. J. E 2017, 40, 76. [PubMed: 28913812]

[419]. Warner M, Terentjev EM, Liquid Crystal Elastomers, OUP Oxford, 2007.

[420]. Bladon P, Terentjev EM, Warner M, Phys. Rev. E 1993, 47, R3838.

[421]. Broer D, Crawford GP, Zumer S, Cross-Linked Liquid Crystalline Systems: From Rigid Polymer Networks to Elastomers, CRC Press, 2011.

[422]. Iqbal D, Samiullah M, Materials 2013, 6, 116. [PubMed: 28809298]

[423]. Wang Z, Cai S, J. Mater. Chem. B 2020, 8, 6610. [PubMed: 32555841]

[424]. White TJ, J. Polym. Sci. Part B Polym. Phys 2018, 56, 695.

[425]. Ware TH, White TJ, Polym. Chem 2015, 6, 4835.

[426]. Wei W-S, Xia Y, Ettinger S, Yang S, Yodh AG, Nature 2019, 576, 433. [PubMed: 31853082]

[427]. McCracken JM, Donovan BR, Lynch KM, White TJ, Adv. Funct. Mater 2021, 31, 2100564.

[428]. Martinez AM, McBride MK, White TJ, Bowman CN, Adv. Funct. Mater 2020, 30, 2003150.

[429]. Jia Y, Zhang B, Zhou E, Feng Z, Zang B, J. Appl. Polym. Sci 2002, 85, 1104.

[430]. Maeng J, Rihani RT, Javed M, Rajput JS, Kim H, Bouton IG, Criss TA, Pancrazio JJ, Black BJ, Ware TH, J. Mater. Chem. B 2020, 8, 6286. [PubMed: 32315020]

[431]. Ware TH, McConney ME, Wie JJ, Tondiglia VP, White TJ, Science 2015, 347, 982. [PubMed: 25722408]

[432]. Roach DJ, Kuang X, Yuan C, Chen K, Qi HJ, Smart Mater. Struct 2018, 27, 125011.

[433]. Ambulo CP, Burroughs JJ, Boothby JM, Kim H, Shankar MR, Ware TH, ACS Appl. Mater. Interfaces 2017, 9, 37332. [PubMed: 28967260]

[434]. Ware TH, Biggins JS, Shick AF, Warner M, White TJ, Nat. Commun 2016, 7, 10781. [PubMed: 26902873]

[435]. Ambulo CP, Tasmim S, Wang S, Abdelrahman MK, Zimmern PE, Ware TH, J. Appl. Phys 2020, 128, 140901. [PubMed: 33060862]

[436]. Song E, Li J, Rogers JA, APL Mater 2019, 7, 050902.

[437]. Ahn, Jeong, Kim, Micromachines 2019, 10, 508.

[438]. Lewis JS, Weaver MS, IEEE J. Sel. Top. Quantum Electron 2004, 10, 45.

[439]. Wang H, Zhao Y, Wang Z, Liu Y, Zhao Z, Xu G, Han T-H, Lee J-W, Chen C, Bao D, Huang Y, Duan Y, Yang Y, Nano Energy 2020, 69, 104375.

[440]. Prodanov D, Delbeke J, Front. Neurosci 2016, 10, DOI 10.3389/fnins.2016.00011.

[441]. Silver IA, Maroudas A, Fell HB, Dingle JT, Philos. Trans. R. Soc. Lond. B Biol. Sci 1975, 271, 261. [PubMed: 239420]

[442]. Kuang W, Nelson SO, Trans. ASAE 1998, 41, 173.

[443]. Reis RL, Román JS, Eds., in Biodegrad. Syst. Tissue Eng. Regen. Med, CRC Press, 2004.

[444]. Mestais CS, Charvet G, Sauter-Starace F, Foerster M, Ratel D, Benabid AL, IEEE Trans. Neural Syst. Rehabil. Eng 2015, 23, 10. [PubMed: 25014960]

[445]. Caldwell R, Mandal H, Sharma R, Solzbacher F, Tathireddy P, Rieth L, J. Neural Eng 2017, 14, 046011. [PubMed: 28351998]

[446]. Liu R, Zhao S, Liu J, ACS Appl. Electron. Mater 2021, 3, 101.

[447]. Song E, Fang H, Jin X, Zhao J, Jiang C, Yu KJ, Zhong Y, Xu D, Li J, Fang G, Du H, Zhang J, Park JM, Huang Y, Alam MA, Mei Y, Rogers JA, Adv. Electron. Mater 2017, 3, 1700077.

[448]. Phan H-P, Zhong Y, Nguyen T-K, Park Y, Dinh T, Song E, Vadivelu RK, Masud MK, Li J, Shiddiky MJA, Dao D, Yamauchi Y, Rogers JA, Nguyen N-T, ACS Nano 2019, 13, 11572. [PubMed: 31433939]

[449]. Le Floch P, Molinari N, Nan K, Zhang S, Kozinsky B, Suo Z, Liu J, Nano Lett 2020, 20, 224. [PubMed: 31775509]

[450]. Song E, Li R, Jin X, Du H, Huang Y, Zhang J, Xia Y, Fang H, Lee YK, Yu KJ, Chang J-K, Mei Y, Alam MA, Huang Y, Rogers JA, ACS Nano 2018, 12, 10317. [PubMed: 30281278]

[451]. Yap CC, Tan D, Brun C, Li H, Teo EHT, Dominique B, Tay BK, in 2013 IEEE 5th Int. Nanoelectron. Conf. INEC, IEEE, Singapore, Singapore, 2013, pp. 4–6.

[452]. Koo JH, Song J-K, Yoo S, Sunwoo S-H, Son D, Kim D-H, Adv. Mater. Technol 2020, 5, 2000407.

[453]. Li H, Ma Y, Huang Y, Mater. Horiz 2021, 8, 383. [PubMed: 34821261]

[454]. Lee Seung Woo, Min Kyou Sik, Jeong Joonsoo, Kim Junghoon, Kim Sung June, IEEE Trans. Biomed. Eng 2011, 58, 2255.

[455]. Lecomte A, Degache A, Descamps E, Dahan L, Bergaud C, Sens. Actuators B Chem 2017, 251, 1001.

[456]. Kirsten S, Schubert M, Uhlemann J, Wolter K-J, in 2014 36th Annu. Int. Conf. IEEE Eng. Med. Biol. Soc, IEEE, Chicago, IL, 2014, pp. 6561–6564.

[457]. Fang H, Zhao J, Yu KJ, Song E, Farimani AB, Chiang C-H, Jin X, Xue Y, Xu D, Du W, Seo KJ, Zhong Y, Yang Z, Won SM, Fang G, Choi SW, Chaudhuri S, Huang Y, Alam MA, Viventi J, Aluru NR, Rogers JA, Proc. Natl. Acad. Sci 2016, 113, 11682. [PubMed: 27791052]

[458]. Wuu DS, Lo WC, Chang LS, Horng RH, Thin Solid Films 2004, 468, 105.

[459]. Kang S-K, Hwang S-W, Cheng H, Yu S, Kim BH, Kim J-H, Huang Y, Rogers JA, Adv. Funct. Mater 2014, 24, 4427.

[460]. Kim KS, Kim KH, Ji YJ, Park JW, Shin JH, Ellingboe AR, Yeom GY, Sci. Rep 2017, 7, 13585. [PubMed: 29051604]

[461]. Andringa A-M, Perrotta A, de Peuter K, Knoops HCM, Kessels WMM, Creatore M, ACS Appl. Mater. Interfaces 2015, 7, 22525. [PubMed: 26393381]

[462]. Carcia PF, McLean RS, Reilly MH, Groner MD, George SM, Appl. Phys. Lett 2006, 89, 031915.

[463]. Song E, Lee YK, Li R, Li J, Jin X, Yu KJ, Xie Z, Fang H, Zhong Y, Du H, Zhang J, Fang G, Kim Y, Yoon Y, Alam MA, Mei Y, Huang Y, Rogers JA, Adv. Funct. Mater 2018, 28, 1702284.

[464]. Kim LH, Kim K, Park S, Jeong YJ, Kim H, Chung DS, Kim SH, Park CE, ACS Appl. Mater. Interfaces 2014, 6, 6731. [PubMed: 24712401]

[465]. Seo S-W, Jung E, Chae H, Cho SM, Org. Electron 2012, 13, 2436.

[466]. Majee S, Geffroy B, Bonnassieux Y, Bourée J-E, Surf. Coat. Technol 2014, 254, 429.

[467]. Chiang CC, Wuu DS, Lin HB, Chen YP, Chen TN, Lin YC, Wu CC, Chen WC, Jaw TH, Horng RH, Surf. Coat. Technol 2006, 200, 5843.

[468]. Xie X, Rieth L, Merugu S, Tathireddy P, Solzbacher F, Appl. Phys. Lett 2012, 101, 093702.

[469]. Boehler C, Carli S, Fadiga L, Stieglitz T, Asplund M, Nat. Protoc 2020, 15, 3557. [PubMed: 33077918]

[470]. Reynolds FH, Proc. IEEE 1974, 62, 212.

[471]. McCreery D, in Neurobionics Biomed. Eng. Neural Prostheses, John Wiley & Sons, Ltd, 2016, pp. 162–185.

[472]. Hogg A, Uhl S, Feuvrier F, Girardet Y, Graf B, Aellen T, Keppner H, Tardy Y, Burger J, Surf. Coat. Technol 2014, 255, 124.

[473]. Kempe MD, Reese MO, Dameron AA, Rev. Sci. Instrum 2013, 84, 025109. [PubMed: 23464253]

[474]. Schubert S, Klumbies H, Müller-Meskamp L, Leo K, Rev. Sci. Instrum 2011, 82, 094101. [PubMed: 21974600]

[475]. Elrawemi M, Blunt L, Fleming L, Sweeney F, Surf. Topogr. Metrol. Prop 2013, 1, 015006.

[476]. Groner MD, George SM, McLean RS, Carcia PF, Appl. Phys. Lett 2006, 88, 051907.

[477]. Coulter AR, Deeken RA, Zentner GM, J. Membr. Sci 1992, 65, 269.

[478]. Mamishev AV, Sundara-Rajan K, Yang Fumin, Du Yanqing, Zahn M, Proc. IEEE 2004, 92, 808.

[479]. Minnikanti S, Diao G, Pancrazio JJ, Xie X, Rieth L, Solzbacher F, Peixoto N, Acta Biomater 2014, 10, 960. [PubMed: 24185000]

[480]. McIntyre JM, Pham HQ, Prog. Org. Coat 1996, 27, 201.

[481]. Yu D, Yang Y-Q, Chen Z, Tao Y, Liu Y-F, Opt. Commun 2016, 362, 43.

[482]. Lasoski SW, Cobbs WH, J. Polym. Sci 1959, 36, 21.

[483]. Diamant Y, Marom G, Broutman LJ, J. Appl. Polym. Sci 1981, 26, 3015.

[484]. Vanlandingham MR, Eduljee RF, Gillespie JW, J. Appl. Polym. Sci 1999, 71, 787.

[485]. Sangaj NS, Malshe VC, Prog. Org. Coat 2004, 50, 28.

[486]. Shahriari L, Mohseni M, Yahyaei H, Prog. Org. Coat 2019, 134, 66.

[487]. Lee TH, Choi MH, Jeon SJ, Moon DK, Polymer 2016, 99, 756.

[488]. Khonakdar HA, Morshedian J, Wagenknecht U, Jafari SH, Polymer 2003, 44, 4301.

[489]. Gupta VB, Brahatheeswaran C, Polymer 1991, 32, 1875.

[490]. Hassler C, von Metzen R, Stieglitz T, in 4th Eur. Conf. Int. Fed. Med. Biol. Eng (Eds.: Vander Sloten J, Verdonck P, Nyssen M, Haueisen) J, Springer, Berlin, Heidelberg, 2009, pp. 2439–2442.

[491]. Seo J, Han H, J. Appl. Polym. Sci 2001, 82, 731.

[492]. DeIasi R, Russell J, J. Appl. Polym. Sci 1971, 15, 2965.

[493]. Rubehn B, Stieglitz T, Biomaterials 2010, 31, 3449. [PubMed: 20144477]

[494]. Tolstosheeva E, Biefeld V, Lang W, Procedia Eng 2015, 120, 36.

[495]. Ceyssens F, Puers R, J. Neural Eng 2015, 12, 054001. [PubMed: 26269487]

[496]. Selbmann F, Baum M, Wiemer M, Gessner T, in 2016 IEEE 11th Annu. Int. Conf. NanoMicro Eng. Mol. Syst. NEMS, 2016, pp. 427–432.

[497]. Seok S, Park H, Kim J, Micromachines 2020, 11, 605.

[498]. Xie Y, Pei W, Guo D, Zhang L, Zhang H, Guo X, Xing X, Yang X, Wang F, Gui Q, Wang Y, Chen H, Sens. Actuators Phys 2017, 260, 117.

[499]. Gwon TM, Kim JH, Choi GJ, Kim SJ, J. Mater. Sci 2016, 51, 6897.

[500]. Lee JH, Hwang KS, Yoon KH, Kim TS, Ahn S, IEEE Trans. Plasma Sci 2004, 32, 505.

[501]. Pham A-V, IEEE Microw. Mag 2011, 12, 83.
[502]. Shin S, Kim J-H, Jeong J, Gwon TM, Lee S-H, Kim SJ, J. Neurosci. Methods 2017, 278, 25. [PubMed: 28040494]
[503]. van Amerongen GJ, Rubber Chem. Technol 1964, 37, 1065.
[504]. Kosiyanon R, McGregor R, J. Appl. Polym. Sci 1981, 26, 629.
[505]. Lal J, Scott KW, J. Polym. Sci. Part C Polym. Symp 1965, 9, 113.
[506]. Bowman L, Meindl JD, IEEE Trans. Biomed. Eng 1986, BME-33, 248.
[507]. Shen K, Maharbiz MM, J. Neural Eng 2021, 18, 025002. [PubMed: 33624611]
[508]. Ardebili H, Zhang J, Pecht MG, Encapsulation Technologies for Electronic Applications, William Andrew, 2018.
[509]. Jeong J, Laiwalla F, Lee J, Ritasalo R, Pudas M, Larson L, Leung V, Nurmikko A, Adv. Funct. Mater 2019, 29, 1806440.
[510]. Ray NH, J. Non-Cryst. Solids 1974, 15, 423.
[511]. Argall F, Jonscher AK, Thin Solid Films 1968, 2, 185.
[512]. Fahlteich J, Fahland M, Schönberger W, Schiller N, Thin Solid Films 2009, 517, 3075.
[513]. Blesa MA, Morando PJ, Regazzoni AE, Chemical Dissolution of Metal Oxides, CRC Press, Boca Raton, 2017.
[514]. Casey WH, Lasaga AC, Gibbs GV, Geochim. Cosmochim. Acta 1990, 54, 3369.
[515]. Lee YK, Yu KJ, Kim Y, Yoon Y, Xie Z, Song E, Luan H, Feng X, Huang Y, Rogers JA, ACS Appl. Mater. Interfaces 2017, 9, 42633. [PubMed: 29178781]
[516]. Rie K-T, Gebauer A, Wöhle J, Surf. Coat. Technol 1996, 86–87, 498.
[517]. Fraga M, Pessoa R, Micromachines 2020, 11, 799.
[518]. Kijima K, Setaka N, Tanaka H, J. Cryst. Growth 1974, 24–25, 183.
[519]. Gupta M, Rathi VK, Thangaraj R, Agnihotri OP, Chari KS, Thin Solid Films 1991, 204, 77.
[520]. Wuu DS, Lo WC, Chiang CC, Lin HB, Chang LS, Horng RH, Huang CL, Gao YJ, Surf. Coat. Technol 2005, 198, 114.
[521]. Li J, Li R, Du H, Zhong Y, Chen Y, Nan K, Won SM, Zhang J, Huang Y, Rogers JA, ACS Nano 2019, 13, 660. [PubMed: 30608642]
[522]. Diaz-Botia CA, Luna LE, Neely RM, Chamanzar M, Carraro C, Carmena JM, Sabes PN, Maboudian R, Maharbiz MM, J. Neural Eng 2017, 14, 056006. [PubMed: 28573982]
[523]. Lei X, Kane S, Cogan S, Lorach H, Galambos L, Huie P, Mathieson K, Kamins T, Harris J, Palanker D, J. Neural Eng 2016, 13, 046016. [PubMed: 27323882]
[524]. Knaack GL, McHail DG, Borda G, Koo B, Peixoto N, Cogan SF, Dumas TC, Pancrazio JJ, Front. Neurosci 2016, 10, DOI 10.3389/fnins.2016.00301.
[525]. Lim JW, Yun SJ, Electrochem. Solid-State Lett 2004, 7, F45.
[526]. Correa GC, Bao B, Strandwitz NC, ACS Appl. Mater. Interfaces 2015, 7, 14816. [PubMed: 26107803]
[527]. Tripp MK, Stampfer C, Miller DC, Helbling T, Herrmann CF, Hierold C, Gall K, George SM, Bright VM, Sens. Actuators Phys 2006, 130–131, 419.
[528]. Elliott SD, Scarel G, Wiemer C, Fanciulli M, Pavia G, Chem. Mater 2006, 18, 3764.
[529]. Elliott SD, Greer JC, J. Mater. Chem 2004, 14, 3246.
[530]. Zhang Y, Seghete D, Abdulagatov A, Gibbs Z, Cavanagh A, Yang R, George S, Lee Y-C, Surf. Coat. Technol 2011, 205, 3334.
[531]. Jung H, Choi H, Jeon H, Lee S, Jeon H, J. Appl. Phys 2013, 114, 173511.
[532]. Le Floch P, Meixuanzi S, Tang J, Liu J, Suo Z, ACS Appl. Mater. Interfaces 2018, 10, 27333. [PubMed: 30016067]
[533]. Wu H, Menon M, Zhu C, Balasubramanian A, Bettinger CJ, Adv. Mater. Interfaces 2014, 1, 1400301.
[534]. Wu H, Kustra S, Gates EM, Bettinger CJ, Org. Electron 2013, 14, 1636.
[535]. Pholpabu P, Kustra S, Wu H, Balasubramanian A, Bettinger CJ, Biomaterials 2015, 39, 164. [PubMed: 25468368]

[536]. Choi YS, Koo J, Lee YJ, Lee G, Avila R, Ying H, Reeder J, Hambitzer L, Im K, Kim J, Lee K-M, Cheng J, Huang Y, Kang S-K, Rogers JA, Adv. Funct. Mater 2020, 30, 2000941.

[537]. Ju J, Hu N, Cairns DM, Liu H, Timko BP, Proc. Natl. Acad. Sci 2020, 117, 15482. [PubMed: 32571918]

[538]. Zhang H, Vecchio D, Emre A, Rahmani S, Cheng C, Zhu J, Misra AC, Lahann J, Kotov NA, bioRxiv 2020, 2020.12.28.424604.

[539]. Khanna VK, J. Phys. D: Appl. Phys 2010, 44, 034004.

[540]. Hora J, Hall C, Evans D, Charrault E, Adv. Eng. Mater 2018, 20, 1700868.

[541]. Sim K, Ershad F, Zhang Y, Yang P, Shim H, Rao Z, Lu Y, Thukral A, Elgalad A, Xi Y, Tian B, Taylor DA, Yu C, Nat. Electron 2020, 3, 775.

[542]. Chen Z, Boyajian N, Lin Z, Yin RT, Obaid SN, Tian J, Brennan JA, Chen SW, Miniovich AN, Lin L, Qi Y, Liu X, Efimov IR, Lu L, Adv. Mater. Technol 2021, 6, 2170041.

[543]. Dual SA, Zambrano BL, Sündermann S, Cesarovic N, Kron M, Magkoutas K, Hengsteler J, Falk V, Starck C, Meboldt M, Vörös J, Daners MS, Adv. Healthc. Mater 2020, 9, 2000855.

[544]. Lee P, Lee J, Lee H, Yeo J, Hong S, Nam KH, Lee D, Lee SS, Ko SH, Adv. Mater 2012, 24, 3326. [PubMed: 22610599]

[545]. Yoon IS, Kim SH, Oh Y, Ju B-K, Hong J-M, Sci. Rep 2020, 10, 5036. [PubMed: 32193483]

[546]. Kim T, Cho M, Yu KJ, Materials 2018, 11, 1163.

[547]. Tan D, Jiang C, Li Q, Bi S, Song J, J. Mater. Sci. Mater. Electron 2020, 31, 15669.

[548]. Zambrano BL, Renz AF, Ruff T, Lienemann S, Tybrandt K, Vörös J, Lee J, Adv. Healthc. Mater 2021, 10, 2001397.

[549]. Merrill DR, Bikson M, Jefferys JGR, J. Neurosci. Methods 2005, 141, 171. [PubMed: 15661300]

[550]. Xu L, Gutbrod SR, Bonifas AP, Su Y, Sulkin MS, Lu N, Chung H-J, Jang K-I, Liu Z, Ying M, Lu C, Webb RC, Kim J-S, Laughner JI, Cheng H, Liu Y, Ameen A, Jeong J-W, Kim G-T, Huang Y, Efimov IR, Rogers JA, Nat. Commun 2014, 5, 3329. [PubMed: 24569383]

[551]. Lee W, Kobayashi S, Nagase M, Jimbo Y, Saito I, Inoue Y, Yambe T, Sekino M, Malliaras GG, Yokota T, Tanaka M, Someya T, Sci. Adv 2018, 4, eaau2426. [PubMed: 30345362]

[552]. Ledochowitsch P, Yazdan-Shahmorad A, Bouchard KE, Diaz-Botia C, Hanson TL, He J-W, Seybold BA, Olivero E, Phillips E. a. K., Blanche TJ, Schreiner CE, Hasenstaub A, Chang EF, Sabes PN, Maharbiz MM, J. Neurosci. Methods 2015, 256, 220. [PubMed: 26296286]

[553]. Zhang J, Liu X, Xu W, Luo W, Li M, Chu F, Xu L, Cao A, Guan J, Tang S, Duan X, Nano Lett 2018, 18, 2903. [PubMed: 29608857]

[554]. Bruegmann T, Malan D, Hesse M, Beiert T, Fuegemann CJ, Fleischmann BK, Sasse P, Nat. Methods 2010, 7, 897. [PubMed: 20881965]

[555]. Adamantidis A, Arber S, Bains JS, Bamberg E, Bonci A, Buzsáki G, Cardin JA, Costa RM, Dan Y, Goda Y, Graybiel AM, Häusser M, Hegemann P, Huguenard JR, Insel TR, Janak PH, Johnston D, Josselyn SA, Koch C, Kreitzer AC, Lüscher C, Malenka RC, Miesenböck G, Nagel G, Roska B, Schnitzer MJ, Shenoy KV, Soltesz I, Sternson SM, Tsien RW, Tsien RY, Turrigiano GG, Tye KM, Wilson RI, Nat. Neurosci 2015, 18, 1202. [PubMed: 26308981]

[556]. Song K-I, Seo H, Seong D, Kim S, Yu KJ, Kim Y-C, Kim J, Kwon SJ, Han H-S, Youn I, Lee H, Son D, Nat. Commun 2020, 11, 4195. [PubMed: 32826916]

[557]. Lee J, Ihle SJ, Pellegrino GS, Kim H, Yea J, Jeon C-Y, Son H-C, Jin C, Eberli D, Schmid F, Zambrano BL, Renz AF, Forró C, Choi H, Jang K-I, Küng R, Vörös J, Nat. Electron 2021, 4, 291.

[558]. Kim B, Soepriatna AH, Park W, Moon H, Cox A, Zhao J, Gupta NS, Park CH, Kim K, Jeon Y, Jang H, Kim DR, Lee H, Lee K-S, Goergen CJ, Lee CH, Nat. Commun 2021, 12, 3710. [PubMed: 34140475]

[559]. Ohm Y, Pan C, Ford MJ, Huang X, Liao J, Majidi C, Nat. Electron 2021, 4, 185.

[560]. Burdușel A-C, Gherasim O, Grumezescu AM, Mogoantă L, Ficai A, Andronescu E, Nanomaterials 2018, 8, 681.

[561]. Zhang J, Mou L, Jiang X, Chem. Sci 2020, 11, 923. [PubMed: 34084347]

[562]. Elahi N, Kamali M, Baghersad MH, Talanta 2018, 184, 537. [PubMed: 29674080]

[563]. Lee J, Shin S, Lee S, Song J, Kang S, Han H, Kim S, Kim S, Seo J, Kim D, Lee T, ACS Nano 2018, 12, 4259. [PubMed: 29617111]

[564]. Boutry CM, Kaizawa Y, Schroeder BC, Chortos A, Legrand A, Wang Z, Chang J, Fox P, Bao Z, Nat. Electron 2018, 1, 314.

[565]. Stauffer F, Zhang Q, Tybrandt K, Zambrano BL, Hengsteler J, Stoll A, Trüeb C, Hagander M, Sujata J-M, Hoffmann F, Stekhoven JS, Quack J, Zilly H, Goedejohann J, Schneider MP, Kessler TM, Taylor WR, Küng R, Vörös J, Adv. Mater. Technol 2018, 3, 1800031.

[566]. Li R, Qi H, Ma Y, Deng Y, Liu S, Jie Y, Jing J, He J, Zhang X, Wheatley L, Huang C, Sheng X, Zhang M, Yin L, Nat. Commun 2020, 11, 3207. [PubMed: 32587309]

[567]. Ausra J, Wu M, Zhang X, Vázquez-Guardado A, Skelton P, Peralta R, Avila R, Murickan T, Haney CR, Huang Y, Rogers JA, Kozorovitskiy Y, Gutruf P, Proc. Natl. Acad. Sci 2021, 118, DOI 10.1073/pnas.2025775118.

[568]. Han M, Chen L, Aras K, Liang C, Chen X, Zhao H, Li K, Faye NR, Sun B, Kim J-H, Bai W, Yang Q, Ma Y, Lu W, Song E, Baek JM, Lee Y, Liu C, Model JB, Yang G, Ghaffari R, Huang Y, Efimov IR, Rogers JA, Nat. Biomed. Eng 2020, 4, 997. [PubMed: 32895515]

[569]. Zhao J, Chi Z, Yang Z, Chen X, Arnold MS, Zhang Y, Xu J, Chi Z, Aldred MP, Nanoscale 2018, 10, 5764. [PubMed: 29542765]

[570]. Ho MD, Liu Y, Dong D, Zhao Y, Cheng W, Nano Lett 2018, 18, 3593. [PubMed: 29767529]

[571]. Matsuhisa N, Chen X, Bao Z, Someya T, Chem. Soc. Rev 2019, 48, 2946. [PubMed: 31073551]

[572]. Ko G-J, Han SD, Kim J-K, Zhu J, Han WB, Chung J, Yang SM, Cheng H, Kim D-H, Kang C-Y, Hwang S-W, NPG Asia Mater 2020, 12, 1.

[573]. Kim H-S, Yang SM, Jang T-M, Oh N, Kim H-S, Hwang S-W, Adv. Healthc. Mater 2018, 7, 1801071.

[574]. Calabrese V, Mancuso C, Calvani M, Rizzarelli E, Butterfield DA, Stella AMG, Nat. Rev. Neurosci 2007, 8, 766. [PubMed: 17882254]

[575]. Förstermann U, Sessa WC, Eur. Heart J 2012, 33, 829. [PubMed: 21890489]

[576]. Nagano T, Luminescence 1999, 14, 283. [PubMed: 10602296]

[577]. Xu S, Zhang Y, Cho J, Lee J, Huang X, Jia L, Fan JA, Su Y, Su J, Zhang H, Cheng H, Lu B, Yu C, Chuang C, Kim T, Song T, Shigeta K, Kang S, Dagdeviren C, Petrov I, Braun PV, Huang Y, Paik U, Rogers JA, Nat. Commun 2013, 4, 1543. [PubMed: 23443571]

[578]. Liu Y, Feig VR, Bao Z, Adv. Healthc. Mater 2021, 10, 2001916.

[579]. Tropp J, Rivnay J, J. Mater. Chem. C 2021, DOI 10.1039/D1TC03600A.

[580]. Rashid RB, Ji X, Rivnay J, Biosens. Bioelectron 2021, 190, 113461. [PubMed: 34197997]

[581]. Prunet G, Pawula F, Fleury G, Cloutet E, Robinson AJ, Hadziioannou G, Pakdel A, Mater. Today Phys 2021, 18, 100402.

[582]. Athukorala SS, Tran TS, Balu R, Truong VK, Chapman J, Dutta NK, Roy Choudhury N, Polymers 2021, 13, 474. [PubMed: 33540900]

[583]. Wang C, Chai Y, Wen X, Ai Y, Zhao H, Hu W, Yang X, Ding M-Y, Shi X, Liu Q, Liang Q, ACS Mater. Lett 2021, 3, 1238.

[584]. Horn CC, Forssell M, Sciullo M, Harms JE, Fulton S, Mou C, Sun F, Simpson TW, Xiao G, Fisher LE, Bettinger C, Fedder GK, J. Neural Eng 2021, 18, 055008.

[585]. Horn CC, Xiao G, Bettinger C, Redder GK, Ong XC, Huang W, Fisher LEB, Gaunt R, Conformable Neural Interface Device with Hydrogel Adhesion and Methods of Using the Same, 2021, US20210268268A1.

[586]. Forssell M, Sciullo M, Mou C, Sun F, Simpson TW, Xiao G, Fisher LE, Bettinger C, Horn CC, Fedder GK, in 2019 IEEE Sens, 2019, pp. 1–4.

[587]. Tran H, Nikzad S, Chiong JA, Schuster NJ, Peña-Alcántara AE, Feig VR, Zheng Y-Q, Bao Z, Chem. Mater 2021, 33, 7465.

[588]. Xu Y, Li Y, Li S, Balestra F, Ghibaudo G, Li W, Lin Y-F, Sun H, Wan J, Wang X, Guo Y, Shi Y, Noh Y-Y, Adv. Funct. Mater 2020, 30, 1904508.

[589]. Xu J, Wu H-C, Mun J, Ning R, Wang W, Wang NG-J, Nikzad S, Yan H, Gu X, Luo S, Zhou D, Tok JB-H, Bao Z, Adv. Mater, DOI: 10.1002/adma.202104747.

[590]. Wang W, Wang S, Rastak R, Ochiai Y, Niu S, Jiang Y, Arunachala PK, Zheng Y, Xu J, Matsuhisa N, Yan X, Kwon S-K, Miyakawa M, Zhang Z, Ning R, Foudeh AM, Yun Y, Linder C, Tok JB-H, Bao Z, Nat. Electron 2021, 4, 143.

[591]. Surgailis J, Savva A, Druet V, Paulsen BD, Wu R, Hamidi-Sakr A, Ohayon D, Nikiforidis G, Chen X, McCulloch I, Rivnay J, Inal S, Adv. Funct. Mater 2021, 31, 2010165.

[592]. Ji X, Paulsen BD, Chik GKK, Wu R, Yin Y, Chan PKL, Rivnay J, Nat. Commun 2021, 12, 2480. [PubMed: 33931638]

[593]. Kim Y, Noh H, Paulsen BD, Kim J, Jo I-Y, Ahn H, Rivnay J, Yoon M-H, Adv. Mater 2021, 33, 2007550.

[594]. Srikantharajah K, Medinaceli Quintela R, Doerenkamp K, Kampa BM, Musall S, Rothermel M, Offenhäusser A, Sci. Rep 2021, 11, 18920. [PubMed: 34556704]

[595]. Musk E, Neuralink, J. Med. Internet Res 2019, 21, e16194. [PubMed: 31642810]

[596]. Chin AL, Jiang S, Jang E, Niu L, Li L, Jia X, Tong R, Nat. Commun 2021, 12, 5138. [PubMed: 34446702]

[597]. Cea C, Spyropoulos GD, Jastrzebska-Perfect P, Ferrero JJ, Gelinas JN, Khodagholy D, Nat. Mater 2020, 19, 679. [PubMed: 32203456]

[598]. Paulk AC, Yang JC, Cleary DR, Soper DJ, Halgren M, O'Donnell AR, Lee SH, Ganji M, Ro YG, Oh H, Hossain L, Lee J, Tchoe Y, Rogers N, Kiliç K, Ryu SB, Lee SW, Hermiz J, Gilja V, Ulbert I, Fabó D, Thesen T, Doyle WK, Devinsky O, Madsen JR, Schomer DL, Eskandar EN, Lee JW, Maus D, Devor A, Fried SI, Jones PS, Nahed BV, Ben-Haim S, Bick SK, Richardson RM, Raslan AM, Siler DA, Cahill DP, Williams ZM, Cosgrove GR, Dayeh SA, Cash SS, Cereb. Cortex 2021, 31, 3678. [PubMed: 33749727]

[599]. Oh JY, Rondeau-Gagné S, Chiu Y-C, Chortos A, Lissel F, Wang NG-J, Schroeder BC, Kurosawa T, Lopez J, Katsumata T, Xu J, Zhu C, Gu X, Bae W-G, Kim Y, Jin L, Chung JW, Tok JB-H, Bao Z, Nature 2016, 539, 411. [PubMed: 27853213]

[600]. Maya-Vetencourt JF, Manfredi G, Mete M, Colombo E, Bramini M, Di Marco S, Shmal D, Mantero G, Dipalo M, Rocchi A, DiFrancesco ML, Papaleo ED, Russo A, Barsotti J, Eleftheriou C, Di Maria F, Cossu V, Piazza F, Emionite L, Ticconi F, Marini C, Sambuceti G, Pertile G, Lanzani G, Benfenati F, Nat. Nanotechnol 2020, 15, 698. [PubMed: 32601447]

[601]. Li M-X, Zhao S-F, Lu Z, Hirata A, Wen P, Bai H-Y, Chen M, Schroers J, Liu Y, Wang W-H, Nature 2019, 569, 99. [PubMed: 31043727]

[602]. Guo H, Yan PF, Wang YB, Tan J, Zhang ZF, Sui ML, Ma E, Nat. Mater 2007, 6, 735. [PubMed: 17704779]

[603]. Jang D, Greer JR, Nat. Mater 2010, 9, 215. [PubMed: 20139966]

[604]. Shi Y, Int. Mater. Rev 2019, 64, 163.

[605]. Greer AL, Science 1995, 267, 1947. [PubMed: 17770105]

[606]. Plummer J, Nat. Mater 2015, 14, 553. [PubMed: 25990901]

[607]. Yan W, Dong C, Xiang Y, Jiang S, Leber A, Loke G, Xu W, Hou C, Zhou S, Chen M, Hu R, Shum PP, Wei L, Jia X, Sorin F, Tao X, Tao G, Mater. Today 2020, 35, 168.

[608]. Yan W, Page A, Nguyen-Dang T, Qu Y, Sordo F, Wei L, Sorin F, Adv. Mater 2019, 31, 1802348.

[609]. Yan W, Richard I, Kurtuldu G, James ND, Schiavone G, Squair JW, Nguyen-Dang T, Das Gupta T, Qu Y, Cao JD, Ignatans R, Lacour SP, Tileli V, Courtine G, Löffler JF, Sorin F, Nat. Nanotechnol 2020, 15, 875. [PubMed: 32747740]

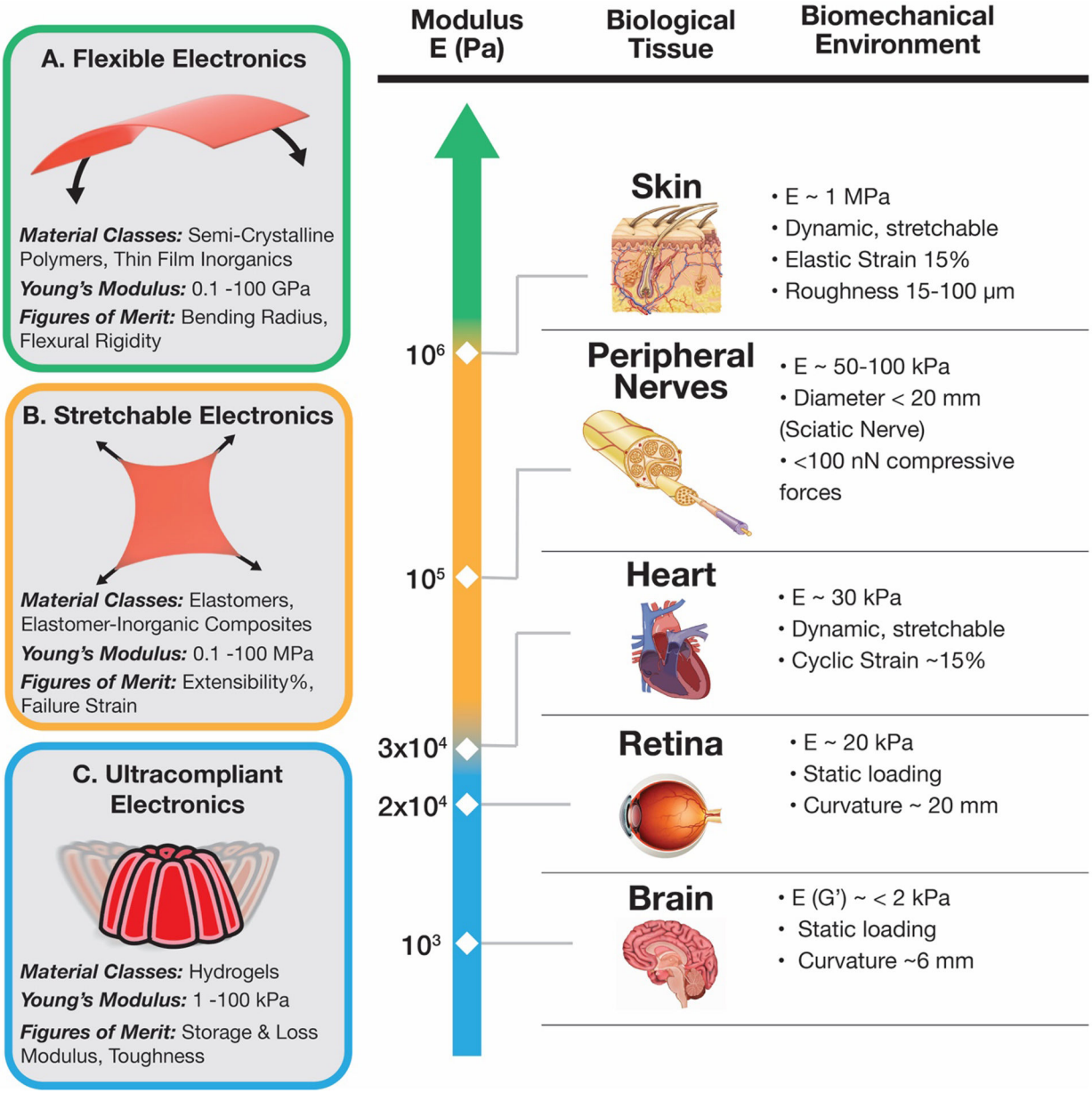

Figure 1.

(Left) The mechanical description and figures of merit of three regimes of bioelectronics devices: A. flexible electronics (0.1–100 GPa),[41] B. stretchable electronics (0.1–100 MPa),[39] and C. ultracompliant electronics (1–100 kPa).[59] (Right) A biomechanical description of target organs and loading conditions for mechanically compliant bioelectronics deployment: skin,[60] peripheral nerves,[61–64] heart,[65–67] retina,[68,69] and brain.[70–72] Reproduced with permission.[73] Copyright 2017, Elsevier.

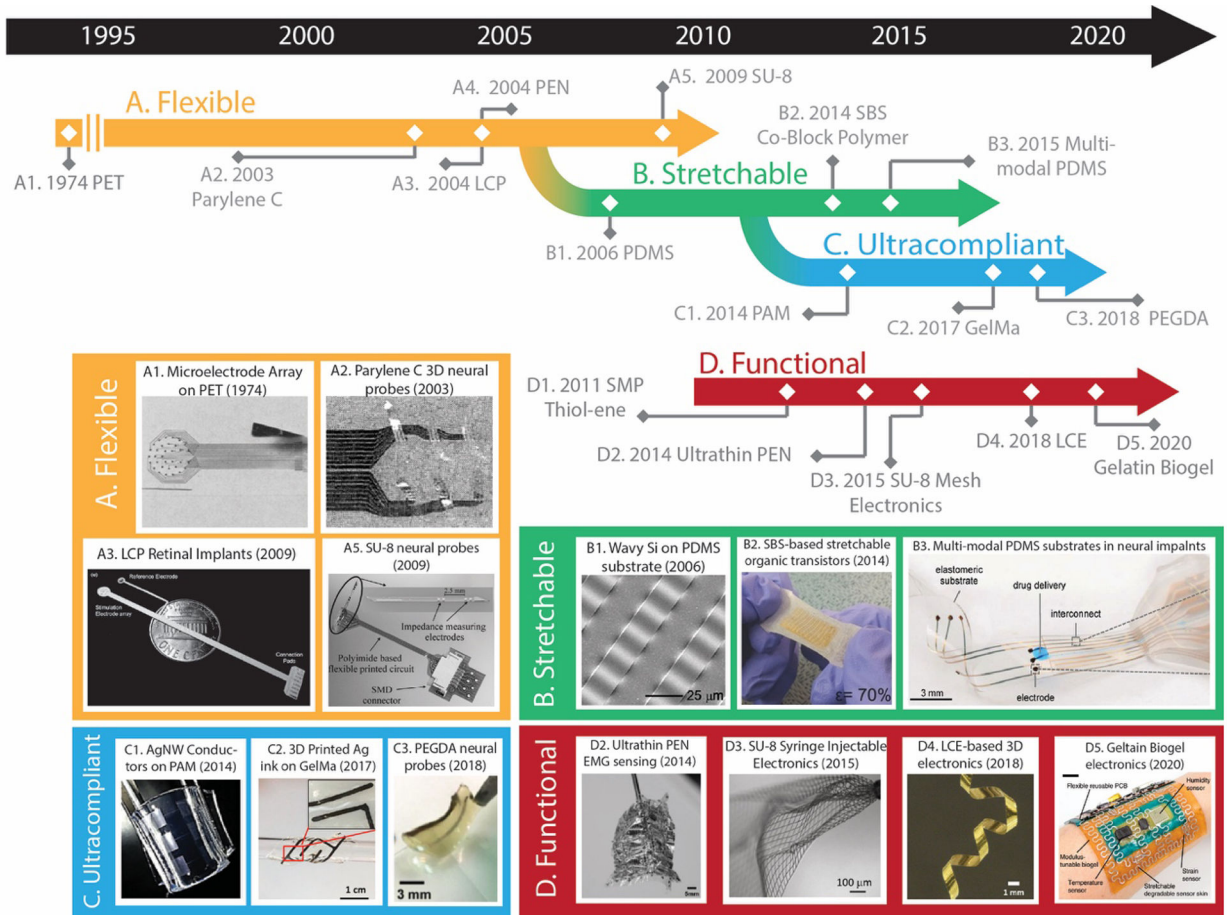

Figure 2.

Timeline outlining the evolution of mechanically compliant substrates in bioelectronics towards softer devices designed to maximize biological integration. Substrate materials are roughly classified into four categories – A. Flexible, B. Stretchable, C. Ultracompliant, and D. Structurally Adaptive. Key advances from each category have been presented on the timeline and select examples have been featured through the following pictures: A1. Polyethylene Terephthalate (PET). Reproduced with permission.[117] Copyright 1974, Springer Nature. A2. Parylene C. Reproduced with permission.[118] Copyright 2003, IEEE. A3. Liquid crystal polymers (LCPs). Reproduced with permission.[119] Copyright 2009, Association for Research in Vision and Ophthalmology. A5. SU-8 epoxy. Reproduced with permission.[120] Copyright 2009, Elsevier. B1. Stretchable Si on PDMS. Reproduced with permission.[121] Copyright 2006, The American Association for the Advancement of Science. B2. Organic transistors on styrene-butadiene-styrene (SBS). Reproduced with permission.[122] Copyright 2014, John Wiley and Sons. B3. Muti-modal PDMS electronic dura mater. Reproduced with permission.[123] Copyright 2015, The American Association for the Advancement of Science. C1. Silver nanowires on polyacrylamide. Reproduced with permission.[124] Copyright 2014, American Chemical Society. C2. Printed silver flakes on gelatin methacrylate (GelMa). Reproduced with permission.[125] Copyright 2017, Elsevier. C3. Transfer printed polyethylene glycol-dopamine (PEGDA). Reproduced with permission.[126] Copyright 2017, John Wiley and Sons. D2. Ultrathin 1 μm polyethylene napthalate

(PEN). Reproduced with permission.[127] Copyright 2014, IEEE. D3. Syringe injectable SU-8. Reproduced with permission.[128] Copyright 2015, Springer Nature. D4. Morphing electronics on a liquid crystal elastomer. Reproduced with permission.[129] Copyright 2019, American Chemical Society. D5. Transient devices on gelatin biogels. Reproduced with permission.[130] Copyright 2020, Springer Nature.

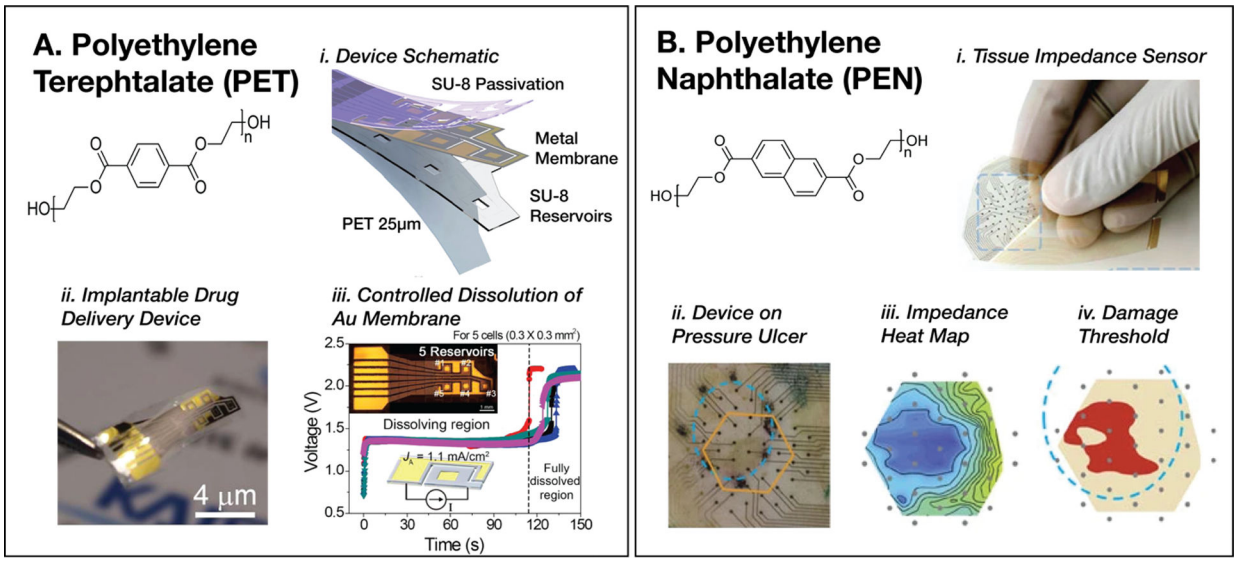

Figure 3.

A. Polyethylene terephthalate (PET)-based bioelectronic device for controlled drug delivery within the cerebral cortex (i, ii). Demonstration of temporal control over dissolution of a gold membrane to release the drug (iii). Reproduced with permission.[159] Copyright 2018, Elsevier. B. Inkjet-printed impedance sensors on polyethylene napthalate (PEN) substrates for early detection of pressure ulcers in mice. Reproduced with permission.[168] Copyright 2015, Springer Nature.

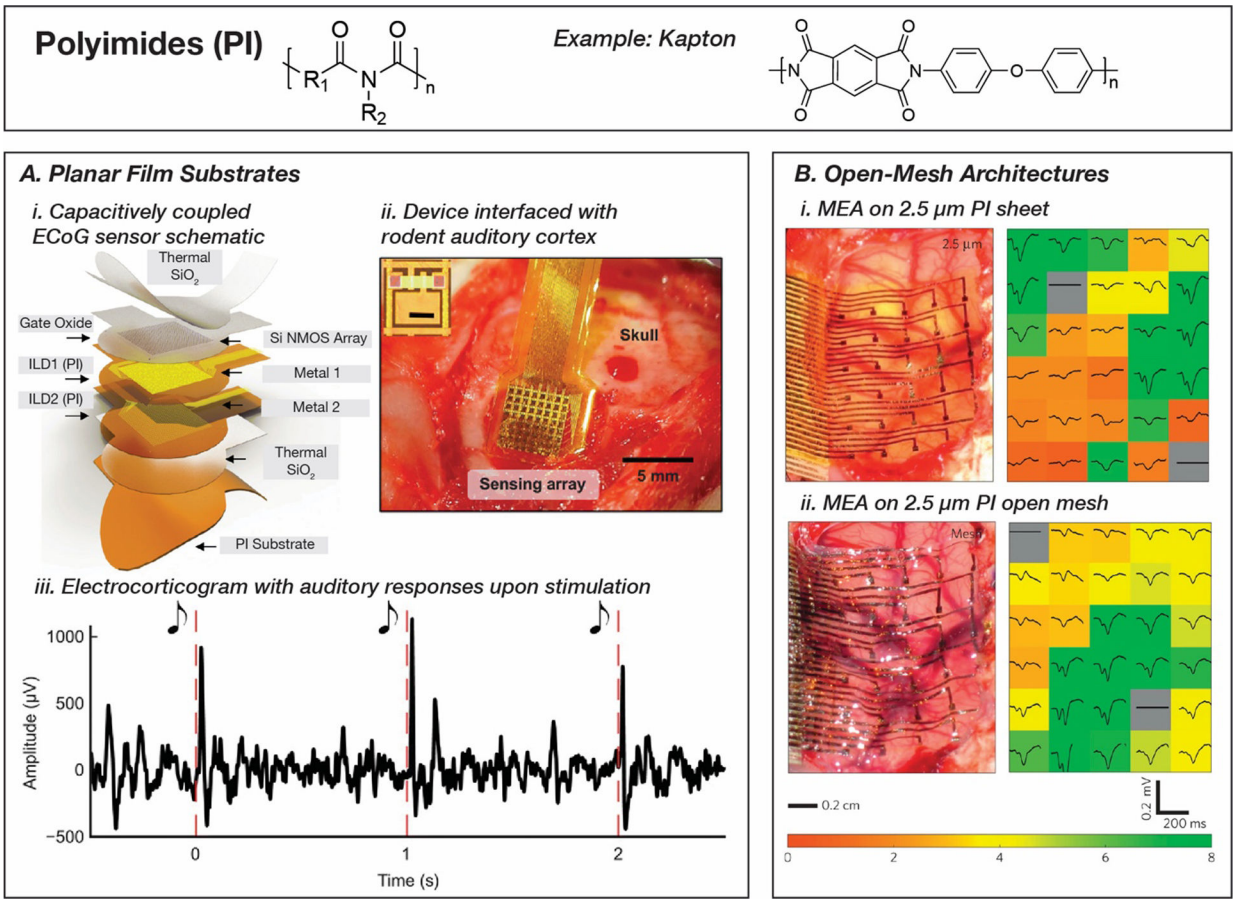

Figure 4.

Polyimide-based bioelectronic implants for electrophysiology. A. Capacitively-coupled neural sensors capable of high density 1008 channel electrodes for multiplexed electrocorticograms on a polyimide substrate. Reproduced with permission.[185] Copyright 2020, The American Association for the Advancement of Science. B. Open-mesh architectures using etched polyimide substrates capable of highly conformal recordings with improved signal-to-noise ratio compared to complete films. Reproduced with permission. [112] Copyright 2010, Springer Nature.

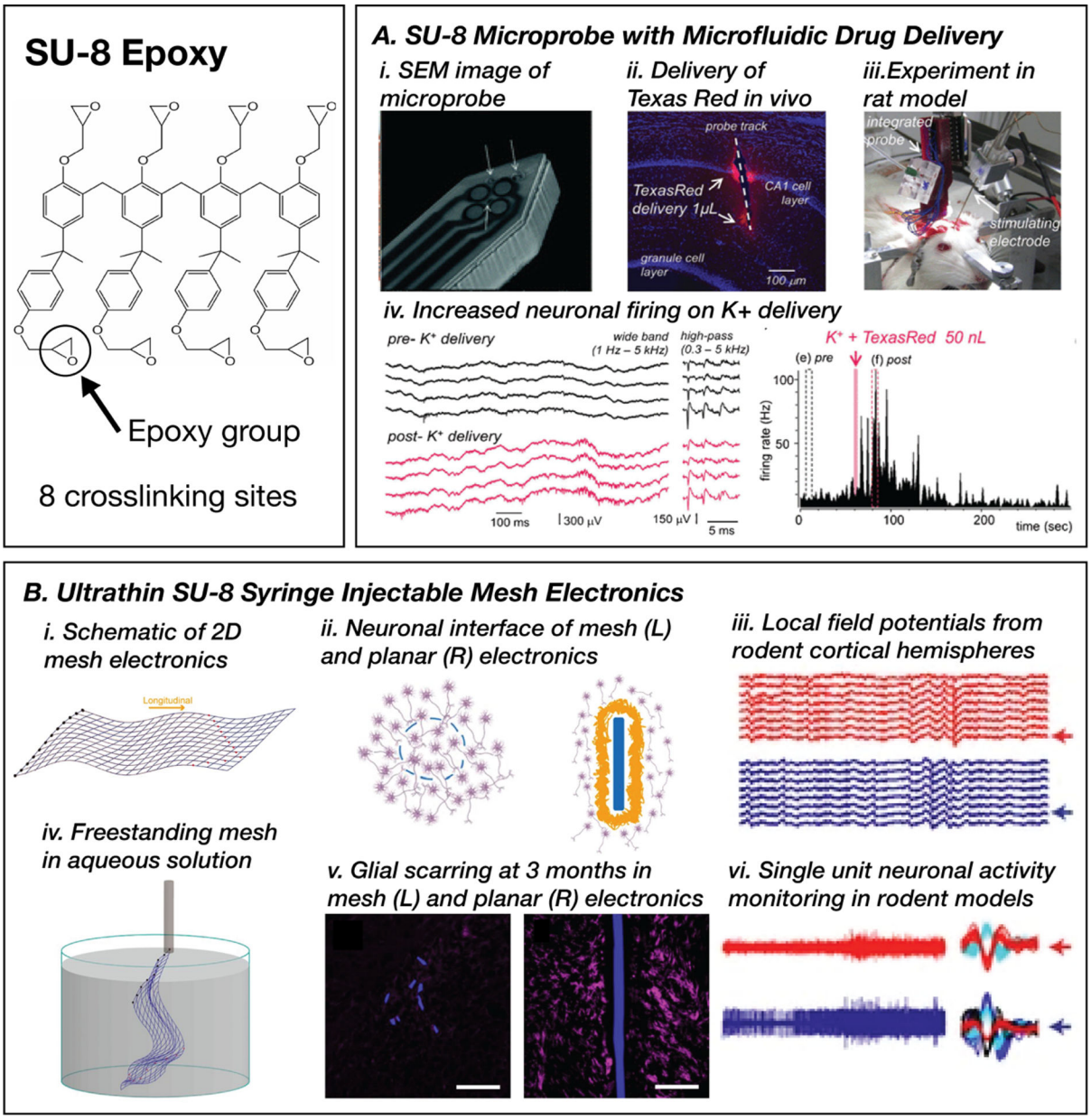

Figure 5.

SU-8 epoxy substrates for flexible neural interfaces. A. A neural probe photopatterned with microfluidic channels for simultaneous drug delivery and electrophysiology (i, iv), demonstrated through increased neural activity on the delivery of potassium ions(iv).Reproduced with permission.[203] Copyright 2012, Elsevier. B. Photopatterned syringe-injectable mesh electronics (i, ii) deployed in murine brains that promote biointegration (ii), reduce glial scarring (v), and can record field potentials (iii) and single neuronal activity (vi). Reproduced with permission.[214] Copyright 2017, National Academy of Sciences. Reproduced with permission.[215] Copyright 2016, Springer Nature.

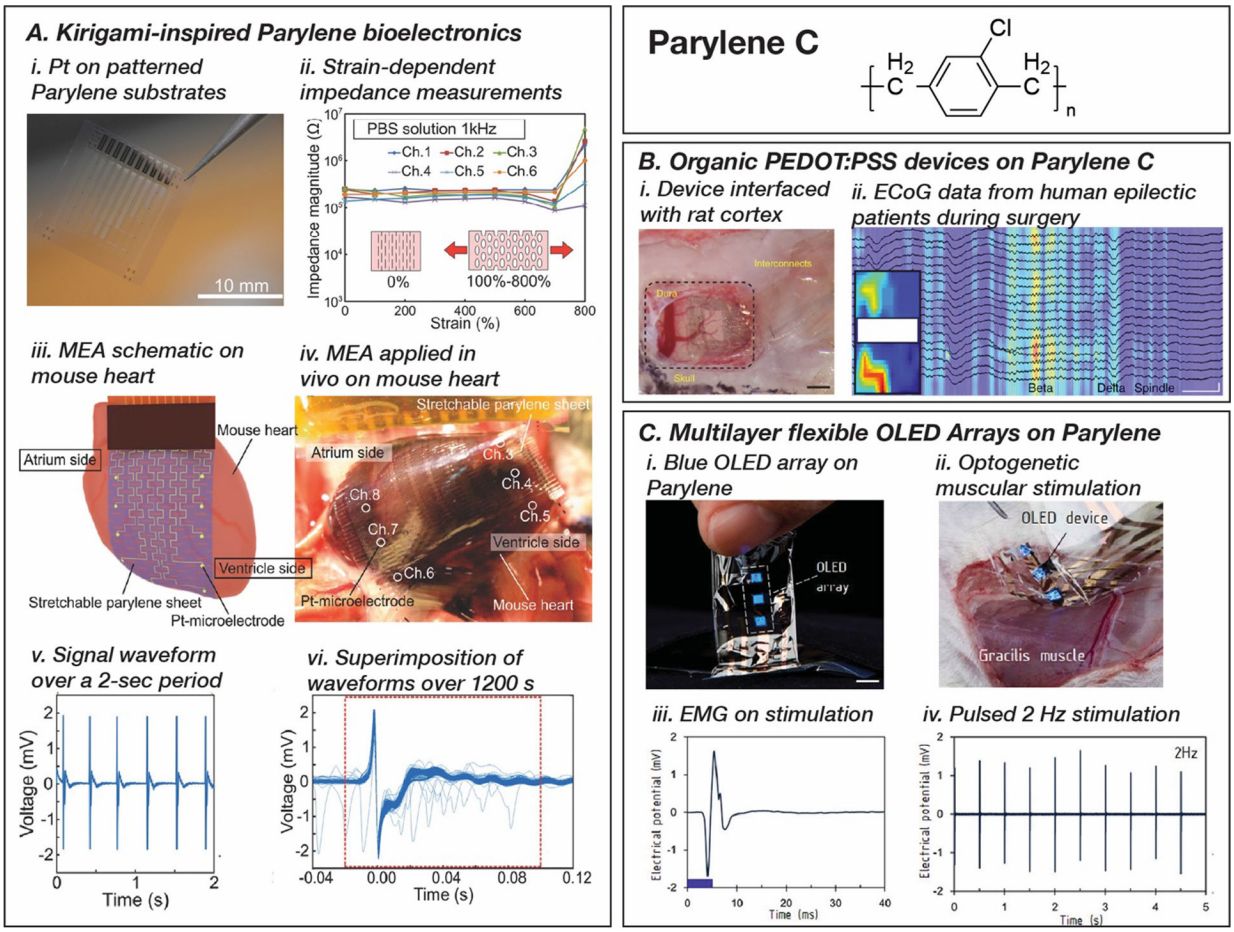

Figure 6.

Parylene C based bioelectronics for implantable applications. A. Laser cut Parylene C substrates for kirigami enabled stretchable multielectrode arrays for electrophysiological monitoring (i, ii, iii, iv), capable of high-resolution electrocardiography (v, vi). Reproduced with permission.[135] Copyright 2018, John Wiley and Sons. B. 265 PEDOT:PSS electrode array on 2 μm Parylene C to record neural activity from human epileptic patients. Reproduced with permission.[220] Copyright 2015, Springer Nature. C. Flexible blue organic light emitting diode (OLED) on Parylene C substrates (i) for optogenetic muscular stimulation (ii) and electromyogram recording (iii, iv). Reproduced with permission.[248] Copyright 2020, National Academy of Sciences.

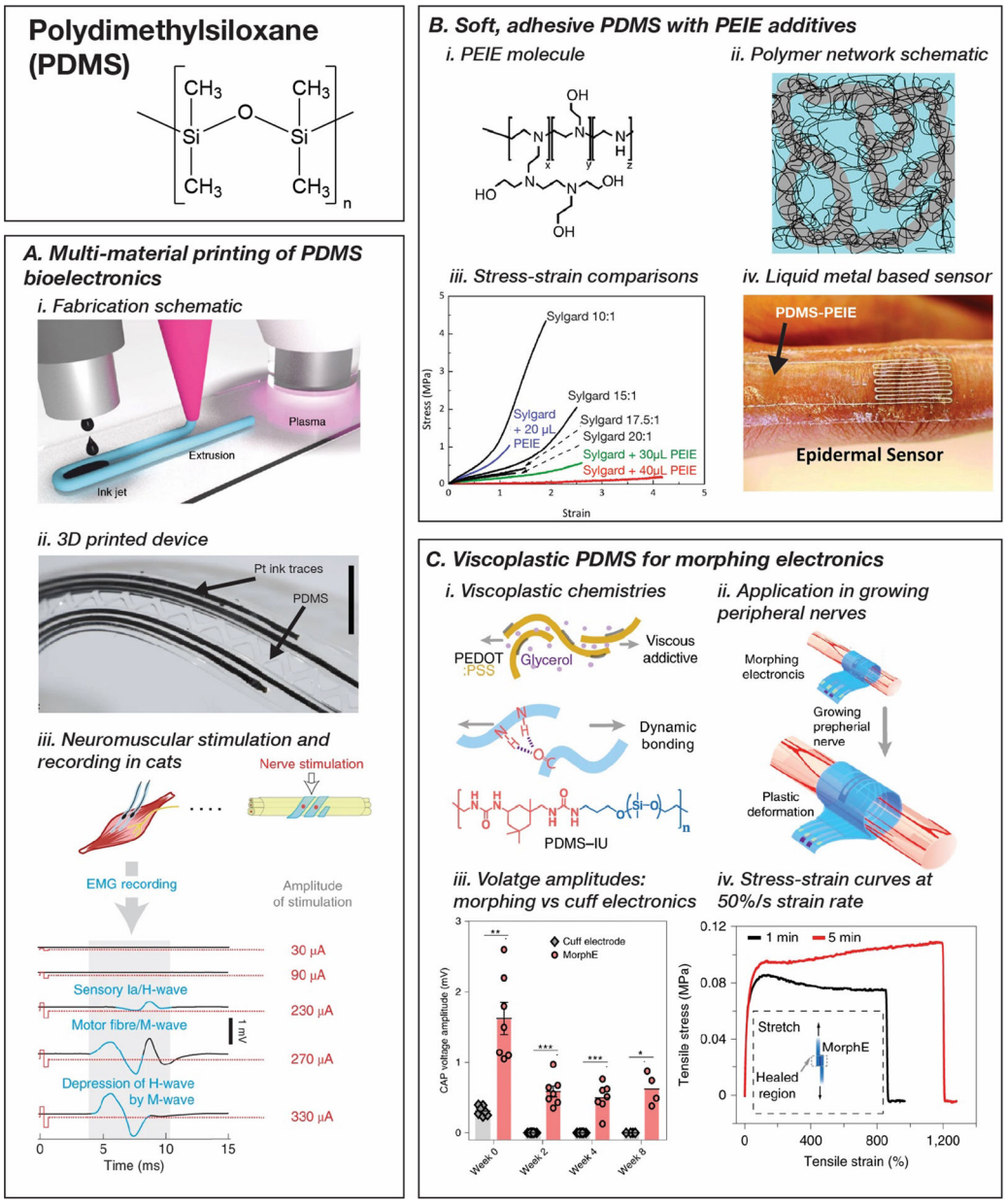

Figure 7.

Polydimethylsiloxane (PDMS) and PDMS derivatives for wearable and implantable bioelectronics. A. 3-dimensional printing strategies for PDMS substrates and platinum nanoparticle inks to form *in situ* stretchable conductors to rapidly prototype electrode arrays (i, ii) for neuromuscular stimulation and recording. Reproduced with permission.[271] Copyright 2020, Springer Nature. B. Ethoxylated polyethylenimine (PEIE) additive in PDMS elastomers to produce softer and stickier elastomers for wearable devices. Reproduced with permission.[273] Copyright 2016, John Wiley and Sons. C. Viscoplastic PDMS derivatives and plasticized PEDOT:PSS conductors for morphing electronics in regenerating peripheral nervous interfaces (i, ii, iv), with superior signal-to-noise

performance compared to fixed cuff electrodes (iii). Reproduced with permission.[276] Copyright 2020, Springer Nature.

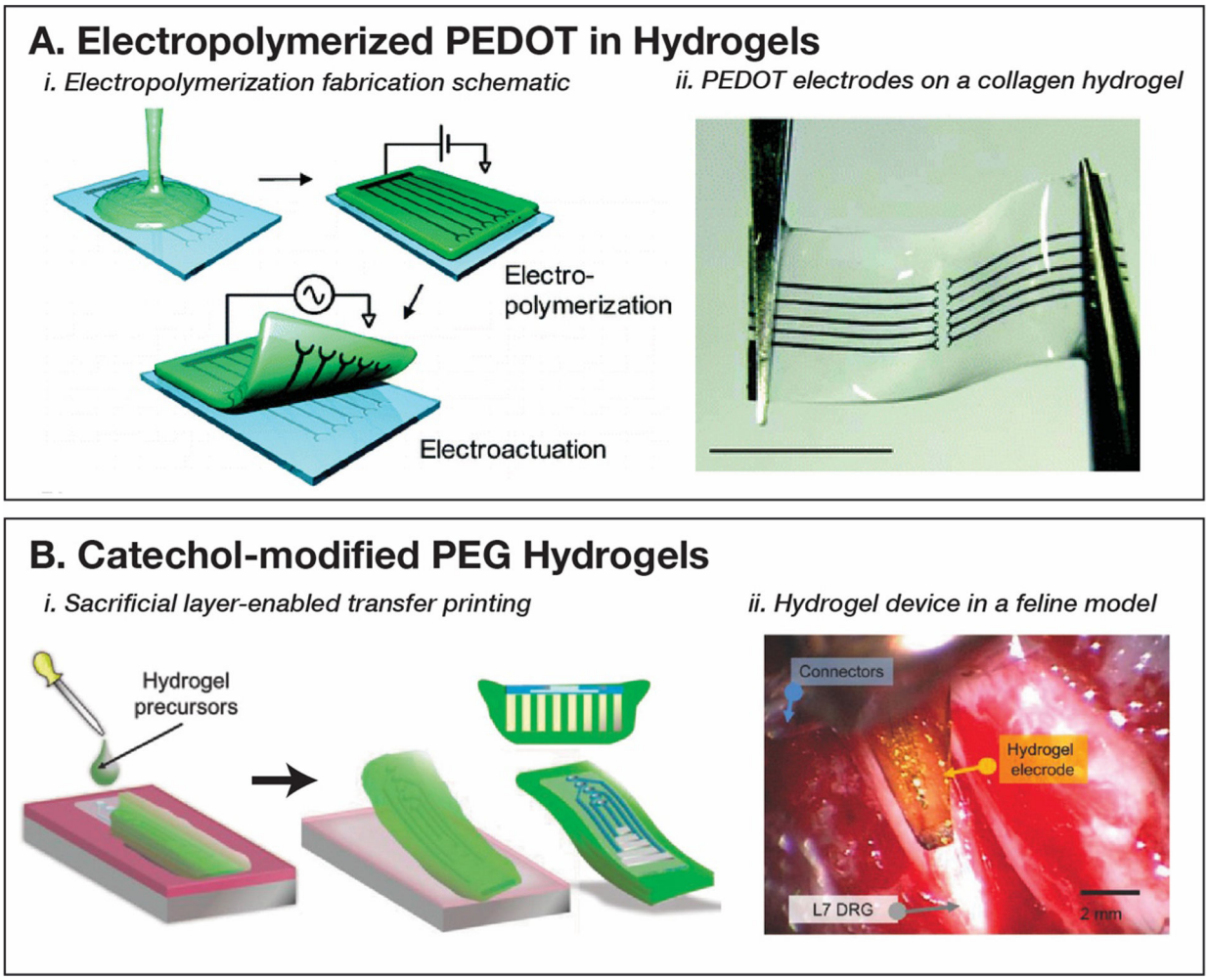

Figure 8.

A. Electropolymerization technique for patterning PEDOT polymer electrodes in hydrogel matrices. Reproduced with permission.[321] Copyright 2010, American Chemical Society. Reproduced with permission.[322] Copyright 2012, American Chemical Society. B. Catechol-modified polyethylene glycol hydrogels (PEGDA) substrates for peripheral nerve interfaces in feline models fabricated using an aqueous phase transfer printing technique. Reproduced with permission.[126] Copyright 2018, John Wiley and Sons.

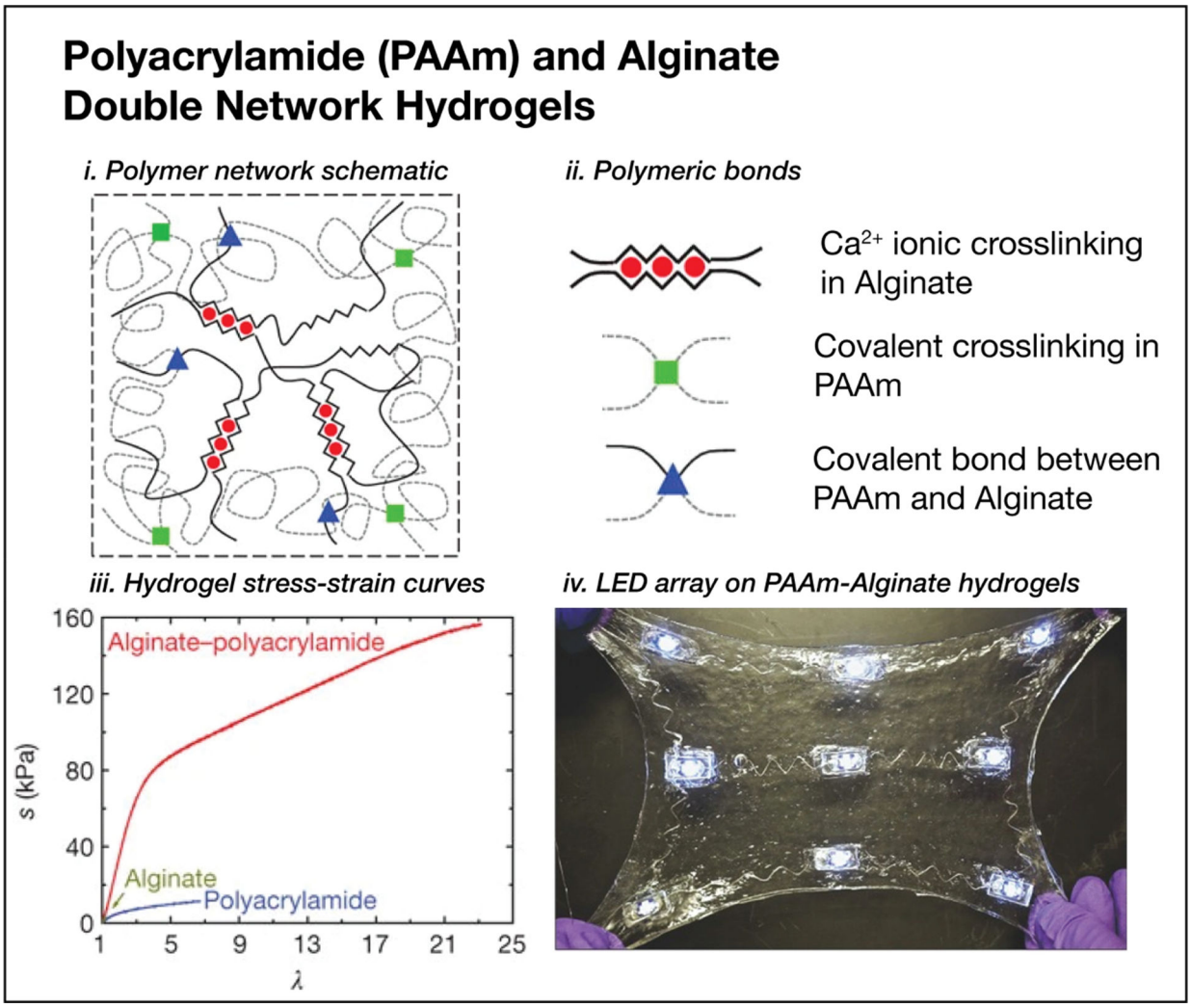

Figure 9.

Polyacrylamide (PAAm) and alginate double network tough hydrogels for ultracompliant, stretchable, and adhesive electronics. (i, ii, iii) Reproduced with permission.[157] Copyright 2012, Springer Nature. (iv) Reproduced with permission.[158] Copyright 2016, John Wiley and Sons.

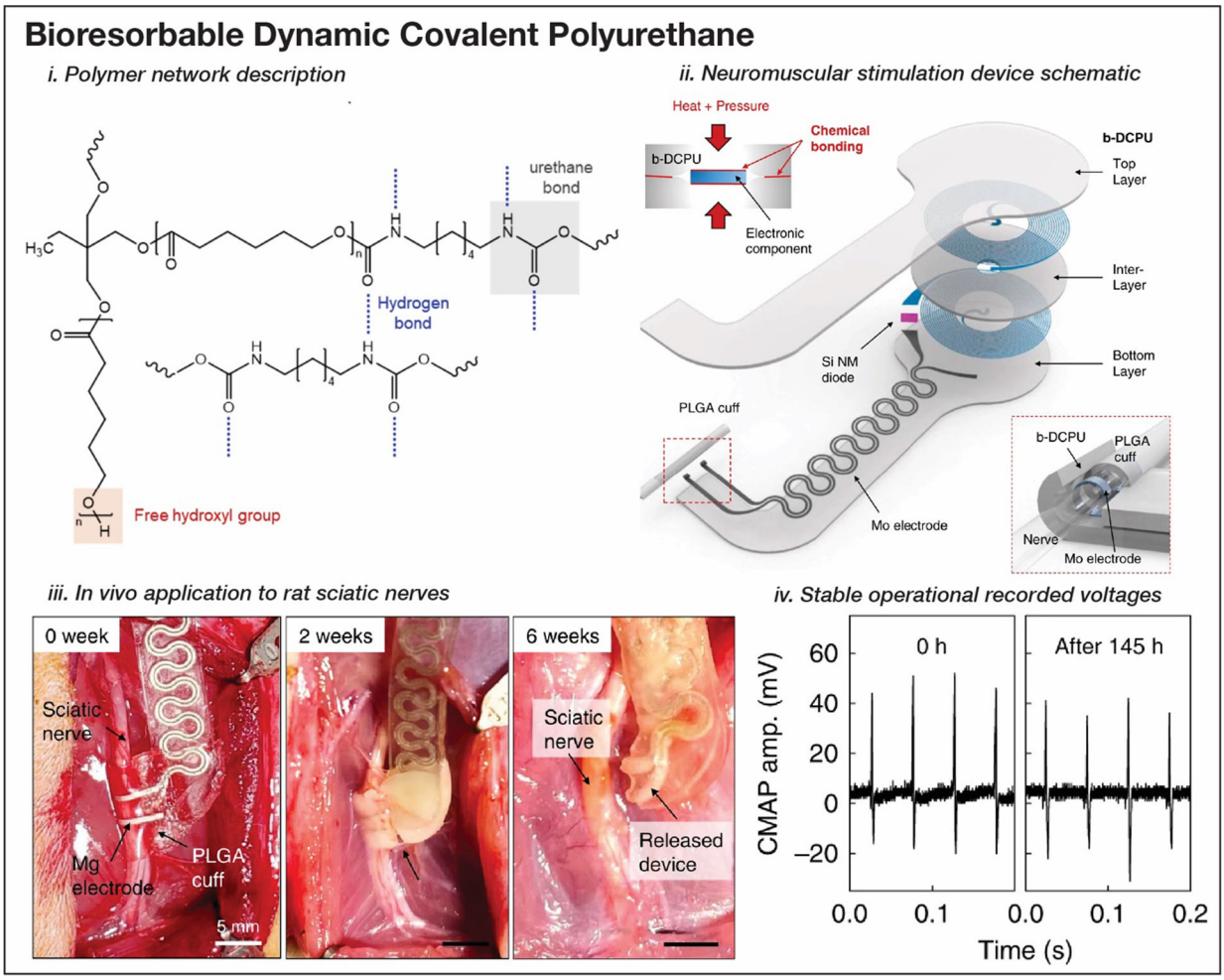

Figure 10.

Bioresobable dynamic covalent polyurethane (b-DCPU)-based neuromuscular stimulation device for peripheral nerve regeneration (i, ii), tested *in vivo* on growing rat sciatic nerves (iii), with stable operational voltages for over 145 hours (iv). Reproduced with permission.[340] Copyright 2020, Springer Nature.

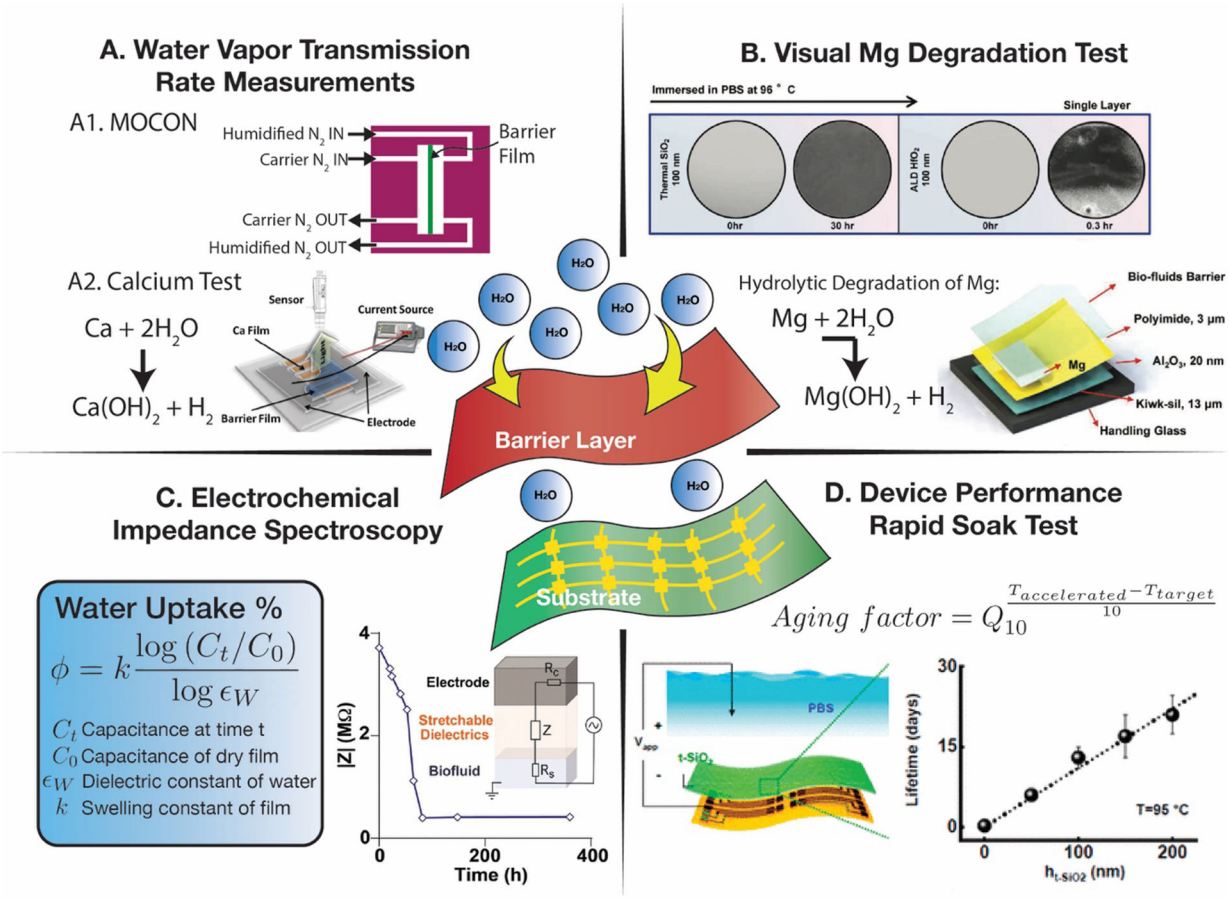

Figure 11.

Schematic describing the four primary techniques to evaluate barrier layer performance. A. Water vapor transmission rate determination using the Ametek MOCON platform or a calcium test, B. Visual degradation studies using dissolvable metals such as magnesium, C. Electrochemical impedance spectroscopy to determine water uptake or delamination, and D. Device performance rapid soak tests at elevated temperatures. A1, calcium test. Reproduced with permission.[481] Copyright 2016, Elsevier. B, visual Mg degradation test. Reproduced with permission.[463] Copyright 2017, John Wiley and Sons. C, electrochemical impedance spectroscopy. Reproduced with permission.[449] Copyright 2020, American Chemical Society. D, rapid soak test. Reproduced with permission.[450] Copyright 2018, American Chemical Society.

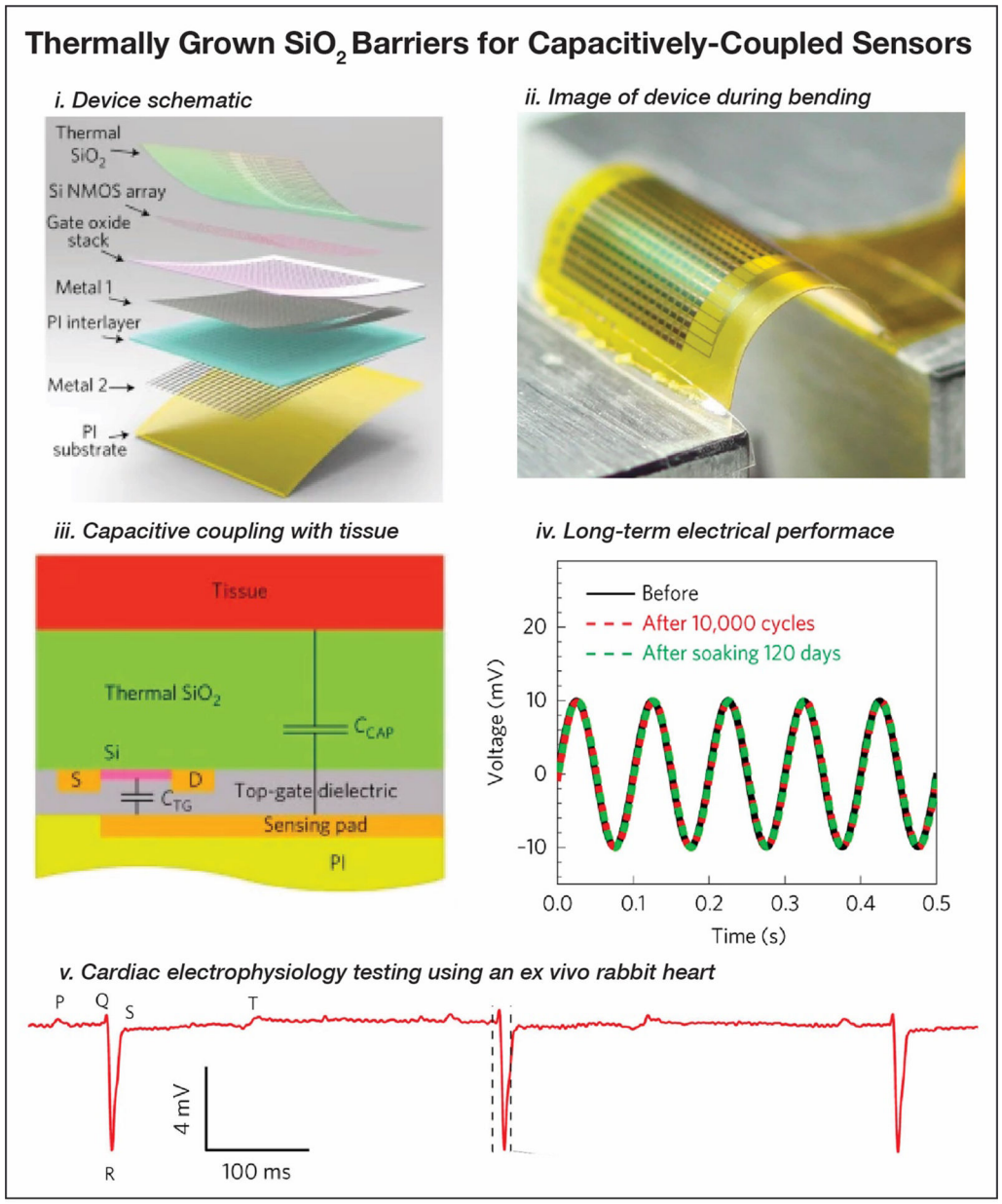

Figure 12.

Thermally grown SiO_2 barrier layer integrated with Si nanomembrane transistor array to function as capacitively coupled interface with cardiac tissue (i-iii), capable of stable electrical performance over time (iv), and monitoring cardiac electrophysiology (v). Reproduced with permission.[182] Copyright 2017, Springer Nature.

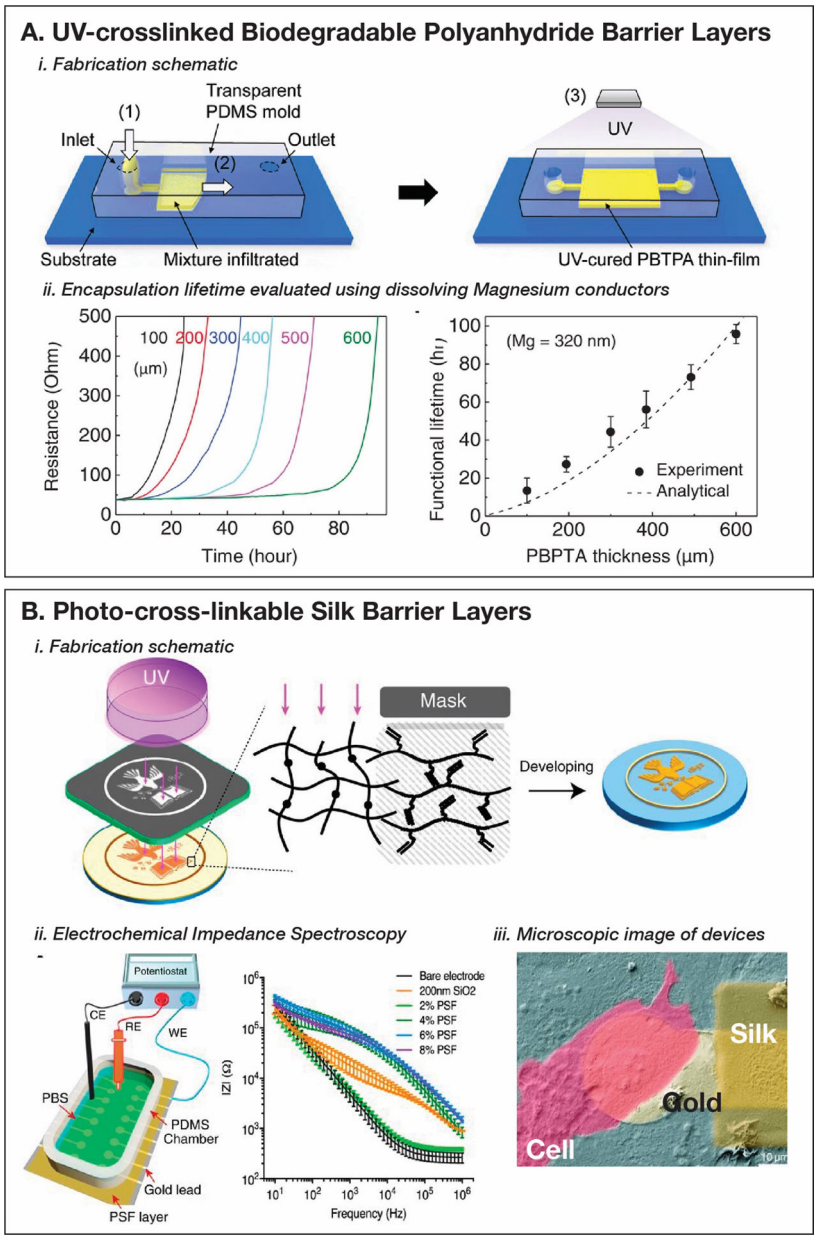

Figure 13.

Novel biocompatible and bioinspired designer barrier materials. A. UV-cured biodegradable polyanhydride barrier layers (i), tested using dissolution experiments with Mg conductors (ii). Reproduced with permission.[536] Copyright 2020, John Wiley and Sons. B. Photo-cross-linkable silk as insulators for multielectrode arrays (i), tested using electrochemical impedance spectroscopy (ii), and *in vitro* cell culture (iii). Reproduced with permission.[537] Copyright 2020, National Academies of Sciences.

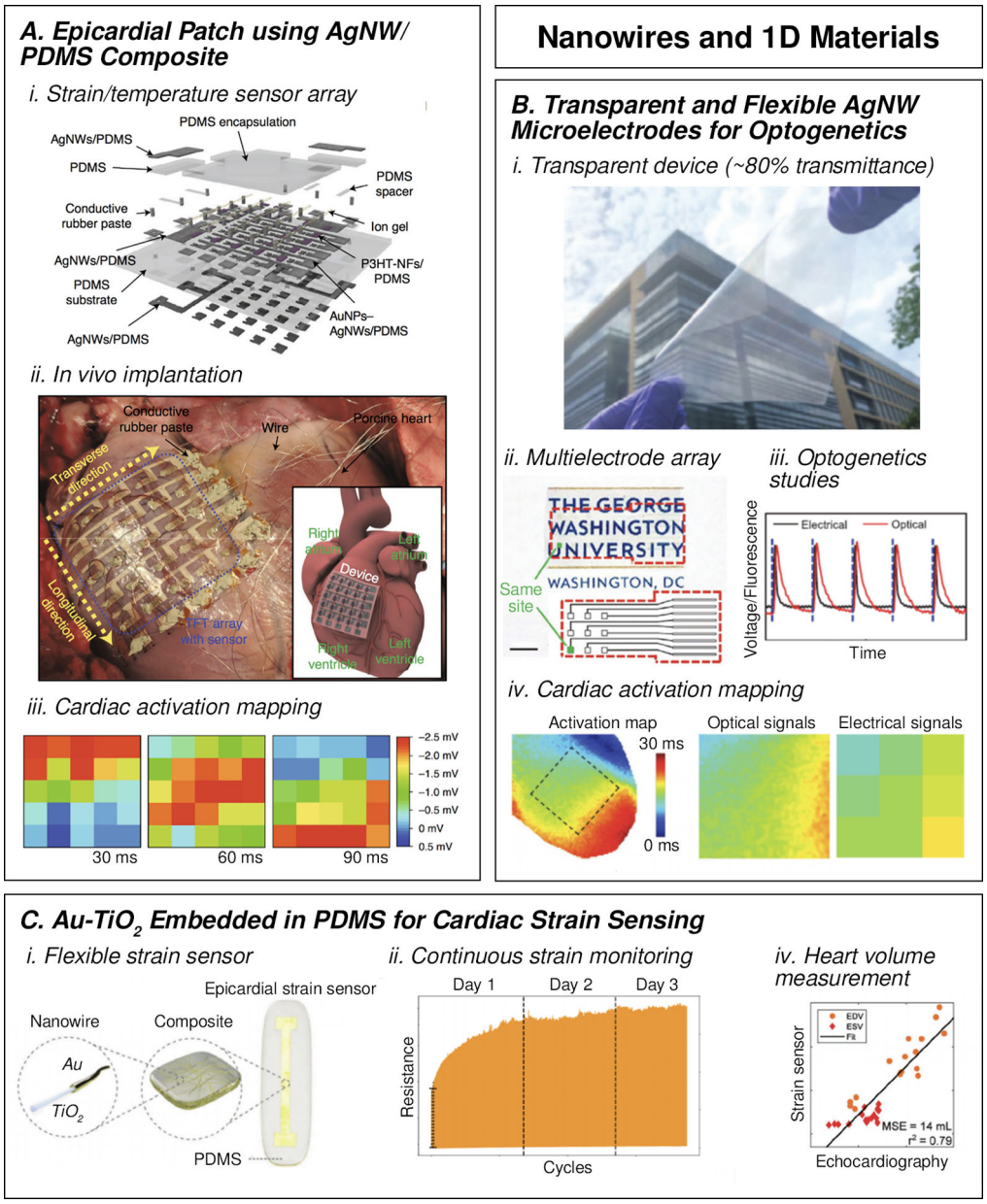

Figure 14.

Recent *in vivo* applications of nanowires. A. Epicardial patch for temperature and strain sensing using a AgNW/PDMS composite as the conductive material and novel rubbery transistors. Reproduced with permission.[541] Copyright 2020, Springer Nature. B. AgNW used in a transparent multielectrode array for optogenetics studies and cardiac activation mapping. Scale bar: 5 mm. Reproduced with permission.[542] Copyright 2021, John Wiley and Sons. C. Au-TiO_2 NW used for cardiac strain sensing. Reproduced with permission.[543] Copyright 2020, John Wiley and Sons.

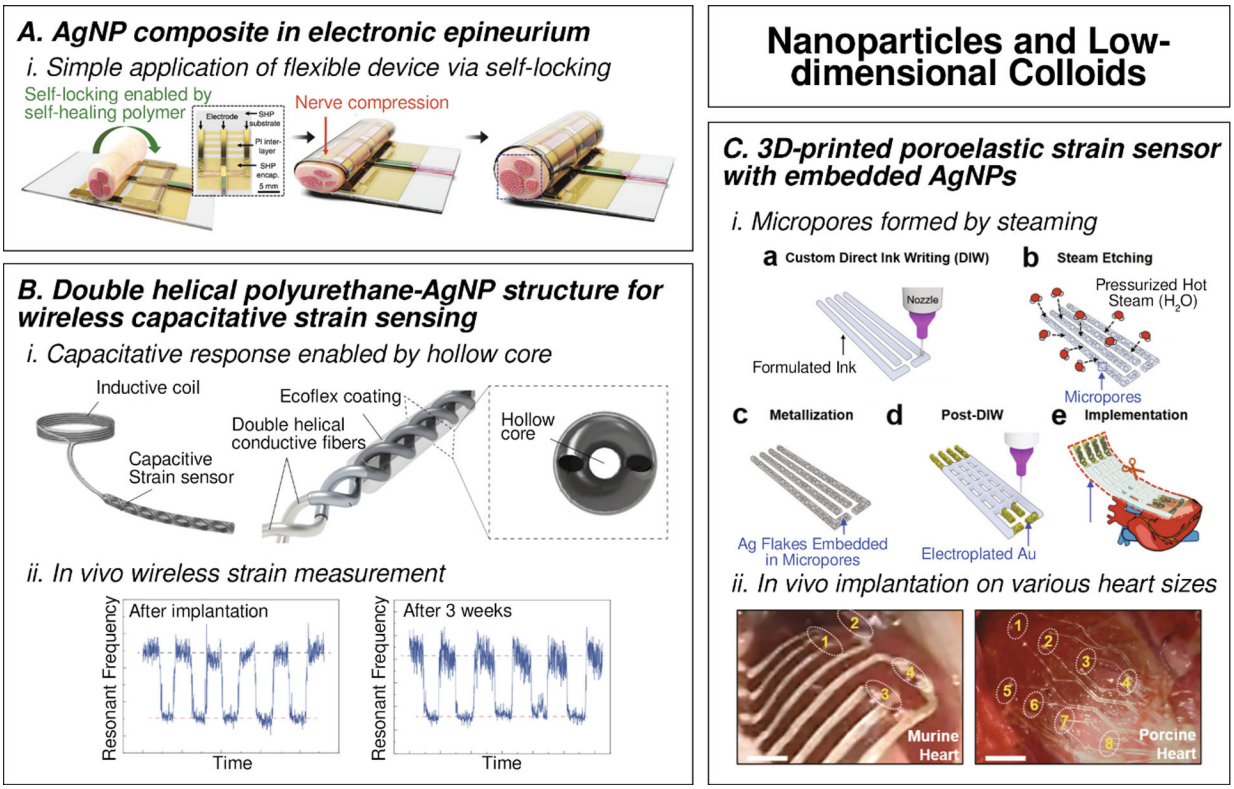

Figure 15.

Recent *in vivo* applications of nanoparticles. A. AgNP used in a self-healing polymer composite for a flexible electronic epineurium. Reproduced with permission.[556] Copyright 2020, Springer Nature. B. AgNP incorporated into double helical polyurethane fibers for wireless capacitive strain sensing. Reproduced with permission.[557] Copyright 2021, Springer Nature. C. AgNP incorporated into a poroelastic 3D-printed cardiac strain sensor. Scale bars: 1.5 mm, 1.5 cm. Reproduced with permission.[558] Copyright 2021, Springer Nature.

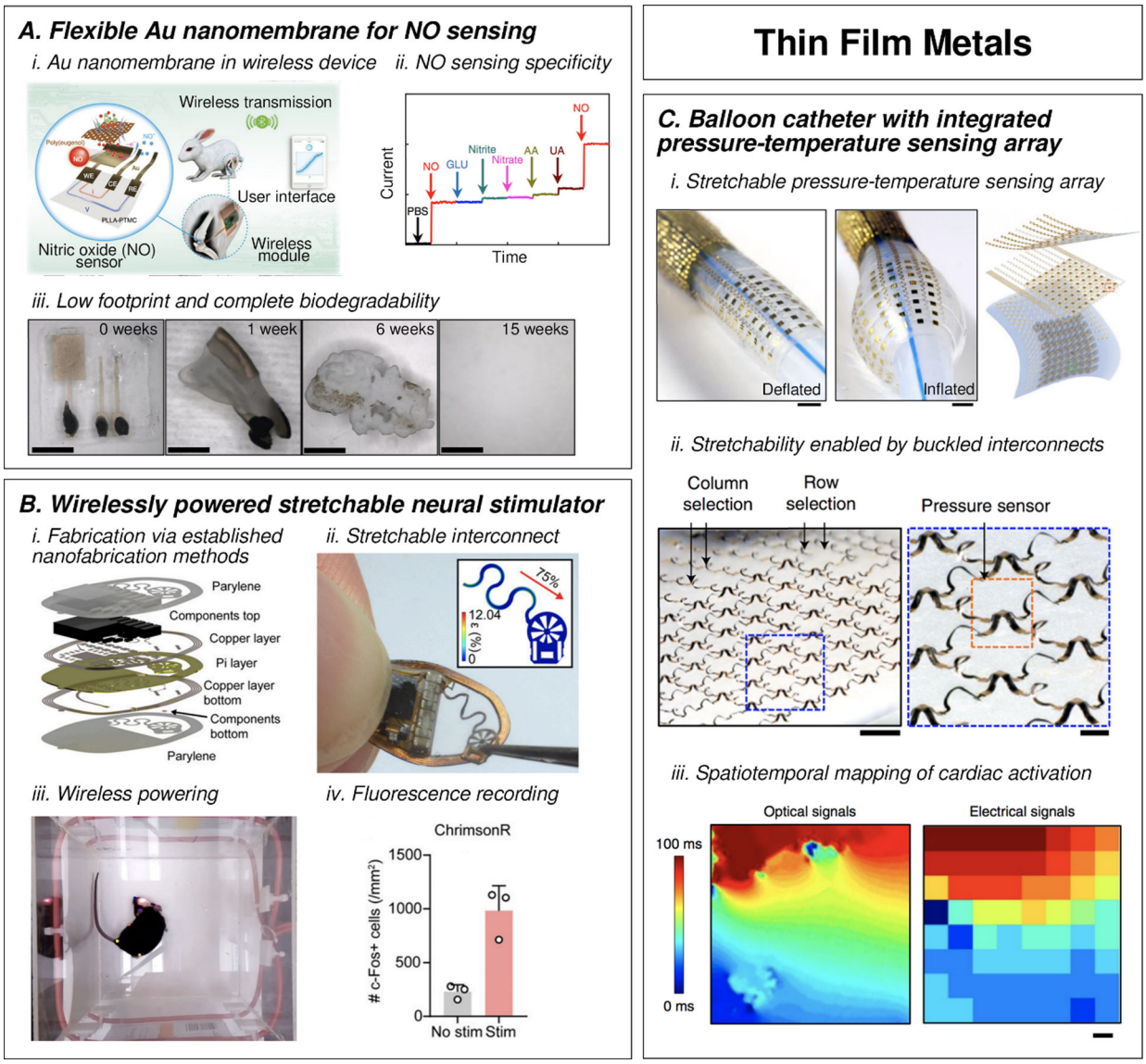

Figure 16.

Recent *in vivo* applications of thin film metals. A. Ultrathin Au nanomembrane used for highly selective and sensitive NO sensing. Scale bars: 5 mm. Reproduced with permission.[566] Copyright 2020, Springer Nature. B. Wirelessly powered neural stimulator made using established nanofabrication techniques and a stretchable copper electrode. Reproduced with permission.[567] Copyright 2020, Springer Nature. C. Stretchable thin film interconnects used in a balloon catheter with integrated pressure and temperature sensing array for cardiac activation mapping. Scale bars in i: 2 mm. Scale bars in ii: 2 mm, 500 μm. Scale bar in iii: 1 mm. Reproduced with permission.[568] Copyright 2021, National Academy of Sciences.

Table 1.

Summary of mechanical and thermal properties of common polymeric substrates.

Material	Modulus [Pa]	Strain at break [%]	T_{glass} a) [°C]	T_{melt} b) [°C]	T_{deg} c) [°C]	Fabrication Methods	Thickness Range [μm]	Refs
Polyesters								
Polyethylene Terephthalate (PET)	3.3×10^9	80–115	78	255	-	Molten extrusion, cold rolling	>1	[138,139]
Polyethylene Naphthalate (PEN)	6.25×10^9	42	120	263	-	Molten extrusion, cold rolling	>1	[138,139]
Polyimides								
Kapton 100 HN	2.5×10^9	72	360–410	-	>500	Film extrusion	12.5–125	[140]
PI 2611	8.5×10^9	100	360	-	620	Spin coating	3–9	[141]
Liquid Crystal Polymers								
Velctra A950	$7–10\times10^9$	5.7	110	280	380	Film extrusion	25–3000	[142–144]
Epoxies								
SU-8	$2–5\times10^9$	6.5	200	-	380	Spin coating, UV curing	0.2–300	[145–147]
Poly(para-xylylene)								
Parylene C	3×10^9	25–200	80–100	290	>125	CVD d)	0.2–100	[148–151]
Elastomers								
PDMS	$5–100\times10^6$	10–1000	−150	-	400–650	Molding, spin coating, 3D printing	>1	[152–154]
Hydrogels								
Polyethylene glycol-dopamine	1.8×10^7	300	-	-	-	Electrochemical gelation, molding	>1000	[126,155,156]
Polyacrylamide-alginate	$1–3\times10^7$	2000	-	-	>225	Molding, 3D printing	1500–3000	[157,158]

a) T_{glass}: glass transition temperature;

b) T_{melt}: melting temperature;

c) T_{deg}: degradation temperature;

d) CVD: Chemical Vapor Deposition

Table 2.

A summary of salient characteristics of polymer, inorganic, multilayer, and composite barrier materials evaluated for flexible electronic applications.

Material	Thickness [μm]	Fabrication Method	WVTR[a] [g m^{-2} day^{-1}]	Accelerated Lifetime Test	Failure Mechanism	Refs
			Polymer Films			
Parylene C	3–4.5	CVD[b]		>4 year at 37°C	Defects (Cracks, pinholes), Delamination	[454,455]
Polyimide PI2611	9	Spin-coat	6	-	Defects (cracks, pinholes)	[456]
Silicone MED6–6606	12	Spin-coat	7	-	High Moisture Diffusivity	[456]
Liquid Crystal Polymer	25	Thermo-press	-	>300 days at 75°C	Diffusivity, Delamination	[454]
			Inorganic Thin Films			
t-SiO_2	0.1	Thermal growth	2E-8	22 days at 70°C	Hydrolytic Degradation (15 nm/year @ 37°C), ionic diffusion	[436,457]
SiO_2	0.1	PECVD[c]	0.1 (double-side)	-	Hydrolytic Degradation, Defects	[458]
SiN_x (Si_3N_4)	0.43	High Freq. PECVD	4.39E-04	-	Hydrolytic Degradation (18.3 nm/day @ 87°C)	[459,460]
	0.01–0.04	PEALD[d]	Order of 1e-6	-		[461]
	0.2	LPCVD	-	2 days at 96°C	Hydrolytic Degradation (0.3 nm day^{-1}), defects (pinholes)	[447]
Al_2O_3	0.025	PEALD	1.7E-05	-	Hydrolytic Degradation	[462]
			Inorganic Multilayers			
SiO_2/SiN_x	0.1/0.2	Thermal growth/ LPCVD[e]	-	16 years at 37°C		[447]
t-SiO_2/HfO_2	0.1/0.1	Thermal growth/ALD		>40 years at 37°C	HfO_2: Pinhole Defects	[463]
Al_2O_3/TiO_2 Nanolaminate	0.003, 12 alternating layers 1.8/0.75Å	PEALD	1.81E-04	-		[464]
Al_2O_3/ZrO_2	0.03	ALD	2.00E-04	-		[465]
			Composite Multilayers			
SiN_x-PMMA-SiN_x	0.05/0.3/0.05	PECVD/Spin-coat/PECVD	8.00E-04	-		[466]
SiN_x-Parylene C	0.1	PECVD/Vacuum Deposition	1.00E-02	-		[467]
Parylene C/HfO_2/t-SiO_2	0.05/0.05/0.1	CVD/ALD/ thermal		13 days at 95°C		[450]
Al_2O_3/Parylene C	0.05/6	PEALD/CVD		>3 years at 37°C		[468]

[a] WVTR- water vapor transmission rate;

[b] CVD- chemical vapor deposition;

[c] PECVD- plasma-enhanced CVD;

[d] PEALD- plasma enhanced atomic layer deposition;

[e] LPCVD- low-pressure CVD